AD NUMBER

AD 023 468

CLASSIFICATION CHANGES

TO

Unclassified

FROM

Confidential

AUTHORITY

USABRL Notice, Oct 30, 1964

AD NUMBER

AD 023468

NEW LIMITATION CHANGE

TO Distribution Statement A
Approved for Public Release: Distribution is Unlimited

Limitation Code: 1

FROM

No Distribution Control Statement

Limitation Code: 9

AUTHORITY

BRL D/A via Ltr, April 22, 1981

BRL

REPORT No. 876

The Effect of Length on the Aerodynamic Characteristics of Bodies of Revolution in Supersonic Flight

C. H. MURPHY
L. E. SCHMIDT

BALLISTIC RESEARCH LABORATORIES

ABERDEEN PROVING GROUND, MARYLAND

WARNING NOTICES

Authority for release of this document to a foreign government must be secured from the Assistant Chief of Staff, G–2, Department of the Army.

When this document is released to a foreign government, it is released subject to the following conditions: This information is furnished with the understanding that it will not be released to another nation without specific approval of the Department of the Army, United States of America; that it will not be used for other than military purposes; that individual or corporation rights originating in the information whether patented or not will be respected; and that the information will be afforded substantially the same degree of security as afforded by the Department of the Army, United States of America.

This document contains information affecting the national defense of the United States within the meaning of the Espionage Laws, Title 18, U.S.C., Sections 793 and 794. The transmission or the revelation of its contents in any manner to an unauthorized person is prohibited by law.

BALLISTIC RESEARCH LABORATORIES

REPORT NO. 876

AUGUST 1953

THE EFFECT OF LENGTH ON THE AERODYNAMIC CHARACTERISTICS OF BODIES OF REVOLUTION IN SUPERSONIC FLIGHT

C. H. Murphy
L. E. Schmidt

Project No. TB3-0240 of the Research and
Development Division, Ordnance Corps

ABERDEEN PROVING GROUND, MARYLAND

TABLE OF CONTENTS

BALLISTIC RESEARCH LABORATORIES

REPORT NO. 876

CHMurphy/LESchmidt/ekb
Aberdeen Proving Ground, Md.
August 1953

THE EFFECT OF LENGTH ON THE AERODYNAMIC CHARACTERISTICS OF BODIES OF REVOLUTION IN SUPERSONIC FLIGHT

ABSTRACT

As a result of a joint interservice research effort, the Army-Navy Spinner Rocket program consisting of more than three hundred models of various lengths has been fired on BRL's precision Free Flight Spark Range. The data obtained from these firings are analysed to provide a good determination of the effect of model length on the aerodynamic coefficients for supersonic Mach numbers. The effect of length on dynamic stability is considered in detail.

Appendices provide a summary of theoretical relations, conversion relations between aerodynamic and ballistic nomenclature, and a full tabulation of the experimental data.

INTRODUCTION

In 1946 an intensive program investigating the dynamic properties of spinning missiles in supersonic flight was instituted as a joint interservice effort. The Army through the Free Flight Aerodynamics Branch of the Ballistic Research Laboratories agreed to manufacture, measure, and fire the one hundred and thirty-five models required by the program and the Navy agreed to contribute the plate measurement and data reduction facilities of its computing group under Dr. Zdenek Kopal at the Massachusetts Institute of Technology. A report on the data reduction process was issued by the M.I.T. group.[1]

The basic interest of the program was in the dynamic stability of spinning bodies of revolution with an emphasis on configurations possessing large fineness ratios. Of the six ballistic coefficients of the Kelly-McShane linearized theory which affect dynamic stability, very few measurements of the Magnus moment coefficient, $K_T(C_{M_{p\alpha}})$[2], and the damping moment coefficient, $K_H(C_{M_q} + C_{M_{\dot{\alpha}}})$, had been made. Information on these coefficients was therefore to be an important result of the program. Since these quantities are functions of the center of mass location, three force coefficients which characterize these functions also had to be found. These were the Magnus force coefficient, $K_F(C_{N_{p\alpha}})$, the damping force coefficient, $K_S(C_{N_q} + C_{N_{\dot{\alpha}}})$, and the normal force coefficient, $K_N(C_{N_\alpha})$. The remaining three ballistic coefficients are the overturning moment, $K_M(C_{M_\alpha})$, which is of prime importance to gyroscopic stability and is essential for consideration of dynamic stability, and the two axial coefficients: axial drag, $K_D(C_D)$, and spin deceleration, $K_A(C_{\not p})$.

The determination of most of these ballistic coefficients especially K_H and K_T is usually quite difficult for wind tunnels and hence the selection of BRL's Free Flight Spark Range for the study was a logical choice. This range at present consists of forty-six spark stations which

---

1. Kopal, Kavanagh, and Rodier, A Manual of Reduction of Spinner Rocket Shadowgrams, Center of Analysis, Tech. Rept. No. 4. (out of print).

2. The symbols appearing in parenthesis after the ballistic coefficient are the corresponding aerodynamic coefficient. See Appendix B for a discussion of the precise correspondence. Brackets will be used to identify the number of individual publications listed in the References.

are distributed over a distance of two hundred and eighty feet.[1] Figure 1 shows a view looking down range with the spark cylinders on the left and the plate holders on the right. The brass squares, located at each station, shield single loops of wire which form part of the electrostatic triggering circuit. As the gun launched models pass each of the spark stations accurately located to 0.001 feet, they are photographed simultaneously in the vertical and horizontal planes by a short duration spark discharge. The time of occurrence of the discharge for ten of the stations is measured to an accuracy of 10^{-6} seconds. From the photographs the spatial coordinates of the missile are obtained to an accuracy of .001 feet in position and three minutes of arc in angular orientation. The ballistic coefficients are computed from these data. [10] .

When the program was originally set up it was decided that five rounds were necessary to determine one value. Since it was planned to obtain reliable values of the force coefficients from the yawing motion of identical shapes possessing different centers of mass, this resulted in the requirement that three different center of mass positions for each shape be fired. In order to study stability over a reasonable range of supersonic Mach numbers data were to be obtained at three Mach numbers, 1.3, 1.9, and 2.5.[2] These considerations meant that forty-five rounds would be needed to complete the study of each design.

Body length was selected to be the basic design variable and the shape was to be representative of service spinner rocket designs. For these reasons the common head shape was chosen to be a secant ogival head two calibers[3] long whose radius of ogive was twice the tangent ogival radius. Three body lengths of three, five, and seven calibers were agreed upon and thus fixed the program size at 135 models. A drawing of the configuration with the actual center of mass location indicated is shown in Figure 2 and a tabulation of the physical characteristics of the models is given in Table C1 in Appendix C.

In order to be able to make flow computations a smooth contour was required and hence no rotating band was used. Spin was imparted by means of a pre-engraved aluminum sabot placed immediately behind the model. At first friction coupling was employed but later it was found to be necessary to connect model and sabot by means of a cruciform key.

---

1. See [8] and [9] for descriptions of the range. Appendix A of [30] gives a more recent description of the range.
2. At the time the intermediate Mach number firings were made, no suitable gun was available and hence the firings were made at the slightly lower Mach number of 1.8. Later using a gun contributed by the Navy, it was possible to fire at the high Mach number of 2.5.
3. A caliber is one diameter. In this program 20mm models were used and hence one caliber corresponded to 20mm.

Finally a copper obturating cup was placed behind the sabot. A model with its key, sabot, and copper cup is shown in Figure 3. Although these auxiliary launching components usually separated quite quickly from the model due to their high drag, for some rounds it was possible to observe this separation. (See Fig. 4). In 4A the missile is about two feet from the gun and none of the components have separated. The fragments above the missile are from paper wadding used in the cartridge case. Figure 4B shows the copper cup separating at five feet from the gun. At twenty-three feet (4C) the sabot is clear of model and the key is dropping free. Finally the sabot separates to over four calibers and the missile is in free flight twenty-eight feet from the gun, (4D).

In the firing portion of the program considerable difficulty was experienced in launching the models properly. In order to obtain the aerodynamic moment coefficients a yawing motion whose magnitude is between half a degree and six degrees is required. The lower limit is imposed by measuring accuracy while the upper indicates the limitations of the linearized theory.

In order to obtain the program requirements, 330 models were launched. It was possible to perform a complete yaw reduction on 109 of these of which 9 had average squared yaw of over 30 and so were not included in the analysis. The overturning moment coefficient was obtained from 19 additional rounds whose yawing motions were too small for a complete reduction. Of the models launched 145 were suitable for drag reductions. A total of 162 rounds provided usable data. A good indication of the improvement in firing efficiency as experience was gained is shown by Figure 5.

The body of this report, which is basically concerned with the data resulting from these firings, will be divided into three major parts. The first part will deal with axial force and moment coefficients, the second with transverse force and moment coefficients, and the third will analyze the dynamic stability characteristics of the configurations. In the appendices all theoretical relations are stated and the conversion from the ballistic nomenclature to aerodynamic is derived.

AXIAL FORCE AND MOMENT COEFFICIENTS

(a) Drag Force Coefficient

Denoting the component of the aerodynamic force along the axis of the missile by F_1, the axial drag coefficient can then be defined by the equation:

$$(1) \quad K_{DA} = -\frac{F_1}{\rho d^2 u_1^2}$$

where ρ = air density

d = diameter

u_1 = axial velocity

If F_1 in (1) is replaced by F_T, the component of the aerodynamic force directed along the trajectory, the more familiar drag coefficient $K_D = \frac{\pi}{8} C_D$ is defined.[1] If cross spin, μ, is neglected, it can be shown that $K_D = K_{DA} \cos \delta + K_N \delta \sin \delta \doteq K_{DA} + \left[K_N - \frac{K_{DA}}{2} \right] \delta^2$ where δ is the magnitude of yaw and K_N is the normal force coefficient. The drag coefficient, K_D, along with the Mach number, is determined for each round by means of a polynomial least squares fit of time-position data. [14]

Since K_D is a function of several parameters, basically shape of missile, Mach number, M, and the squared magnitude of the yaw, the effect of the different parameters have to be separated.[2] The assumption, therefore, is made that the drag dependence on yaw is linear in the average squared yaw, δ^2, for the particular round. This average is over the distance between the first and last timing stations and can easily be computed from the parameters of yaw reductions. Drag values were grouped in intervals of Mach number less than 0.1 long and the parameters of this linear function for each group found from a least squares fit of the drag coefficients and corresponding mean squared yaws. The zero yaw values of the drag coefficients, K_{D_o}, were then computed and use was made of the empirical Q function derived by Thomas [9], [12], to derive their dependence on Mach number.[3] The Q function essentially assumes an inverse quadratic dependence of K_D on Mach number and can be written in the form

$$(2) \quad Q = \sqrt{1 + M^2 K_{D_o}} = a + bM$$

where a and b are empirical constants. This function provides a good description of the drag coefficient's dependence on Mach number for supersonic Mach numbers. The constants a and b for each model length were determined by the usual least squares method.

Since the yaw drag coefficient $K_{D_{\delta^2}}$ was contaminated by Mach number effects, the rounds of each interval were converted to central Mach numbers by means of (2) and new yaw drag coefficients determined. The process can now be iterated and convergence is rapid. Table I

---

1. Throughout the report we will indicate for each ballistic K its exact relationship to the corresponding aerodynamic C's (See Appendix B for details of the conversion process.)

2. In [37] a dependence of K_D on spin which has been measured is described.

3. In [19] the technique for handling drag data which is employed here is described and applied to a study of the effect on drag of systematically blunting the headshape.

presents the final values of the a's and b's together with the $K_{D_{\delta 2}}$ used. (These $K_{D\delta 2}$ may be converted from 1/sq. radian to 1/sq. degree by the factor 3280 $\frac{\text{sq. degree}}{\text{sq. rad.}}$) The defining relation for $K_{D_{\delta^2}}$ is

$$(3)\quad K_D = K_{D_o} + K_{D_{\delta^2}} \overline{\delta^2}$$

TABLE I[1]

Q - Function Parameters

	5 cal.	7 cal.	9 cal.
a	.927	.924	.920
b	.157	.164	.172

	$K_{D_{\delta^2}}$ $\frac{1}{\text{Square radians}}^2$		
Mach No	5 cal.	7 cal.	9 cal.
1.3	3.1 ± .2	4.7 ± .6	3.4 ± .4
1.8	2.6 ± .3	2.6 ± .2	2.3 ± .3
2.5	2.7 ± 11	2.7 ± .3	2.9 ± 1.0

1. All errors calculated in this report are standard errors. In order to convert to probable error, the multiplicative factor 0.6745 should be employed.

2. Since K_N is about 1.0 this table indicates that the axial drag coefficient, K_{DA} is also strongly dependent on the magnitude of yaw.

The original K_D's for each round and their mean squared yaws are tabulated in Appendix C. An indication of their internal statistical accuracy is provided by the representative standard errors provided by Table C7. These standard errors of about 0.5% seem to conflict with the actual dispersion of about 3% as seen in Figures 9, 10, and 11. This spread is quite easily explainable by the wide variation of boundary layers. Figures 6 and 7 clearly illustrate this point.

A further check on this explanation can be obtained by means of a simple computation. It is possible to compute approximate values of the skin friction drag coefficient K_{DSF} for both turbulent and laminar boundary layers.[1] The results of this computation are listed in Table II.

TABLE II

Skin Friction Drag Coefficient, $K_{DSF} \times 10^2$

M	5 cal.			7 cal.			9 cal.		
	turb.	lam.	% diff.[2]	turb.	lam.	% diff.	turb.	lam.	% diff.
1.3	2.1	.5	10	3.0	.6	14	3.8	.7	17
1.8	1.9	.4	10	2.6	.5	14	3.4	.6	18
2.5	1.6	.3	11	2.2	.4	14	2.8	.5	18

An interesting use this drag data can be put to is the rather indirect measurement of the base pressure. The drag coefficient is usually broken up into the head drag, skin friction drag, and base drag coefficients.

$$(3) \quad K_D = K_{DH} + K_{DSF} + K_{DB}$$

---

1. The Blasius flat plate values with the Van Driest correction for compressible flow were used for the laminar flow computation and the recently derived formula obtained by Van Driest [31], [32] was employed for the turbulent boundary layer. The Reynolds numbers based on diameter, R_d, were:

M	$R_d \times 10^{-5}$
1.3	5.90
1.8	8.17
2.5	11.34

2. The percent difference was computed with respect to the total drag coefficient.

Since the head drag arises from compressible fluid pressure difference on the head, it can be computed exactly by means of characteristics. This was done by the ENIAC and the results are given in Table III. The corresponding values obtained by the linearized theory are also listed for comparison purposes. In Figure 8 the pressure ratio, as obtained from the ENIAC is plotted against distance along the model.

TABLE III

Head Drag Coefficients K_{DH}

M	Exact Theory	Linearized Theory
1.3	.0719[1]	.0790
1.8	.0603	.0660
2.5	.0549	.0555

An examination of Table III, the turbulent values of Table II and Figures 9, 10, 11 shows that K_{DSF} contributes about 20% of the drag while K_{DH} and K_{DB} each contribute about 40%. The ratio of base pressure p_B to free stream pressure can now be computed by means of the relation

$$(4) \quad \frac{p_B}{p_0} = 1 - \frac{4M^2}{\pi} \gamma \left[K_D - K_{DH} - K_{DSF} \right]$$

$$\gamma = 1.405.$$

Charters and Turetsky, [13] , were able to make an independent determination by means of measuring the wake angle and assuming a Prandtl-Meyer flow around the base to this wake angle. A comparison of these methods is provided in Table IV. The values for Mach number 1.3 are omitted as the ENIAC computations of ratio of pressure at end of cylinder to free stream were made only as low as Mach number 1.5.

---

1. This is an extrapolated value as K_{DH} was computed only for $M \geq 1.5$.

TABLE IV

Model Number[1]	K_D	K_{DSF}	K_{DH}	K_{DB}	$\frac{p_B}{p_0}$	$\frac{p_B}{p_0}$
		M = 1.8			Total Drag	Wake Angle
5-47	.1431	.0190	.0603	.0638	.63	.67
7-48	.1497	.0263	.0598	.0636	.62	.64
9-09	.1586	.0342	.0607	.0637	.64	.68
		M = 2.5				
5-56	.1198	.0158	.0552	.0488	.48	.46
7-50	.1277	.0218	.0548	.0511	.42	.44
9-13	.1322	.0282	.0548	.0492	.45	.43

The descrepancy between the two methods is caused by the measurement error in the wake angle. The estimated error in $\frac{p_B}{p_0}$ from wake angle is .04 while the total drag method has an estimated error of .01.

An examination of Table IV indicates that K_{DB} does not vary with the length of the cylinder and hence K_{DSF} is the only varying drag component. This conclusion is further substantiated by comparing the change in K_D with length with $\frac{\partial K_{DSF}}{\partial L}$ in Table V. The change in K_D was found by fitting it to a linear function of length by least squares and $\frac{\partial K_{DSF}}{\partial L}$ was found by differentiating the Van Driest formula.

TABLE V

M	$\frac{\partial K_{DSF}}{\partial L} \times 10^3$	Slope of K_D vs L line $\times 10^3$
1.3	4.08	$4.11 \pm .48$
1.8	3.57	$3.74 \pm .37$
2.5	3.00	$3.13 \pm .30$

1. The first digit in the model number indicates its length.

It is interesting to note that this variation decreases with increasing Mach number.

(b) Spin Deceleration Moment Coefficient

The spin deceleration moment coefficient may be defined by

$$(5)\quad K_A = \frac{-M_1}{\rho d^3 u_1^2 \nu} = -\frac{\pi}{8} C_{\ell_p}$$

where

M_1 is component of aerodynamic moment along the symmetry axis

$\nu = \frac{\omega_1 d}{u_1}$ is spin in radians per caliber

ω_1 is axial component of angular velocity

Although it is possible to determine this coefficient from the yawing motion, after part of the program had been fired it was found that this determination was not very accurate. It was, therefore, decided to place pins in the bases of the remaining missiles and measure the rolling motion directly[1]. Figures 6 and 7 show models with and without pins respectively. The individual round values of K_A are tabulated in Appendix C and plotted in Figure 12.

Since the spin deceleration moment is a pure viscous effect, it seemed probable that it could be related to K_{DSF}. Charters and Kent [11] have shown that for a cylinder $K_A = 1/4\ K_{DSF}$. This appeared to be a good approximation for our configuration. (The 1/4 appears because the diameter and not the radius is used as characteristic length). K_{DSF} was obtained from Table IV and $1/4\ K_{DSF}$ is plotted in Figure 12. The agreement seems to be quite good. Since the moments are small and the surface conditions from round to round are clearly not identical, the experimental scatter is not unexpected. The usual values of the individual statistical standard errors as given in Appendix C seem to support this consideration.

---

1. In Appendix A, the exact relations employed are listed.

In Figure 13 K_A is plotted against length. The slopes of least squares fitted lines are compared with $1/4 \frac{\partial K_{DSF}}{\partial L}$ in Table V.

TABLE V

M	Slope	$1/4 \frac{\partial K_{DSF}}{\partial L}$
1.3	.00106 ± .00006	.00102
1.8	.00099 ± .00004	.00089
2.5	.00079 ± .00004	.00075

TRANSVERSE FORCE AND MOMENT COEFFICIENTS

From Appendix A we have the statement of the Kelley-McShane linearity assumption.

If F_2 and F_3 are the components of the transverse aerodynamic force, then

$$(A2) \quad F_2 + iF_3 = \rho d^2 u_1^2 \left[(-K_N + i\nu K_F)\lambda + (\nu K_{XF} + iK_S)\mu\right]$$

where ν is the spin in radians per caliber

$\lambda = \lambda_2 + i\lambda_3$ is the complex yaw

$\mu = \frac{(\omega_2 + i\omega_3)d}{u_1}$ is the complex angular velocity

and the K_i's are the ballistic coefficients. They are identified in both Appendix A and the Table of Symbols and Coefficients. Similarly for the components of the transverse moment there results

$$(A4) \quad M_2 + iM_3 = \rho d^3 u_1^2 \left[(-\nu K_T - iK_M)\lambda + (-K_H + i\nu K_{XT})\mu\right]$$

By assuming a reasonable size for the Magnus cross spin coefficients K_{XF} and K_{XT}, it can be shown that they have little effect on the motion of a body of revolution [28]. In none of the firings made on the BRL Spark Ranges has this assumption seemed unreasonable and hence only the remaining six coefficients will be considered.

In Appendix B an aerodynamic nomenclature is defined and their relation with the ballistic coefficients stated. The conversion equations are:

$$K_N = \frac{-\pi}{8} C_{N_\alpha} \qquad K_M = \frac{\pi}{8} C_{M_\alpha}$$

$$K_F = \frac{\pi}{16} C_{N_{p\alpha}} \qquad K_T = -\frac{\pi}{16} C_{M_{p\alpha}}$$

$$K_S = \frac{\pi}{16} (C_{N_q} + C_{N_{\dot{\alpha}}}) \qquad K_H = -\frac{\pi}{16} (C_{M_q} + C_{M_{\dot{\alpha}}})$$

Note that the last pair of relations are written with an equality sign and not in the manner they appear in (B10). This is due to the fact that in this report K_S and K_H are measured solely by means of their effect on H in the homogeneous part of equation (A8) and as is stated in Appendix B the equality sign is proper.

Throughout this section use will be made of the symmetry argument that all coefficients are even functions of the magnitude of yaw. It is assumed that the yawing motion of each round may be characterized by its mean squared yaw, $\overline{\delta^2}$, and that the coefficient obtained from each firing is constant for the yaw encountered in each flight and may be associated with $\overline{\delta^2}$. It was found that a simple linear dependence on $\overline{\delta^2}$ was sufficient to describe the data for $\overline{\delta^2} < 30$ square degrees.

(a) Normal Force and Overturning Moment Coefficients

The overturning moment coefficient can be obtained accurately from the turning rates of the two arms of the characteristic epicyclic yawing motion of a spinning missile. Actually small corrections are necessary which involve the damping exponents and the Magnus force coefficient K_F, and although these are usually less than one percent all of the data in this report contain them. These corrections are explicitly stated in Appendix A. A further correction is necessitated by the variation in center of mass from round to round. Since this variation is less than .02 calibers for models of the same type all the models are corrected to a standard center of mass location for each type by means of an approximate K_N in equation (A5.7).

These final results were examined for yawing motions of different amplitudes. It was found that the seven caliber forward c.m. models together with the nine caliber forward and middle c.m. models had definite dependence on the magnitude of yaw. Values for a fixed Mach number were fitted to a linear function of mean squared yaw:

(6) $K_M = K_{M_o} + K_{M_{\delta^2}} \overline{\delta^2}$

The resulting values of $K_{M_{\delta^2}}$ are listed in Table VI together with their standard errors:

TABLE VI

	$K_{M_{\delta^2}}$ $\frac{1}{\text{Square radians}}$		
Mach No.	7 F	9 F	9 M
1.3	-36 ± 7	-85 ± 16	-53 ± 26
1.8	-23 ± 3	-16 ± 3	-59 ± 3
2.5	-53 ± 7	-20 ± 20*	-56 ± 16
Eq. (7)	-41.	-83.	-39.

* This value is poorly determined since the total variation of $\overline{\delta^2}$ is from 1 to 5.7 square degrees.

The values provided by Table VI should be considered only good qualitative results since they were obtained by a rather crude technique. Since the samples are small the standard errors have only qualitiative significance. With this in mind we see that the effect of yaw on the overturning moment has a stabilizing influence and that the explanation of these indications of non-linearity lies in a non-linear pressure distribution over the rear of the models[1]. This distribution probably starts about six calibers from the nose and increases in its non-linear character with increasing length. From this we would expect the longer missiles to exhibit non-linearity and that this effect will become more pronounced as the center of mass is moved forward and thereby accentuates the effect of force on the missile's rear. This prediction is roughly verified by Table VI.

H. R. Kelly [36] has recently developed a simple relation for $K_{M_{\delta^2}}$ and $K_{N_{\delta^2}}$ by considering the viscous cross flow. His results can be written in the following form:

(7) $K_{M_{\delta^2}} = 1/4\ C_{D_c}\ L^2 \left[3r - 2L\right]$

(8) $K_{N_{\delta^2}} = 3/4\ C_{D_c}\ L^2$

1. This explanation was suggested by J. D. Nicolaides.

where r is distance to center of mass from the nose and C_{D_c} is the drag coefficient for an infinite cylinder in a cross flow. For laminar boundary layers C_{D_c} is 1.2 and for turbulent boundary layers it is .35. Since the average transition point is about 1.5 cal. rear of the shoulder for the seven and nine caliber models a weighted value[1] for C_{D_c} of .78 was used for the seven caliber models and .68 for the nine caliber models. $K_{M_{\delta^2}}$ and $K_{N_{\delta^2}}$ have been computed by equations (7) - (8), and are tabulated in Tables VI and VIII respectively. Considering the roughness of the experimentally determined values and the use of a "weighted" C_{D_c} the agreement is good.

Using Table VI and the round values for K_M and $\overline{\delta^2}$, individual values of K_{M_o} were then computed and in Figures 14-16 are plotted against Mach number. The maximum scatter is about 2%. The circled points were computed by fitting K_{M_o} for each Mach number to a line as a function of center of mass location: (See Eq. A5.7). The slopes of these lines are the normal force coefficients and are tabulated in Table VII.

TABLE VII

Normal Force Coefficient, $K_N = -\frac{\pi}{8} C_{N_\alpha}$

M	5	7	9
1.3	.98 ± .01	1.02 ± .02	1.06 ± .01
1.8	1.13 ± .01	1.13 ± .01	1.16 ± .01
2.5	1.26 ± .02	1.21 ± .01	1.28 ± .01

As is described in Appendix A it is also possible to measure K_N by means of the swerving motion. Values of K_N were obtained by this means from all rounds with large enough swerving motion[2]. These data also exhibited a dependence on yaw for the seven and nine caliber rounds. The values of $K_{N_{\delta^2}}$ are given in Table VIII.

1. More precisely for the seven caliber models $C_{D_c} = \frac{(1.2)3.5 + (.35)3.5}{7} = .78$ A similar computation was performed for the nine caliber models.
2. The criterion was that the swerving motion be six times the linear measurement accuracy of .010".

The swerve K_{N_o}'s were computed in a manner similar to the K_{M_o}'s and are plotted in Figure 17.

TABLE VIII

	$K_{N_\delta}{}^2$, $\frac{1}{\text{Square radians}}$	
Mach No.	7	9
1.3	23 ± 7	20 ± 3
1.8	13 ± 3	26 ± 3
2.5	46 ± 3	33 ± 13
Eq. (8)	29.	41.

The circled values are those obtained from the K_{M_o}'s at different center of mass locations and crosses are based on tests in BRL's Supersonic Wind Tunnel. The agreement is fairly good. In Figure 18 the distance to the center of pressure from the nose in calibers C_{P_N}, is plotted as obtained from the individual swerving motion, the center of mass method, and the wind tunnel. Since this scale is larger than model size, in order to show individual points, the curves are replotted against model length at the actual model size of 20mm per caliber in Figure 19. Finally Figure 20 shows K_N's dependence on length. Note that both center of pressure and normal force are relatively insensitive to length. (A mild exception to this is the behavior of the center of pressure at Mach number of 1.3) In this characteristic they follow the slender body prediction that cylindrical afterbodies have no effect on normal force or center of pressure[1].

(b) Magnus Force and Moment Coefficients

In this section and the next one we will discuss those coefficients which at the present time can only be determined by the precision Range Technique. The determination of the quantities is difficult, and, quite naturally, is not as accurate as K_D, K_M, or K_N. The difficulty lies in the fact that the dynamic coefficients affect only the damping of the epicyclic yawing motion. The damping is difficult to determine as it is the rate of change of a small quantity. For 20mm models a

1. The data, however, is not very close to the slender body values of $K_N = .78$ and $CP_N = 1.14$. This discrepancy has been observed by many investigators and is probably due to the inappropriateness of the theory.

reasonable estimate for the size of error of a damping coefficient α_i is 2×10^{-5} 1/calibers. Since for the five caliber models $\alpha_i \sim 25 \times 10^{-5}$, this is roughly an 8% error. (The figure 2×10^{-5} is sensitive to the frequency of the two modes, their amplitude, and the distribution of the observation.)

An inspection of the Magnus moment coefficient data for the 7F, 9F, and 9M models shows that, in common with the normal force and overturning moment coefficients, they are functions of yaw. This dependence is clouded by the scatter of the data and hence $K_{T_\delta 2}$ as tabulated in Table IX is poorly determined for some Mach numbers and can only be estimated for others.

TABLE IX

	$K_{T_\delta 2}$ $\frac{1}{\text{Square radians}}$		
Mach No.	7F	9F	9M
1.3	-26 ± 10	-43^*	-16^*
1.8	-43 ± 20	-43 ± 16	-16^{**}
2.5	-72 ± 20	-43^*	-16^*

* Estimated value

** Obtained from two points

For fixed Mach number, K_T is a linear function of center of mass location (see (A5.8)). K_{T_o} is plotted against c.m. in Figures 21-23 and its rather large scatter verifies the prediction that dynamic data is certainly not of as good quality as that for K_M. In Table X, the slopes of the least squares fitted lines, which are the Magnus force coefficients, are tabulated. This linear relationship is used to obtain "average" values of K_{T_o} which are exhibited as a function of Mach number in Figure 24. For some rounds where the yawing motion is such that the Magnus force has a measurable effect on the swerving motion an independent measurement of K_F is possible.[1] In Figure 25, K_F's as obtained from the center of mass method together with those obtained from the swerving motion of individual rounds are plotted against Mach numbers. The agreement of such delicate measurements is quite encouraging.

1. Appendix A provides the exact relations employed in this determination.

TABLE X

Magnus Force Coefficient, K_F, From C.M. Method

Mach number	1.3	1.8	2.5
5 cal.	.14 ± .01	.14 ± .04	.05 ± .02
7 cal.	.20 ± .02	.20 ± .02	.16 ± .02
9 cal.	.31 ± .03	.33 ± .02	.26 ± .02

J. C. Martin has recently suggested a simple model by which K_F and K_T may be computed theoretically [29] . He shows that the effect of spin on a body of revolution at an angle of attack is to rotate the plane of symmetry of the boundary layer configuration slightly out of the plane of yaw. The linearized flow over the resulting shape then provides a force which is perpendicular to the plane of yaw and proportional to the magnitude of spin. These considerations result in the following formula for the radio of slender body Magnus force coefficient K_F to slender body normal force coefficient K_N for incompressible flow.

(9) $$\frac{K_F}{K_N} = 6.93 \hat{L} \delta^*$$

where L is the equivalent cylinder length in calibers[1]

and δ^* is the boundary layer displacement thickness in calibers.

Since our main interest is in compressible turbulent boundary layers, we have to assume that Equation (9) will apply to this case. From [33] and [34] , it can be shown that a good approximation for δ^* is

$\frac{c}{6.93} (1 - .14 M) \hat{L}^{4/5} R_d^{-1/5} \frac{4}{\pi}$ where R_d is the Reynolds' number based on the diameter and c depends on the velocity profile. Inserting this value of δ^* together with the slender body normal force coefficient

1. Since Martin's calculations are based on the usual flat plate boundary layer assumptions, his results are for a circular cylinder whose boundary layer build up is equivalent to the body of revolution.

value of $\frac{\pi}{4}$ in (9) there results:

$$\hat{K}_F = c(1 - .14\,M)\hat{L}^{9/5}\ R_d^{-1/5} \tag{10}$$

From (10) it is now possible to compute the center of pressure of the Magnus force by the formula:

$$C.P._F = \frac{1}{\hat{K}_F}\int_0^{\hat{L}} \hat{L}\,\frac{d\hat{K}_F}{d\hat{L}}\,d\hat{L}$$

$$= \frac{9}{14}\,\hat{L}$$

where $\hat{C.P.}_F$ is the equivalent cylinder distance to Magnus force center of pressure.

We now assume that $\hat{L}$, the equivalent cylinder length, can be written $L - L_n$ where L is the model length and L_n is a correction due to the nose and is a function of Mach number.

$$\hat{C.P.}_F = C.P._F - L_n$$

and

$$C.P._F = \frac{9}{14}\,L + \frac{5}{14}\,L_n \tag{11a}$$

$$\hat{K}_F = c(1 - .14\,M)\ (L - L_n)^{9/5}\ R_d^{-1/5} \tag{11b}$$

In Figure 19 $C.P._F$ is plotted against length and it can be seen that the predicted slope of $\frac{9}{14}$ is very good. For fixed Mach number we fit Equation (11a) and obtain the following values for L_n:

Mach number	1.3	1.8	2.5
L_n	.52 ± .15	1.34 ± .08	2.55 ± .12

Using equation (11b) as an empirical relation and fitting the data shown in Figure 25 there results c = .19 ± .03. These results are plotted in Figure 19. The agreement is fair for such a rough theory, although it is certainly not as good as the $C.P._F$ slope. Finally it is important to note that the slope of the $C.P._F$ curve versus length of 9/14 is independent of the Mach number and velocity profile and depends only on the assumption that for turbulent boundary layers $\frac{\delta^*/d}{L}$ varies inversely as the 1/5th power of the Reynolds number based on length.

(c) Damping Force and Moment Coefficients

When the data on the damping moment coefficient K_H is examined, once again the existence of non-linearity in the 7F, 9F, and 9M models can be seen. In Table XI are tabulated the values of $K_{H_{\delta^2}}$ which were employed to obtain the K_{H_o}'s.

TABLE XI

	$K_{H_{\delta^2}}$ $\frac{1}{\text{Square radians}}$		
Mach No.	7F	9F	9M
1.3	590*	650*	650*
1.8	590 ± 361	490 ± 230	720**
2.5	590 ± 230	650*	650*

* estimated

** two values of K_H

These values are inserted in a modified form of (A5.9) and K_S, the damping force coefficient at the centroid, is obtained.[1] The desired form of (A5.9) is

$$\left[K_H\right] = K_H^* - qK_M^* = K_H + qK_S$$

where q is measured from the centroid and unstarred quantities are for c.m. at centroid.

In Figures 26-28, $\left[K_H\right]$ is plotted against c.m. location and lines are fitted. The scatter indicates the poor quality of K_S. In order to obtain other values of K_S for c.m.'s which are not at the centroid, relation (A5.4) must be used. Table XII presents K_S at the centroid and it is plotted against Mach number in Figure 29.

1. The middle center of mass rounds have their centers of mass located at their geometric centroid.

TABLE XII

K_S at Centroid

Mach No.	5	7	9
1.3	-3.8 ± .1	-5.3 ± .6	-8.6 ± .8
1.8	-3.1 ± .5	-5.4 ± .1	-9.2 ±1.2
2.5	-1.1 ± .2	-3.8 ± .1	-6.6 ±1.4
Eq. (13)	-4.6	-7.0	-9.3

In Figure 30 K_H at the centroid is plotted against Mach number while Figures 31 and 32 give the centroid values of K_S and K_H as functions of length.

In order to get some theoretical basis for predicting K_H it is necessary to use certain results recently obtained by W. Dorrance [35]. According to Dorrance's "zero order" slender body theory for missiles without boattails:[1] [The relations for C_{M_q} and C_{N_q} were first obtained by M. Munk.]

$$C_{M_{\dot{\alpha}}} = \frac{16v}{\pi} (r - r_c)$$

$$C_{M_q} = -4 \left[(L - r)^2 + \frac{4v}{\pi} (r - r_c) \right]$$

$$C_{N_{\dot{\alpha}}} = -\frac{16v}{\pi}$$

$$C_{N_q} = -4 (L - r)$$

where L is length in calibers

r is distance to the c.m. from the nose in calibers

v is volume in cal.^{3}

r_c is distance to the centroid from the nose in calibers

From these equations there results

(12) $$K_H = \frac{\pi}{4} (L - r)^2$$

(13) $$K_S = -\frac{\pi}{4} (L - r) - v$$

1. Care has to be used in order to transform the symbols of [35] to those of this report. C_{n_w} and C_{M_w} of [35] actually correspond to $C_{N_{\dot{\alpha}}}$ and and $C_{M_{\dot{\alpha}}}$ while $C_{n_{\dot{\alpha}}}$ and $C_{m_{\dot{\alpha}}}$ of [35] correspond to $C_{N_q} + C_{N_{\dot{\alpha}}}$ and $C_{M_q} + C_{M_{\dot{\alpha}}}$ of this report.

Equation (12) predicts that K_H at the centroid is a pure quadratic function of the distance of the centroid from the base which has $\frac{\pi}{4} = .79$ as its coefficient. If we fit K_H at the centroid to such a function, there results the values of 1.19, 1.43, 1.50 for Mach numbers 1.3, 1.8, and 2.5 respectively. Since the fit is quite good, we will consider $K_H = C\,(L - r_c)^2$ as a good empirical formula for the damping moment at the centroid. Table XII compares K_S at centroid with Dorrance's K_S. The agreement is not too satisfactory. It is finally of interest to note that within the accuracy of this elementary theory K_H has no contribution from $C_{M_{\dot{\alpha}}}$ when the c.m. is at the centroid.

DYNAMIC STABILITY

A study of the dynamic stability of the rounds fired in this program provides some of the most interesting results of this report. As in [28] a missile is defined to be dynamically stable if the yawing motion described by the solution of the homogeneous equation of the yawing motion does not increase. It is proven in [28] that a sufficient condition for dynamic stability of a statically unstable[1] missile traveling over a flat trajectory is

$$(14a) \qquad h - K_N - K_D + k_2^{-2}K_H - k_1^{-2}K_A > 0$$

$$(14b) \qquad s > \frac{1}{\bar{s}\,(2 - \bar{s})} \quad ; \quad 0 < \bar{s} < 2$$

where $s = \dfrac{A^2 \nu^2}{4B \rho d^5 K_M}$ (Gyroscopic stability factor)

A = axial moment of inertia

B = transverse moment of inertia

ρ = air density

d = diameter

$\nu = \dfrac{\omega_1 d}{u_1}$; spin in radians per caliber

1. A missile is statically unstable if $K_M > 0$.

$$\bar{s} = \frac{2(K_N - K_D - k_1^{-2}K_T)}{K_N - K_D + k_2^{-2}K_H - k_1^{-2}K_A} \quad \text{(Dynamic Stability Factor)}$$

$k_1^{-2} = \frac{md^2}{A}$ (k_1 is axial radius of gyration in calibers)

m = mass

$k_2^{-2} = \frac{md^2}{B}$ (k_2 is transverse radius of gyration in calibers)

If $\bar{s} < 0$ or $\bar{s} > 2$, it is further shown that a statically unstable missile can not be stabilized by spin. The curve $s = \frac{1}{\bar{s}(2 - \bar{s})}$ is plotted in Figure 33 and the stable and unstable regions are identified.

This requirement is much more complete than the classical gyroscopic stability requirement that $s \geq 1$. Since h is usually positive for missiles in supersonic flight[1], conditions (14) will reduce to the classical inequality for $\bar{s} = 1$. $\bar{s}$ is tabulated in Appendix C for all rounds and it can be seen there that it definitely departs from this optimum value of unity. For some of the 9F models $\bar{s}$ exceeds two and hence these models are dynamically unstable and cannot be stabilized by spin! $\bar{s}$ has the further property that the slower arm has the smaller damping rate ($\alpha_2 < \alpha_1$) when $\bar{s} < 1$ and the reverse is true ($\alpha_2 > \alpha_1$) when $\bar{s} > 1$. This therefore, means that the faster arm will grow for the 9F models irrespective of spin. (Unless h is negative the slower arm, however, will always shrink.)

It is possible to make an important generalization of the dynamic stability in the following way, (see [28]).

Theorem

The damping exponents α_1 and α_2 of the epicyclic yawing motion of a statically unstable missile are greater than or equal to an assigned value, α if the following relations are satisfied:

$$h - \alpha > 0$$

$$s \geq \frac{1}{\bar{s}(\alpha)\left[2 - \bar{s}(\alpha)\right]}$$

1. It was positive for all missiles fired in this program.

$$0 < \bar{s}(a) < 2$$

$$\text{where } \bar{s}(a) = \frac{2\,(K_N - K_D - k_1^{-2} K_T) - a}{K_N - K_D + k_2^{-2} K_H - k_1^{-2} K_A - a}$$

(Note that $\bar{s}(0)$ is the dynamic stability factor.)

With the above information in mind we will now move on to a consideration of the various applications of our experimental information to the stability problem. First the effect of center of mass location is of interest.

Looking over the $\bar{s}$'s for the five caliber models in Table C-2b, it can be seen that $\bar{s}$ lies between .40 and 1.30 and hence the dynamic stability is of little interest for these models. The dynamic stability of the seven calibers, and especially the nine calibers, is more interesting. In order to obtain a rough picture of the effect of c.m. we will assume that c.m. may be changed while the masses and radii of gyration remain constant. An examination shows that with the exception of the bimetal middle c.m.'s (9 M2, 9 M3) and two of the rear c.m.'s (9 R2, 9 R3), these assumptions are roughly true.

With these assumptions in mind, v^2 required for stability is plotted in Figure 34 against c.m. position for M = 1.3[1]. v^2 was selected as one of the variables in this plot so that the gyroscopic stability curve, s = 1, appears as a straight line. According to this plot the interval of c.m. location where spin stabilization is possible, identified in this figure by $a = 0$, is relatively small and even there a rather high twist is required[2]. The rear asymptote corresponds to $\bar{s} = 0$ while the forward one is caused by $\bar{s} = 2$. Note that 0.3 cal. rear of the centroid is located at the "optimum point" where $\bar{s} = 1$.

Now it is shown in [28] that the situation is improved by increasing k_2^{-2}. Since k_2^{-2} is 40% larger for the bimetals (9 M2 and 9 M3), the stability curves are replotted for their masses and radii of gyration in Figure 35 (The physical constants for both figures are listed in Table XIII).

---

1. In the two stability plots c.m.'s forward of the centroid are plotted positively.
2. This fact was first observed by R. Turetsky in [18] which was an interim report on the program.

TABLE XIII

	m gms	k_1^{-2}	k_2^{-2}
Standard	137	8.3	.19
Bimetal	200	7.6	.26

The bimetals as can be easily seen are much more stable than the solid models. These figures become, of course, more inaccurate as the c.m. is moved from the centroid. If the exact physical characteristics of the 9 F's are used, a much better determination of the c.m. position for which $\bar{s} = 2$ may be made. Similarly better values for the "optimum point" and the point at which $\bar{s} = 0$ can be found when the physical characteristics of the 9 M's and 9 R's respectively are used. These calculations have been made and the results appear in Table XIV. Note that according to Table XIV it is impossible to spin stabilize the 9 F's and furthermore that at M = 1.8 they should be markedly unstable. This is verified by Table C-4b. As the yaw increases, however, the non-linearities which have been observed throughout the program have a destabilizing effect and increase the size of $\bar{s}$ considerably.

TABLE XIV

Location of C.M. From Centroid For Dynamically Stable Nine Caliber Models

M	$\bar{s} = 0$	$\bar{s} = 1$ (standard)	$\bar{s} = 1$ (bimetal)	$\bar{s} = 2$
1.3	-1.09	-.32	.05	.97
1.8	-1.59	-.70	-.28	.30
2.5	-2.03	-.73	-.28	.94

As a final application of the data obtained by this program we will make rough estimates of the stability of models which are longer than nine calibers. (Since these estimates are based on linear theory, they are at the mercy of non-linearities which seem to increase with length.) For simplicity the center of mass will be located at the centroid. The data for nine-caliber length models definitely shows a bimetal design to be superior and we will thus consider models possessing cylindrical center sections of length $2\ell_B$ and of density different from the remainder of the model. Finally the following formulas for centroid, mass, and moments of inertia will be needed. They are good approximations for models over eight caliber long:

c.m. from base = 1/2 $(\ell_C + \ell_N)$

ℓ_C = length of cylinder in calibers

$\ell_N = \frac{4}{\pi}$ (volume of nose in calibers) = .857

$$m = \frac{\pi}{4} (\rho_1 d^3) \left[\ell_N + \ell_C + \left(\frac{\rho_2}{\rho_1} - 1\right) 2\ell_B \right]$$

where ρ_1 is density of nose and tail material

ρ_2 is density of center section material

$$\frac{A}{\rho_1 d^5} = \frac{A_N}{\rho_1 d^5} + \frac{\pi}{32} \left[\ell_C + \left(\frac{\rho_2}{\rho_1} - 1\right) 2\ell_B \right]$$

where A_N = axial moment of inertial of ogival nose
= .0565 $(\rho_1 d^5)$

$$\frac{B}{\rho_1 d^5} \doteq \frac{\pi}{48} (\ell_C + \ell_N)^3 + \left(\frac{\rho_2}{\rho_1} - 1\right) \frac{(\pi \ell_B)}{2} \left(\frac{1}{16} + \frac{\ell_N^2}{4} + \frac{\ell_B^2}{3} \right)$$

In order to get some idea of the stability situation for these long missiles, we will select $\frac{\rho_2}{\rho_1} = 3$ and ℓ_B so that the spin required for gyroscopic stability will be a minimum. This is equivalent to requiring that $\frac{A^2}{B}$ be a maximum. In addition we will also specify ρ_1 be equal to the density of dural. In Table XV are tabulated the resulting ℓ_B, A B, m, and $\bar{s}$'s.

TABLE XV

L	ℓ_B (cal.)	A(gm-cal^2)	B(gm-cal^2)	m(gm)	$\bar{s}$
9	2.44	38	1060	310	1.0
11	3.05	48	2080	387	1.2
13	3.66	57	3600	465	2.2
16	4.58	72	7062	582	3.2

According to Table XV, models with c.m. at centroid and longer than eleven calibers are impossible to stabilize by spin. It is possible to make a rough calculation as to the location of the optimum points for the models in Table XV. This would give some indication of possible improvement of dynamic stability by varying c.m. location and is done in Table XVI. In this table the location of the optimum point is given together with the gun twist, $\frac{l}{n}$, required for stability.

TABLE XVI

L	c.m. shift from centroid	l/n
9	-.05	1/20
11	-.63	1/15
13	-1.03	1/12
16	-1.46	1/9

From this table are observed the very important facts that dynamic stability can be improved by moving c.m. rearward and that quite long models can be stabilized with reasonable gun twists. The rather crude approximation on which the above is based should be reemphasized and it should be remembered that the above is done only as a rather weak aid to designers of longer missiles.

C. H. Murphy
C. H. MURPHY

L. E. Schmidt
L. E. SCHMIDT

REFERENCES

1. R. H. Fowler, E. G. Gallop, C. N. H. Lock, H. W. Richmond, The Aerodynamics of a Spinning Shell, Phil. Trans. Roy Soc. London (A) 221, 295-387 (1920).

2. R. H. Fowler, C. N. H. Lock, The Aerodynamics of a Spinning Shell Part II, Phil. Trans. Roy. Soc. London (A) 221, 295-387 (1920).

3. K. L. Nielsen, J. L. Synge, On the Motion of a Spinning Shell, Q. A. M. Vol. IV, No. 3 (1946).

4. C. G. Maple, J. L. Synge, Aerodynamic Symmetry of Projectiles Q. A. M. Vol. VI, No. 4 (1949).

5. J. L. Kelley, E. J. McShane, On the Motion of a Projectile with Small or Slowly Changing Yaw, BRL Report 446 (1944).

6. E. J. McShane, J. L. Kelley, F. Reno, Exterior Ballistics, University of Denver Press, (1953).

7. R. H. Kent, An Elementary Treatment of the Motion of a Spinning Projectile about it's Center of Gravity, BRL Report 85 (1937), and revision with E. J. McShane, BRL Report 459 (1944).

8. A. C. Charters, R. N. Thomas, The Aerodynamic Performance of Small Spheres from Subsonic to High Supersonic Velocities, JAS, Vol 12, No. 4, (1945).

9. A. C. Charters, Some Ballistic Contributions to Aerodynamics, JAS, Vol. 14, No. 3, (1947).

10. R. A. Turetsky, Reduction of Spark Range Data, BRL Report 684 (1948).

11. A. C. Charters, R. H. Kent, The Relation Between the Skin Friction Drag and the Spin Reducing Torque, BRL Report 287 (1942).

12. R. N. Thomas, Some Comments on the Form of the Drag Coefficient at Supersonic Velocity, BRL Report 542, (1945).

13. A. C. Charters, R. A. Turetsky, Determination of Base Pressure from Free-Flight Data, BRL Report 653, (1948).

14. B. G. Karpov, The Accuracy of Drag Measurements as a Function of Number and Distribution of Timing Stations, BRL Report 658 (1948).

15. R. A. Turetsky, Cone Cylinder Model E12M3, BRL Memorandum Report 435 (1946).

16. S. J. Zaroodny, On Jump Due to Muzzle Disturbances, BRL Report 703 (1949).

17. R. E. Bolz, J. D. Nicolaides, A Method of Determining Aerodynamic Coefficients from Supersonic Free-Flight Test of a Rolling Missile, BRL Report 711 (1949).

18. R. A. Turetsky, Dynamic Stability of Spinner Rocket Model Fired in the Free-Flight Aerodynamics Range, BRL Memorandum Report 526 (1950).

19. A. C. Charters, H. Stein, The Drag of Projectiles with Truncated Cone Headshapes, BRL Report 624 (1952).

20. L. E. Schmidt, Aerodynamic Coefficients Determined from the Swerve Reduction, BRL Memorandum Report 599 (1952).

21. L. C. MacAllister, Drag Properties and Gun Launching Long Arrow Projectiles, BRL Memorandum Report 600 (1952).

22. C. H. Murphy, Analogue Computor Determination of Certain Aerodynamic Coefficients, BRL Report 807 (1952).

23. C. H. Murphy, Comment on Kelley-McShane Solution of Yawing Motion of Missiles, BRL Technical Note 703 (1952).

24. C. H. Murphy, Effect of Gravity on Yawing Motion, BRL Technical Note 713 (1952).

25. C. H. Murphy, Effect of Symmetry on the Linearized Force System, BRL Technical Note 743 (1952).

26. J. D. Nicolaides, Variation of the Aerodynamic Force and Moment Coefficients With Reference Position, BRL Technical Note 746 (1952).

27. J. D. Nicolaides, On the Free-Flight Motion of Missiles Having Slight Configurational Asymmetries, Institute of Aeronautical Sciences, Preprint No. 395 and BRL Report 858 (1953).

28. C. H. Murphy, On the Stability Criteria of the Kelley-McShane Linearized Theory of Yawing Motion, BRL Report 853 (1953).

29. J. C. Martin, On Magnus Effect Caused by the Boundary Layer Displacement Thickness on Bodies of Revolution at Small Angle of Attack, BRL Report 870 (1953).

30. W. K. Rogers, The Transonic Free-Flight Range, BRL Report 849 (1953).

31. E. R. Van Driest, Turbulent Boundary Layer for Compressible Fluids on an Insulated Flat Plate, N.A. Aviation Rep. AL 958, (1949).

32. E. R. Van Driest, Turbulent Boundary-Layer in Compressible Fluids, J.A.S. Vol. 18, No. 3, p. 145, March 1951.

33. M. Tucker, Approximate Calculation of Turbulent Boundary-Layer Development in Compressible Flow, N.A.C.A. Technical Note 2337 (1951)

34. M. W. Rubesin, R. C. Maydew, and S. A. Varga, An Analytic and Experimental Investigation of the Skin Friction of the Turbulent Boundary-Layer at Supersonic Speeds, N.A.C.A. Technical Note 2305 (1950).

35. W. Dorrance, Nonsteady Supersonic Flow About Pointed Bodies of Revolution, J.A.S. Vol. 18, No. 8, p. 505, Aug. 1951.

36. H. R. Kelley, The Estimation of Normal Force and Pitching Moment Coefficients For Blunt Base Bodies of Revolution at Large Angles of Attack. N.O.T.S. TM - 998 (1953).

37. L. E. Schmidt, C. H. Murphy, The Effect of Spin on Aerodynamic Properties of Bodies of Revolution, BRL Memorandum Report 715 (1953).

TABLE OF SYMBOLS AND COEFFICIENTS[1]

A	Axial moment of inertia
A_N	Axial moment of inertia of the nose
B	Transverse moment of inertia
C	Empirical constant defined by $K_H = C(L - \gamma_c)^2$
C_{D_C}	Two dimensional cylinder drag coefficient
CP_F	Magnus force center of pressure
CP_N	Normal force center of pressure
D	$J_D - k_1^{-2} J_A$
(F_1, F_2, F_3)	Aerodynamic force
G	$\gamma' - \left[(J_D - k_2^{-2} J_H) + i\bar{\nu}\right] \gamma$
H	$J_N - 2J_D + k_2^{-2} J_H$
J_i	$\frac{\rho d^3}{m} K_i$
$K_A(C_{\ell_p})$	Spin deceleration moment coefficient
$K_D(C_D)$	Drag coefficient
K_{DA}	Axial drag coefficient
K_{DB}	Base drag coefficient
K_{DH}	Head drag coefficient
K_{DSF}	Skin friction drag coefficient
$K_F(C_{N_{p\alpha}})$	Magnus force coefficient
$\hat{K}_F$	Slender body Magnus force coefficient

1. The symbols which appear only in Appendix B are omitted from this table.

$K_H(C_{Mq} + C_{M\dot{\alpha}})$	Damping moment coefficient
$\left[K_H\right]$	$K_H^* - qK_M^*$
K_L	Lift force coefficient
$K_M(C_{M\alpha})$	Overturning (restoring) moment coefficient
$K_N(C_{N\alpha})$	Normal force coefficient
$\hat{K}_N$	Slender body normal force coefficient
$K_S(C_{N\dot{\alpha}} + C_{Nq})$	Damping force coefficient
$K_T(C_{M_{p\alpha}})$	Magnus moment coefficient
K_{XF}	Magnus cross force coefficient
K_{XT}	Magnus cross moment coefficient
K_{i_o}	Zero-yaw coefficient
$K_{i_{\delta^2}}$	Coefficient of yaw squared term
K_1, K_2	Complex constants in yaw equation
L	Length of projectile
L_n	Length of nose which is uneffective in Martin's theory
$\hat{L}$	Equivalent cylinder length in Martin's theory
M	Mach number
M	$k_2^{-2} J_M$
(M_1, M_2, M_3)	Aerodynamic moment
$N - N_T$	Number of yaw stations and timing stations
$O - O^*$	Shift in c.m.

P	Constant term in the swerve equation
Q	Coefficient of linear term in the swerve equation
$Q = \sqrt{1 + K_D M^2}$	The "Q"-function
R_d	The Reynolds number based on diameter
R_i	The coefficients of the exponential terms in the swerve equation
R_{ij}	Constants defined by $R_i = R_{i1} + iR_{i2}$
$(R_i)_L$	Contribution of the lift force to the swerve
$(R_i)_F$	Contribution of the Magnus force to the swerve
T	$J_L - k_1^{-2} J_T$
a	The constant term in the "Q" function
a_i	The coefficients in the polynomial expression for t
a_{ij}	The coefficient of $J_N - J_D$ in R_{ij}
b	The coefficient of the linear term in the "Q" function
b_i	The coefficients in the polynomial expression for θ
b_{ij}	The coefficient of J_F in R_{ij}
c	Empirical constant defined by $K_F = c(1 - .14M)L^{\frac{9}{5}} R_d^{-\frac{1}{5}}$
c_{ij}	The coefficient of J_S in R_{ij}
c.m.	Center of mass in calibers from the nose
d	Diameter
d_{ij}	The coefficient of J_{XF} in R_{ij}
g	Acceleration due to gravity
(g_1, g_2, g_3)	Vector acceleration due to gravity

h	$K_N - K_D + k_2^{-2}K_H - k_1^{-2}K_A$
$k_1^{-2} = \frac{md^2}{A}$	k_1 is the axial radius of gyration in calibers
$k_2^{-2} = \frac{md^2}{B}$	k_2 is the transverse radius of gyration in calibers
ℓ_B	One-half length of center cylinder in bimetal design
ℓ_c	Length of cylinder
$\ell_N = \frac{4}{\pi}$ (volume of nose)	Equivalent length of nose
m	Mass
n	The reciprocal of the gun twist
$p = \int_{t_0}^{t} \frac{u_1}{d}\, dt$	Independent variable
p_B	Base pressure
p_0	Free stream pressure
q	$O - O^*$ (distance from centroid in definition of K_H*
r	Distance in calibers from the nose to the center of mass
r_c	Distance in calibers from the nose to the centroid
s	Stability factor
$\bar{s}$	Dynamic stability factor
t	Time
$u = (u_1, u_2, u_3)$	Velocity vector
v	Volume
x	Lateral displacement
y	Vertical displacement
α	Assigned lower limit of α_i

α_i	Yaw damping rates
γ	Ratio of specific heat of air at constant pressure to that at constant volume
Υ	$\left[(g_2 - g_1 \lambda_2) + i(g_3 - g_1 \lambda_3)\right] d/u_1^2$
$\delta = \lvert\lambda\rvert$	Magnitude of yaw angle
$\overline{\delta^2}$	Mean squared yaw
δ^*	Boundary layer displacement thickness
ϵ_1	Perturbation term in solution of yaw differential equation
ϵ_{Ki}	Standard error in ballistic coefficient
θ	Roll angle
$\lambda = \frac{(u_2 + iu_3)}{u_1}$	Complex yaw
λ_R	Yaw of repose
$\mu = \frac{(\omega_2 + i\,\omega_3)d}{u_1}$	Complex angular velocity
$\nu = \frac{\omega_1 d}{u_1}$	Spin in radians per caliber
$\overline{\nu}$	$\frac{A}{B}\ \nu$
ρ	Density of air
ρ_i	Density of the material
ϕ_i'	Yaw turning rates
$(\omega_1, \omega_2, \omega_3)$	Angular velocity of the missile
$(\ )'$	Primes denote differentiation with respect to p
$\frac{\partial K_{DSF}}{\partial L}$	Partial derivative of skin friction drag coefficient with respect to length
$\lvert\ \rvert$	Bars denote absolute value

APPENDIX A: SUMMARY OF THEORETICAL RELATIONS AND SPARK RANGE TECHNIQUE

In the bibliography the classical publications are listed and a fairly complete list of BRL publications which would have a bearing on this report is provided. Most of the theoretical relations used here are taken from [24] or [28]. The data reduction technique is described in [10] or in the Kopal report mentioned in the introduction. In this appendix we will state but not prove the relations referred to in the body of the report.[1] Although these relations will be in terms of the ballistic K's they can be easily converted to the aerodynamic C's where necessary by use of Appendix B.

We first define a right handed orthogonal coordinate system with axes numbered 1, 2, 3 moving with the missile and so orientated that the 1 axis always points along the missile's axis and the 2 axis lies in the horizontal plane and points to the right. The linear velocity of the center of mass and angular velocity of the missile are expressed in this coordinate system as the vectors (u_1, u_2, u_3) and $(\omega_1, \omega_2, \omega_3)$ respectively. Employing the convenient representation of complex variables the basic Kelley-McShane linear force system for a missile possessing an angle of rotational symmetry less than 120° and a plane of mirror symmetry is defined by the following equations:

$$(A1) \quad F_1 = -\rho d^2 u_1^2 K_{DA} \quad ; \quad F_T = -\rho d^2 u_1^2 K_D$$

$$(A2) \quad F_2 + iF_3 = \rho d^2 u_1^2 \left[(-K_N + i\nu K_F)\lambda + (\nu K_{XF} + iK_S)\mu \right]$$

$$(A3) \quad M_1 = -\rho d^3 u_1^2 \nu K_A$$

$$(A4) \quad M_2 + iM_3 = \rho d^3 u_1^2 \left[(-\nu K_T - iK_M)\lambda + (-K_H + i\nu K_{XT})\mu \right]$$

where

(F_1, F_2, F_3) is the aerodynamic force vector

F_T is component of aerodynamic force vector directed along the trajectory

(M_1, M_2, M_3) is the aerodynamic moment vector

ρ is the density of air

d is the diameter of the model

---

1. Although all of the relations stated are true for all missiles possessing the proper symmetry required for (A1) - (A4), some of the remarks on range technique refer only to spinning bodies of revolution.

$\lambda = \dfrac{u_2 + iu_3}{u_1}$ is the complex yaw

$\nu = \dfrac{\omega_1 d}{u_1}$ is nondimensional spin

$\mu = \dfrac{(\omega_2 + i\omega_3)d}{u_1}$ is complex angular velocity

K_D Drag Force Coefficient[1]

K_{DA} Axial Drag Force Coefficient

K_A Spin Deceleration Moment Coefficient

K_N Normal Force Coefficient

K_F Magnus Force Coefficient

K_{XF} Cross Spin Magnus Force Coefficient

K_S Damping Force Coefficient

K_T Magnus Moment Coefficient

K_M Overturning Moment Coefficient

K_H Damping Moment Coefficient

K_{XT} Cross Spin Magnus Moment Coefficient

Since the moments are defined with respect to center of mass and λ is defined from the motion of the center of mass, these ballistic K's are functions of center of mass location. Since we require symmetric

---

1. For zero cross spin it can be easily shown that $K_D = K_{DA} \cos\delta + K_N \delta \sin\delta \doteq K_{DA} + \left[K_N - \dfrac{K_{DA}}{2}\right] \delta^2 \doteq K_{DA}$ where $\delta = |\lambda|$

mass distribution, all c.m.'s are on the axis. The explicit form of these functions is:

(A5.1) $K_D^* = K_D$

(A5.2) $K_N^* = K_N$

(A5.3) $K_F^* = K_F$

(A5.4) $K_S^* = K_S + qK_N$

(A5.5) $K_{XF}^* = K_{XF} + qK_F$

(A5.6) $K_A^* = K_A$

(A5.7) $K_M^* = K_M + qK_N$

(A5.8) $K_T^* = K_T + qK_F$

(A5.9) $K_H^* = K_H + q(K_S + K_M) + q^2K_N$

(A5.10) $K_{XT}^* = K_{XT} + q(K_{XF} + K_T) + q^2K_F$

where the starred quantities correspond to the center mass located at point O* and the unstarred quantities to center of mass at O. q is the axial distance from O to O* in calibers[1] and is considered positive when measured toward the base from the nose.

Placing these definitions in the equations of motion we obtain the following equations for the axial and yawing motion for a flat trajectory:

(A6) $\dfrac{u_1'}{u_1} = -J_D$

(A7) $\nu' = D\nu$

(A8) $\lambda'' + (H - i\bar{\nu})\lambda' + (-M - i\bar{\nu}T)\lambda = G$

where primes denote differentiation with respect to nondimensional axial arc length $p = \int_{t_o}^{t} \dfrac{u_1 dt}{d}$ and t is time.[2]

$$J_i = \frac{\rho d^3}{m} K_i$$

$$D = J_D - k_1^{-2} J_A$$

$k_1^{-2} = \dfrac{md^2}{A}$ (k_1 is axial radius of gyration in calibers)

A is axial moment of inertia

m is the mass

1. A caliber is a unit of length equal to the missile's diameter.
2. Equation (A8) is based on the size assumption or convention that J^2 terms may be omitted in comparison with J terms.

$$H = J_N - 2J_D + k_2^{-2} J_H$$

$$k_2^{-2} = \frac{md^2}{B}$$ (k_2 is transverse radius of gyration in calibers)

B is the transverse moment of inertia

$$\bar{\nu} = \frac{A}{B} \nu$$

$$M = k_2^{-2} (J_M + \nu^2 k_1^2 J_F) \doteq k_2^{-2} J_M$$

$$T = J_N - J_D - k_1^{-2} J_T$$

$$G = \gamma' - \left[(J_D - k_2^{-2} J_H) + i\bar{\nu}\right] \gamma$$

$$\gamma = \frac{\left[(g_2 - g_1\lambda_2) + i(g_3 - g_1\lambda_3)\right] d}{u_1^2}$$

(g_1, g_2, g_3) is the vector acceleration due to gravity

$$\lambda_2 + i\lambda_3 = \lambda$$

The solution to the equation of yawing motion can be written in the form:

$$\text{(A9)} \quad \lambda = K_1 e^{(-\alpha_1 + i\phi_1')p} + K_2 e^{(-\alpha_2 + i\phi_2')p} + \lambda_R$$

where

$$|\phi_1'| \gtrless |\phi_2'|$$

K_1, K_2 are complex constants depending on initial conditions

$$\lambda_R \doteq - \frac{g d\bar{\nu}}{u_1^2 M}$$ (yaw of repose)

g is acceleration due to gravity

α_i are constants and ϕ_i' are linear functions of p

The exponents of (A9) may be related to the coefficients of equation (A8) by:

(A10) $\bar{\nu} = \phi_1' + \phi_2'$

(A11) $H = (\alpha_1 + \alpha_2) - D\varepsilon_1$

(A12) $M = \phi_1' \cdot \phi_2' - \alpha_1\alpha_2 + \frac{D}{2}\varepsilon_1\left[\alpha_1 + \alpha_2 - \frac{D}{2}\varepsilon_1\right]$

(A13) $T = -1/2 \left[(\alpha_1 - \alpha_2)\left(\frac{\phi_1' - \phi_2'}{\phi_1' + \phi_2'}\right) - H - D\right]$

(A14) $D = \frac{\phi_1^n + \phi_2^n}{\phi_1' + \phi_2'}$

where a very good approximation to the perturbation term ε_1 is $\left[\frac{\phi_1' + \phi_2'}{\phi_1' - \phi_2'}\right]^2$

A missile is said to be statically stable if $K_M \leqq 0$. A statically unstable missile is said to be gyroscopically stable if $s = \frac{\bar{\nu}^2}{4M} \geqq 1$. A missile is dynamically stable if the yaw described by the homogeneous solution to (A8) does not increase. For a statically unstable missile the exponents α_1 and α_2 are greater than or equal to an assigned value α if

(A15) $H + D - \alpha > 0$;

(A16) $s \geqq \frac{1}{\bar{s}(2 - \bar{s})}$ and

(A17) $0 < \bar{s} < 2$

where $\bar{s}(\alpha) = \frac{2T - \alpha}{H + D - \alpha}$ is the generalized dynamic stability factor.

If $\alpha = 0$, $\bar{s}$ becomes the dynamic stability factor $\bar{s}(0)$ and (A15) - (A17) become conditions for dynamic stability. If $\bar{s}(0)$ does not satisfy (A17), a statically unstable missile can never be dynamically stabilized by spin[1].

1. For a statically stable missile (A15) and (A16) apply when $\bar{s}$ is outside the interval $[0, 2]$ while only (A15) is needed when $\bar{s}$ is inside.

If the position of the missile is calculated from the equations of motion, and the p axis is taken to be down range in the horizontal plane, the y axis pointing up, and the x axis determined by the right hand rule, we have the relation

$$(A18)\quad x + iy = P + Qp + R_1K_1\, e^{(-\alpha_1 + i\phi_1')p} + R_2K_2\, e^{(-\alpha_2 + i\phi_2')p}$$

$$+ \iint \lambda_R(J_N - J_D + i\nu\, J_F)\,dp\,dp - \iint \frac{igd}{u^2}\,dp\,dp$$

where

P and Q are complex constants determined by initial conditions

x and y are in calibers

$$R_i = R_{i1} + iR_{i2}$$

$$R_{i1} = a_{i1}\,(J_N - J_D) + b_{i1}\,J_F + c_{i1}\,J_S + d_{i1}\,J_{XF}$$

$$= \frac{(\phi_i'^2 - \alpha_i^2)}{(\phi_i'^2 + \alpha_i^2)^2}\,(J_N - J_D) + \frac{2\nu\,\alpha_i\,\phi_i'}{(\phi_i'^2 + \alpha_i^2)^2}\,J_F$$

$$+ \frac{\alpha_i}{(\phi_i'^2 + \alpha_i^2)}\,J_S + \frac{\nu\phi_i'}{(\phi_i'^2 + \alpha_i^2)}\,J_{XF}$$

$$R_{i2} = a_{i2}(J_N - J_D) + b_{i2}\,J_F + c_{i2}\,J_S + d_{i2}\,J_{XF}.$$

$$= \frac{2\phi_i'\,\alpha_i}{(\phi_i'^2 + \alpha_i^2)^2}\,(J_N - J_D) + \frac{\nu(\phi_i'^2 - \alpha_i^2)}{(\phi_i'^2 + \alpha_i^2)^2}\,J_F$$

$$+ \frac{\phi_i'}{(\phi_i'^2 + \alpha_i^2)}\,J_S - \frac{\alpha_i\,\nu}{(\phi_i'^2 + \alpha_i^2)}\,J_{XF}$$

The first integral is the displacement due to yaw of repose and can usually be estimated to a sufficient accuracy for range work. The real part of this integral is called the "drift". The second integral is, of course, the gravity drop. The expression $J_N - J_D$ can be replaced by J_L, the lift force coefficient.

On the BRL Spark Photography Range the drag coefficient is found by means of up to twelve time-distance measurements. The distance error is less than .001 feet and the least count for the time is 5/8 of a microsecond. The data are usually fitted to a cubic in distance.

$$(A19) \quad t = a_o + a_1 p + a_2 p^2 + a_3 p^3$$

where t is time

The velocity u at point p is then given by

$$(A20) \quad \frac{u}{d} = \frac{1}{a_1 + 2\,a_2 p + 3\,a_3 p^2}$$

and J_D at point p can then be computed from (A6).

$$(A21) \quad J_D = \frac{2a_2 + 6a_3 p}{a_1 + 2a_2 p + 3a_3 p^2} \,.$$

u and J_D are usually evaluated at the center of the data. The temperature and pressure are measured before each firing, thereby providing the velocity of sound and density of air. From this the Mach number and the density factor $\frac{\rho d^3}{m}$ may be computed. (m, A, B, and center of mass location are precisely measured for each model before firing).

D can be directly determined by measuring the spatial location at each station of two pins placed in the base of the model. This then determines the roll angle θ as a function of position, p, on the range. These data are then fitted to a cubic polynomial

$$(A22) \quad \theta = b_o + b_1 p + b_2 p^2 + b_3 p^3$$

From (A7) we have:

$$(A23) \quad D = \frac{2b_2 + 6b_3 p}{b_1 + 2b_2 p + 3a_3 p_1^2} \,.$$

From (A23) and (A21) we can then obtain J_A.

The two components of the yaw of the missile are usually measured to an accuracy of .001 radians. They are then fitted by a combination graphical and analytical technique to equation (A9). From the coefficients of this fit by means of (A11) - (A14) we can obtain J_M, H, T, and a relatively poor second determination of D. The spatial position

of the center of mass is now measured to an accuracy of .001 feet and fitted to equation (A18). Of the form R_{ij} usually, however, only R_{21} is well determined. Fortunately $J_N - J_D$ is the principal constituent for most firings and can then be determined. This plus the values of J_D, H, and T then provide us with J_H and J_T. In certain cases R_{22} can be determined, and from this follow values of J_F. By firing different center of mass positions, equations (A5) then provide us with J_S, J_F and a second determination of J_N.

In summary we see that the firing of a single model with satisfactory initial yawing motion (large enough to measure and small enough to be linear) and satisfactory swerving motion[1] will provide values K_D, K_A, K_M, K_N, K_T, K_H, and possibly K_F at a given Mach number. Firings of identical models with different center of mass positions at the same Mach number then yield additional values of K_N, K_F, and K_S.

---

1. It can easily be shown that the lift force contribution to the slow swerve arm is $(R_2)_L = |K_2|\sqrt{a_{21}^2 + a_{22}^2}\, J_L$ and the corresponding contribution from the Magnus force is $(R_2)_F = |K_2|\sqrt{b_{21}^2 + b_{22}^2}\, J_F$. For most rounds J_S and J_{XF} may be omitted, $a_{22}^2 < a_{21}^2$, and $b_{21} J_F \ll a_{21} J_L$

   Hence $(R_2)_L \sim |K_2|\,|R_{21}|$. Swerving motion is satisfactory for K_N when $(R_2)_L$ is more than six times the experimental accuracy. Since our Magnus force measures were limited in number, K_F values are considered when $(R_2)_F$ is twice the experimental accuracy.

APPENDIX B: CONVERSION OF THE BALLISTIC COEFFICIENTS TO AERODYNAMIC COEFFICIENTS

The work of this report has been done in terms of the ballistic K's which are little known outside the field of ballistics and may be quite confusing to an aerodynamicist who does his dynamic stability analyses in terms of the aerodynamic C's. It is therefore worthwhile to express the results of this report in terms of these symbols. This effort is handicapped however, by the three facts:

1. The missiles usually treated in ballistics have a rotation symmetry which results in pairs of aerodynamic coefficients being equal and hence corresponding to only one ballistic coefficient.

2. In ballistics the missiles usually have a high rate of spin and Magnus effects have to be considered to which there are no corresponding aerodynamic coefficients.

3. Terms involving the rate of change of angle of attack appear in most aerodynamic stability analysis while no such terms appear in the usual ballistic force system.

The axial components of the aerodynamic force and moment are usually defined in aerodynamic nomenclature as:

$$X = -\tfrac{1}{2}\rho V^2 S C_D$$

$$L = -\tfrac{1}{2}\rho V^2 S b\left(\frac{pb}{2V}\right) C_{\ell_p} \tag{B1}$$

where ρ is air density

V is axial velocity

S is a reference area

b is the wing span

From this we see that

$$K_D = \tfrac{1}{2} S/d^2 C_D$$

$$K_A = -\tfrac{1}{4}\left(Sb^2/d^4\right) C_{\ell_p} \tag{B2}$$

$$\nu = \frac{2d}{b}\left(pb/2V\right)$$

If the transverse components of the aerodynamic force and moment are assumed to be linear functions of yaw, change in yaw, and angular velocity, and Magnus coupling is introduced, we have the following definitions:

$$Y = (1/2\ \rho\ V^2\ S)\left\{\left[C_{Y_\beta}\ \beta + C_{Y_r}\ (\frac{br}{2V}) + C_{Y_{\dot\beta}}\ (\frac{b\dot\beta}{2V})\right] + \left[C_{Y_{p\alpha}}\ \alpha + C_{Y_{pq}}\ (\frac{cq}{2V}) + C_{Y_{p\dot\alpha}}\ (\frac{c\dot\alpha}{2V})\right]\ (\frac{pb}{2V})\right\}$$

$$Z = (1/2\ \rho\ V^2\ S)\left\{\left[C_{Z_\alpha}\ \alpha + C_{Z_q}\ (\frac{cq}{2V}) + C_{Z_{\dot\alpha}}\ (\frac{c\dot\alpha}{2V})\right] + \left[C_{Z_{p\beta}}\ \beta + C_{Z_{pr}}\ (\frac{br}{2B}) + C_{Z_{p\dot\beta}}\ (\frac{b\dot\beta}{2V})\right]\ (\frac{pb}{2V})\right\}$$

(B3)
$$M = (1/2\ \rho\ V^2\ S\ c)\left\{\left[C_{m_\alpha}\ \alpha + C_{m_q}\ (\frac{cq}{2V}) + C_{m_{\dot\alpha}}\ (\frac{c\dot\alpha}{2V})\right] + \left[C_{m_{p\beta}}\ \beta + C_{m_{pr}}\ (\frac{br}{2V}) + C_{m_{p\dot\beta}}\ (\frac{b\dot\beta}{2V})\right](\frac{pb}{2V})\right\}$$

$$N = (1/2\ \rho\ V^2\ S\ b)\left\{\left[C_{n_\beta}\ \beta + C_{n_r}\ (\frac{br}{2V}) + C_{n_{\dot\beta}}\ (\frac{b\dot\beta}{2V})\right] + \left[C_{n_{p\alpha}}\ \alpha + C_{n_{pq}}\ (\frac{cq}{2V}) + C_{n_{p\dot\alpha}}\ (\frac{c\dot\alpha}{2V})\right]\ (\frac{pb}{2V})\right\}$$

where c is the wing chord and the angles α, β and angular velocities $\dot\alpha$, $\dot\beta$, q and ν are those defined in the standard aerodynamic nomenclature.

If the missile is assumed to possess trigonal or greater rotational symmetry, it follows from [4] [6] [25] [27]

$$C_{Y_\beta} = C_{Z_\alpha} \equiv C_{N_\alpha} \qquad -C_{Y_{p\alpha}} = C_{Z_{p\beta}} \equiv C_{N_{p\alpha}}$$

$$-C_{Y_r}\frac{b}{c} = C_{Z_q} \equiv C_{N_q} \qquad C_{Y_{pq}} = C_{Z_{pr}}\frac{b}{c} \equiv C_{N_{pq}}$$

$$C_{Y_{\dot\beta}}\frac{b}{c} = C_{Z_{\dot\alpha}} \equiv C_{N_{\dot\alpha}} \qquad C_{Y_{p\dot\alpha}} = C_{Z_{p\dot\beta}}(\frac{b}{c}) \equiv C_{N_{p\dot\alpha}}$$

(B4)
$$-C_{m_\alpha} = C_{n_\beta}\left(\frac{b}{c}\right) = -C_{M_\alpha} \qquad C_{m_{p\beta}} = C_{n_{p\alpha}}\left(\frac{b}{c}\right) = C_{M_{p\alpha}}$$

$$C_{m_q} = C_{n_r}\left(\frac{b}{c}\right)^2 = C_{M_q} \qquad -C_{m_{pr}}\left(\frac{b}{c}\right) = C_{n_{pq}}\left(\frac{b}{c}\right) = -C_{M_{pq}}$$

$$-C_{m_{\dot\alpha}} = C_{n_{\dot\beta}}\left(\frac{b}{c}\right)^2 = -C_{M_{\dot\alpha}} \qquad C_{m_{p\dot\beta}}\left(\frac{b}{c}\right) = C_{n_{p\dot\alpha}}\left(\frac{b}{c}\right) = C_{M_{p\dot\alpha}}$$

The third set of symbols is introduced in order to emphasize the existence of symmetry and will be employed throughout the remainder of this appendix. If we insert these symbols into (B3), multiply the second and fourth equations by i and add to the first and third respectively these results:

$$Y + iZ = (1/2\ \rho\ V^2\ S)\left\{\left[C_{N_\alpha} + i\ \left(\frac{pb}{2V}\right) C_{N_{p\alpha}}\right](\beta + i\ \alpha) + \left[\left(\frac{pb}{2V}\right) C_{N_{pq}} + i\ C_{N_q}\right]\frac{(cq + i\ cr)}{2V} + \left[C_{N_{\dot\alpha}} + i\ \frac{pb}{2V}\ C_{N_{p\dot\alpha}}\right]\frac{(c\dot\beta + i\ c\dot\alpha)}{2V}\right\}$$

(B5)
$$M + iN = (1/2\ \rho\ V^2\ c\ S)\left\{\left[\left(\frac{pb}{2V}\right) C_{M_{p\alpha}} - i\ C_{M_\alpha}\right](\beta + i\alpha) + \left[C_{M_q} - i\ \left(\frac{pb}{2V}\right) C_{M_{pq}}\right]\frac{(cq + i\ cr)}{2V} + \left[\left(\frac{pb}{2V}\right) C_{M_{p\dot\alpha}} - i\ C_{M_{\dot\alpha}}\right]\frac{(c\dot\beta + i\ c\dot\alpha}{2V}\right\}$$

If equation (B5) is compared with equations (A2) and (A4), the Magnus and non-Magnus static coefficients are easily related.

$$K_N = -\ 1/2\ S/d^2\ C_{N_\alpha}$$

$$K_M = 1/2\ Sc/d^3\ C_{M_\alpha}$$

$$K_F = 1/4\ Sb/d^3\ C_{N_{p\alpha}}$$

$$K_T = -\ 1/4\ Scb/d^4\ C_{M_{p\alpha}}$$

The relationships between the remaining dynamic coefficients is somewhat more complicated. Fortunately it can easily be shown that the remaining Magnus coefficients are lost in the differential equations of yawing motion due to the J^2 convention. It therefore, remains only to connect two ballistic coefficients, K_S and K_H, with four aerodynamic coefficients, C_{N_q}, $C_{N_{\dot{\alpha}}}$, C_{M_q} and $C_{M_{\dot{\alpha}}}$.

In order to do this we need only to consider the purpose of this work, namely to state the results of this report in aerodynamic nomenclature. Since this report is concerned with stability, the only contribution of the aerodynamic coefficients is how they appear in the basic differential equations. This means that in order to obtain the partner of K_H we see what coefficient appears in the corresponding point of the differential equation similar to (1) which is based on the aerodynamic force system (see [27] for example). By this tactic we have:

$$(B7) \qquad K_H \rightarrow -1/4 \frac{c^2 S}{d^4} \left(C_{M_q} + C_{M_{\dot{\alpha}}}\right)$$

Since the major function of K_S is its contribution to K_H when the center of mass is altered we have:

$$K_H \rightarrow 1/4 \frac{cS}{d^3} \left(C_{N_q} + C_{N_{\dot{\alpha}}}\right)$$

Note: The method of obtaining (B7) and (B8) is not too desirable. It would, of course, be more satisfying to enlarge the ballistic force system so that there would exist a one-to-one correspondence. It also should be noted that (B7) follows from a comparison of the homogeneous equations. In the yaw of repose, equation (A9), K_H should be replaced by $-1/4 \frac{c^2 S}{d^4} C_{M_q}$.

By use of (B2), (B6), (B7) and (B8) it is now possible to convert our symbols. We will merely tabulate the results.[1] (K_L will be replaced by $K_N - K_D$ for this purpose.)

$$H = \frac{-\rho d S}{2m} \left[C_{N_\alpha} + 2 C_D + 1/2 \, k_2^{-2} \left(\frac{c}{d}\right)^2 \left(C_{M_q} + C_{M_{\dot{\alpha}}}\right) \right]$$

$$\bar{\nu} = \frac{2d}{b} \left(\frac{pd}{2V}\right) \frac{A}{B}$$

$$M = k_2^{-2} \frac{\rho c S}{2m} C_{M_\alpha}$$

1. In order to avoid confusion α^* in $\bar{s}$ (α^*) will be replaced by γ^*.

(B9) $$T = \frac{-\rho dS}{2m}\left[C_{N_\alpha} + C_D - k_1^{-2}\left(\frac{cb}{2d^2}\right) C_{M_{p\alpha}}\right]$$

$$D = \frac{\rho dS}{2m}\left[C_D + k_1^{-2}\ \frac{b^2}{2d^2}\ C_{\ell_p}\right]$$

$$s = \frac{A^2 p^2}{4B\ (1/2\ V^2\ \rho\ Sc C_{M_\alpha})}$$

$$\bar{s} = (\gamma^*) = \frac{2\left[C_{N_\alpha} + C_D - k_1^{-2}\left(\frac{cb}{2d}\right)_2 C_{M_{p\alpha}}\right] + \gamma^*}{C_{N_\alpha} + C_D + 1/2\ k_2^{-2}\left(\frac{c}{d}\right)^2 (C_{M_q} + C_{M_{\dot\alpha}}) - k_1^{-2}\ \frac{b^2}{2d^2}\ C_{\ell_p} + \gamma^*}$$

For bodies of revolution if S is the maximum cross-sectional area[1]

$$\frac{b}{d} = 1;\ \frac{S}{d^2} = \frac{\pi}{4};\quad \frac{c}{d} = 1$$

$$\therefore K_D = \frac{\pi}{8}\ C_D;\ K_A = -\frac{\pi}{8}\ C_{\ell_p}$$

$$K_N = -\frac{\pi}{8}\ C_{N_\alpha};\ K_M = \frac{\pi}{8}\ C_{M_\alpha}$$

(B10) $$K_F = \frac{\pi}{16}\ C_{N_{p\alpha}};\ K_T = -\frac{\pi}{16}\ C_{M_{p\alpha}}$$

$$K_S \to \frac{\pi}{16}\ (C_{N_q} + C_{N_{\dot\alpha}});\ K_H \to -\frac{\pi}{16}\ (C_{M_q} + C_{M_{\dot\alpha}})$$

$$s = \frac{2\ A^2 p^2}{\pi\ B(\rho v^2 d^3\ C_{M_\alpha})};\quad \bar{s} = \frac{2(C_{N_\alpha} + C_D - \frac{1}{2}k_1^{-2}\ C_{M_{p\alpha}}) + \gamma^*}{C_{N_\alpha} + C_D + \frac{1}{2}k_2^{-2}\ (C_{M_q} + C_{M_{\dot\alpha}}) - \frac{1}{2}k_1^{-2} C_{\ell_p} + \gamma^*}$$

---

1. Some authors prefer $\frac{c}{d} = L$ where L is the model length in calibers. This selection seems to complicate our equations unnecessarily.

APPENDIX C: TABLES OF DATA

In Table C-1, the physical characteristics of the twenty-seven model types are tabulated. The types are identified by two numerals separated by a letter. The first number gives the model length, the letter specifies whether the center of mass is forward (F), middle (M), or rear (R), and the second number identifies different types of the same length and center of mass location. The composition of each model is given by three letters which specify the metals used in the nose, center, and base sections respectively.

In Tables C-2, C-3, and C-4, the aerodynamic data for each round are given. The mean squared yaw, δ^2, is in square degrees and is effectively zero for those rounds where it is omitted. The drag coefficient, K_D, is tabulated for all rounds possessing over five timing stations, and the spin decelerating coefficient, K_A, for only rounds with pins. Values of K_M are given for those rounds for which both arms of their epicyclic yawing motion exceed .005 radians. Values of K_H and K_T are listed when both arms exceed .007 radians. In addition to the arm size requirement there must be fifteen observations and a favorable distribution of the observations on the epicycle. For some rounds it was possible to calculate K_M from the spin and the turning rate of one arm when only one arm exceeded .005 radians in size and the model possessed pins. K_N was calculated when the swerve associated with it, $(R_2)_L$, was greater than .06 inches. For those rounds which did not have K_D or K_N values, K_H and K_T were computed using values corresponding to the same type at the same Mach number.

The column marked $N - N_T$ gives the total number of observations and the number of time measurements. α_1 and α_2 are in 1/calibers and ν is in radians/caliber. ν may be converted to gun twist 1: n by the relation $n = \frac{2\pi}{\nu}$.

In Table C-5, the aerodynamic data for models possessing mean squared yaws of over thirty square degrees can be found. Table C-6 gives values of Magnus force coefficients measured from the swerving motion of those models whose Magnus swerving motion, $(R_2)_F$, is greater that .02 inches. Since the statistical error of the various ballistic coefficients was fairly uniform for model types possessing the same spin, only representative values are given in Table C-7. Finally the turning rates of the two epicycle arms are provided by Table C-8.

In conclusion the numbering system for the models should be described. This can be done by the following table for the five caliber length models.

5-01 to 5-29	Forward c.m.
5-31 to 5-59	Middle c.m.
5-61 to 5-89	Rear c.m.
5-91 to 5-99	Large yaw ($\overline{\delta^2} > 30^{o2}$)

The numbers for the 7 and 9 caliber length are divided in the same way.

TABLE C-1

PHYSICAL CONSTANTS OF MODELS[1]

Type	Composition	Roll Pins	C.M. from nose in calibers	m (grams)	k_1^{-2}	k_2^{-2}	Number fired	Data providing rounds
5 F1	BMM	No	2.375	117.0	9.69	.916	6	4
5 F2	BDD	No	2.517	128.5	9.43	.801	7	4
5 F3	BDD	Yes	2.501	113.4	9.58	.726	19	7
5 M1	BBB	No	3.032	202.3	8.70	.706	14	8
5 M2	SSS	No	3.034	189.1	8.65	.700	10	2
5 M3	DDD	No	3.028	67.4	8.60	.701	11	7
5 M4	DDD	Yes	3.024	67.2	8.60	.712	18	11
5 M5	BBB	Yes	3.032	200.2	8.60	.714	2	1
5 R1	MMB	No	3.740	101.2	8.74	.879	6	4
5 R2	DDB	No	3.526	127.0	8.49	.843	12	1
5 R3	DDB	Yes	3.538	114.2	8.58	.768	22	15
7 F1	BDD	No	3.248	176.3	8.98	.349	18	7
7 F2	BDD	Yes	3.251	173.8	8.96	.346	16	9
7 M1	DDD	No	4.036	102.7	8.38	.330	29	18
7 M2	DBD	Yes	4.037	148.2	7.57	.458	11	4
7 R1	DDB	No	4.804	188.3	8.32	.381	6	2
7 R2	DDB	Yes	4.812	174.4	8.36	.355	13	10
9 F1	BDD	No	3.988	241.7	8.67	.204	8	5
9 F2	BDD	Yes	3.996	234.2	8.68	.199	18	8
9 F3	BDD	Yes	3.996	235.0	8.69	.200	13	8
9 M1	DDD	No	5.047	137.4	8.27	.189	14	6
9 M2	DBD	No	5.050	201.0	7.60	.265	6	2
9 M3	DBD	Yes	5.053	198.0	7.51	.260	10	2
9 M4	TTT	Yes	5.038	220.7	8.29	.189	4	4
9 R1	DDB	No	6.074	250.0	8.25	.214	6	3
9 R2	DDB	Yes	5.884	304.3	8.24	.246	11	7
9 R3	DDB	Yes	5.885	302.1	8.23	.246	3	3
							313	162

B Bronze, D Dural, M Magnesium, S Steel, T Titanium Diameter = 20mm = .787".

1. Only those types which provided at least one piece of data are listed. Other types were built and fired which failed to provide any data due to faulty flight performance.

TABLE C-2a

DATA FOR FIVE-CALIBER MODELS

Model No.	Type	M	$\overline{\delta^2}$	K_D	K_A	K_M	K_N	$(R_2)_L$ (inches)	$N - N_T$
5-01	5 F1	1.247	15.1	.1845		0.900[1]	1.00	.26	21 - 7
5-02	5 F1	1.251	12.3			0.904[1]	0.98	.25	21 - 5
5-03	5 F1	1.256	15.7	.1831		0.948[1]	0.98	.26	21 - 8
5-04	5 F1	1.284	16.0			0.913[1]	1.00	.25	12 - 5
5-05	5 F2	1.285	11.4	.1788		1.038	1.02	.21	21 - 7
5-06	5 F2	1.523	4.7			1.003	1.14	.11	20 - 5
5-07	5 F2	1.754	2.4			0.913	1.20	.17	18 - 5
5-08	5 F2	1.783	2.4	.1452		0.916	1.14	.17	17 - 8
5-09	5 F3	1.805	4.4	.1476	.0046	0.883	1.13	.36	21 - 10
5-10	5 F3	1.845	13.2	.1531	.0047				15 - 6
5-11	5 F3	2.454	0.3	.1218	.0039	0.642[2]	1.22	.32	19 - 8
5-12	5 F3	2.480	4.2	.1237	.0038	0.654	1.27	.86	23 - 8
5-13	5 F3	2.498	1.5	.1193	.0040	0.665	1.30	.63	24 - 9
5-14	5 F3	2.542	3.3	.1189	.0037				13 - 6
5-15	5 F3	2.550	0.7	.1156	.0034				23 - 6
5-31	5 M4	1.230	26.5	.1918	.0053	1.525	0.97	.20	16 - 6
5-32	5 M1	1.288	1.9	.1659		1.572	0.99	.06	24 - 7
5-33	5 M1	1.303	2.3	.1659		1.560	1.00	.13	25 - 7
5-34[r]	5 M1	1.305	0.6	.1686					- 6
5-35	5 M1	1.316	2.3	.1676		1.551	0.98	.10	25 - 7
5-36	5 M1	1.324	1.6	.1675			1.00	.11	23 - 7
5-37	5 M4	1.330	16.7	.1798	.0050	1.553	0.99	.16	17 - 7
5-38[s]	5 M4	1.383	11.6	.1717	.0043	1.547	1.00	.18	21 - 9
5-39	5 M2	1.469		.1585					- 6

1. Note position of c.m. for this model type.

2. K_M determined from one arm and spin

r. Rough

s Smooth

TABLE C-2a

DATA FOR FIVE-CALIBER MODELS (CONTD)

Model No.	Type	M	$\overline{\delta^2}$	K_D	K_A	K_M	K_N	$(R_2)_L$ (inches)	$N - N_T$
5-40	5 M2	1.560		.1529					- 6
5-41	5 M3	1.684		.1481					- 7
5-42	5 M3	1.718	0.7	.1498					- 6
5-43	5 M3	1.730	1.0	.1512		1.487	1.16	.08	24 - 6
5-44	5 M3	1.768		.1486					- 6
5-45[r]	5 M3	1.797	1.5	.1458		1.495	1.22	.14	19 - 7
5-46[r]	5 M1	1.809	17.3	.1601		1.475	1.28	.11	24 - 7
5-47	5 M4	1.816	2.6	.1431	.0046	1.482	1.12	.07	20 - 6
5-48	5 M1	1.832	10.0	.1502		1.511	1.20	.08	19 - 6
5-49	5 M1	1.860		.1402					- 6
5-50	5 M4	1.861	0.5	.1376	.0039				- 8
5-51[r]	5 M4	2.218	1.6	.1286	.0041	1.368	1.23	.14	24 - 10
5-52[r]	5 M3	2.338		.1307					- 7
5-53[r]	5 M3	2.366		.1281					- 6
5-54	5 M4	2.426	3.4		.0044	1.356	1.26	.11	14 - 5
5-55	5 M4	2.443	2.6	.1237	.0037	1.341	1.24	.13	24 - 10
5-56	5 M5	2.450	0.8	.1198	.0037				- 6
5-57	5 M4	2.501		.1213	.0041				- 6
5-58[s]	5 M4	2.561	1.6	.1180	.0038	1.297	1.23	.16	23 - 8
5-61[s]	5 R1	1.222	0.2	.1620					- 8
5-62	5 R3	1.256	8.8	.1804	.0056	2.045	0.95	.14	20 - 7
5-63	5 R1	1.256		.1648					- 6
5-64[s]	5 R1	1.259		.1668					- 8
5-65[s]	5 R1	1.263		.1586					- 9
5-66[s]	5 R3	1.269	12.8	.1783	.0044	2.071	1.00	.19	22 - 9
5-67[r]	5 R2	1.282	2.7	.1782		2.045	0.96	.24	24 - 7
5-68	5 R3	1.306	26.7	.1900	.0056	2.063	1.04	.28	16 - 7
5-69	5 R3	1.329	6.4	.1726	.0055	2.063	0.99	.13	22 - 9

r Rough

s Smooth

TABLE C-2a

DATA FOR FIVE-CALIBER MODELS (CONTD)

Model No.	Type	M	$\overline{\delta^2}$	K_D	K_A	K_M	K_N	$(R_2)_L$ (inches)	$N - N_T$
5-70	5 R3	1.722	21.6	.1642	.0046	2.082	1.17	.33	20 - 10
5-71	5 R3	1.732	3.0	.1483	.0044	2.057	1.18	.08	23 - 10
5-72	5 R3	1.771	12.5	.1561	.0044	2.071	1.17	.18	17 - 7
5-73	5 R3	1.796	9.6	.1504	.0043	2.079	1.17	.21	22 - 9
5-74	5 R3	2.436	0.6	.1210	.0040	1.958			26 - 8
5-75	5 R3	2.444	2.4	.1230	.0039	1.956	1.21	.16	22 - 9
5-76	5 R3	2.521	2.3	.1217	.0037	1.947	1.23	.13	20 - 9
5-77	5 R3	2.559	0.9	.1178	.0035				22 - 7
5-78	5 R3	2.559	1.4	.1191	.0038	1.935	1.25	.11	27 - 8
5-79	5 R3	2.576	6.8		.0037	1.951[2]	1.24	.20	15 - 5
5-80	5 R3	2.604	1.2	.1170	.0037	1.968[2]			22 - 6

2 K_M determined from one arm and spin

TABLE C-2b

DATA FOR FIVE-CALIBER MODELS

Model No.	$\lvert K_1 \rvert$	$\lvert K_2 \rvert$	K_H	K_T	$\alpha_1 \times 10^3$	$\alpha_2 \times 10^3$	ν	s	$\bar{s}$
5-01	.0311	.0529	7.0[1]	-.205[1]	.382	.208	.254	2.15	0.78
5-02	.0238	.0516	6.6[1]	-.161[1]	.388	.165	.255	2.18	0.69
5-03	.0233	.0605	7.0[1]	-.133[1]	.451	.125	.254	2.07	0.58
5-04	.0410	.0550	6.4[1]	-.162[1]	.375	.167	.255	2.09	0.72
5-05	.0280	.0507	5.7	-.163	.233	.169	.252	1.87	0.89
5-06	.0245	.0215	5.9	-.191	.220	.209	.250	1.89	0.98
5-07	.0073	.0256					.249	2.07	
5-08	.0053	.0264					.249	2.06	
5-09	.0325	.0166	7.0	-.216	.256	.255	.447	5.45	1.01
5-10							.442	5.60	
5-11	.0069	.0071					.447	7.52	
5-12	.0302	.0182	4.7	-.096	.210	.177	.445	7.01	0.91
5-13	.0173	.0129	4.6	-.080	.221	.165	.448	7.00	0.87
5-14							.42		
5-15							.42		
5-31	.0729	.0524	4.9	-.078	.440	.184	.449	2.24	0.68
5-32	.0079	.0223	5.9	-.170	.139	.109	.212	1.42	0.93
5-33	.0128	.0226	4.6	-.193	.068	.125	.305	2.96	1.24
5-34							:27		
5-35	.0106	.0237	5.8	-.145	.137	.094	.269	2.33	0.85
5-36							.313	2.75	
5-37	.0566	.0416	5.0	-.073	.461	.178	.449	2.18	0.66
5-38	.0349	.0462	5.0	-.067	.474	.172	.451	2.21	0.64
5-39							.63		
5-40							.63		
5-41							.63		
5-42							.637	4.84	
5-43	.0131	.0063					.641	4.72	
5-44							.63		
5-45	.0254	.0110	4.9	-.040	.442	.186	.637	4.63	0.63
5-46	.0436	.0562	4.7	-.105	.135	.099	.187	1.19	0.92
5-47	.0120	.0191	5.2	-.103	.430	.241	.401	1.85	0.80

1. Note position of c.m. for this model type.

TABLE C-2 b

DATA FOR FIVE-CALIBER MODELS (CONTD)

Model No.	$\|K_1\|$	$\|K_2\|$	K_H	K_T	$a_1 \times 10^3$	$a_2 \times 10^3$	ν	s	$\bar{s}$
5-48	.0367	.0366	4.3	-.052	.162	.051	.197	1.26	0.74
5-49							.63		
5-50							.40		
5-51	.0105	.0202	5.0	-.089	.423	.251	.453	2.54	0.81
5-52							.63		
5-53							.63		
5-54	.0295	.0157	4.5	-.096	.347	.278	.447	2.49	0.91
5-55	.0210	.0175	4.5	-.066	.389	.226	.452	2.60	0.78
5-56							.42		
5-57							.45		
5-58	.0096	.0196	4.5	-.074	.372	.236	.451	2.67	0.82
5-61							.63		
5-62	.0349	.0362	3.6	+.004	.254	.047	.448	3.04	0.42
5-63							.63		
5-64							.63		
5-65							.63		
5-66	.0402	.0477	4.0	+.003	.279	.049	.447	3.01	0.41
5-67	.0240	.0235	4.2	-.020	.256	.066	.641	7.80	0.44
5-68	.0604	.0678	4.3	-.015	.285	.065	.446	2.99	0.48
5-69	.0287	.0330	3.7	.032	.286	.025	.447	2.98	0.30
5-70	.0493	.0690	4.7	-.044	.292	.102	.448	2.98	0.73
5-71	.0250	.0148	4.9	-.039	.307	.098	.447	3.01	0.73
5-72	.0490	.0365	4.8	-.013	.322	.074	.447	2.99	0.48
5-73	.0325	.0430	5.1	-.060	.299	.114	.448	3.00	0.63
5-74	.0108	.0066	4.8	-.030	.303	.101	.498	2.92	0.58
5-75	.0066	.0272	4.7	-.049	.286	.114	.447	3.16	0.65
5-76	.0125	.0215	5.1	-.049	.314	.114	.447	3.16	0.61
5-77							.441	3.06	
5-78	.0097	.0188	4.6	.010	.333	.064	.424	2.96	0.45
5-79	.0242	.0362	5.1	-.055	.298	.112	.416	2.93	0.64
5-80									

TABLE C-3a

DATA FOR SEVEN-CALIBER MODELS

Model No.	Type	M	$\overline{\delta^2}$	K_D	K_A	K_M	K_N	$(R_2)_L$ (inches)	$N - N_T$
7-01	7 F1	1.208	6.9			1.491	1.01	.65	19 - 4
7-02	7 F1	1.275	1.3	.1778		1.642	1.00	.20	22 - 6
7-03	7 F1	1.275	4.2	.1822		1.581	1.06	.64	23 - 7
7-04	7 F1	1.283	17.4			1.476	1.06	.99	19 - 4
7-05	7 F1	1.289	13.2			1.481	1.07	.86	18 - 5
7-06	7 F1	1.297	4.9	.1811		1.672	1.03	.57	24 - 8
7-07	7 F1	1.310	2.4	.1771		1.602	0.99	.29	24 - 6
7-08	7 F2	1.741	22.4	.1663	.0060	1.695	1.18	.26	19 - 6
7-09	7 F2	1.757	4.8	.1512	.0059	1.823	1.07	.10	20 - 9
7-10	7 F2	1.768	9.4	.1584	.0066	1.769	1.16	.13	20 - 9
7-11	7 F2	1.798	16.1	.1618	.0062	1.737	1.20	.24	23 - 9
7-12	7 F2	2.357	5.1	.1310	.0055	1.627	1.20	.25	18 - 9
7-13	7 F2	2.434	1.5	.1287	.0057	1.667	1.26	.11	18 - 9
7-14	7 F2	2.454	19.5	.1422	.0061	1.374	1.40	.50	16 - 7
7-15	7 F2	2.487	7.3	.1322	.0058	1.541	1.31	.26	22 - 9
7-31	7 M1	1.080	3.9	.1865		2.267	0.96	.13	22 - 6
7-32	7 M1	1.230	4.5	.1856		2.394	0.99	.14	23 - 6
7-33	7 M1	1.259		.1725					- 6
7-34	7 M1	1.273	8.5	.1864		2.399	1.01	.16	23 - 7
7-35	7 M1	1.277	6.1	.1859		2.423	0.99	.10	22 - 7
7-36	7 M1	1.312		.1671					- 6
7-37	7 M1	1.320		.1725					- 8
7-38	7 M1	1.381		.1707					- 9
7-39	7 M1	1.643	1.9	.1633		2.658	1.20	.07	20 - 7
7-40	7 M1	1.708		.1540					- 8
7-41	7 M1	1.710	0.7	.1485					- 9
7-42	7 M1	1.717	0.9	.1552					- 9
7-43	7 M1	1.763	2.5	.1512		2.692			21 - 9
7-44	7 M1	1.770	4.4	.1511		2.706	1.22	.09	20 - 6
7-45	7 M2	1.776	2.9	.1504	.0066	2.702	1.12	.08	28 - 8
7-46	7 M1	1.801	5.0	.1563		2.669	1.17	.10	20 - 6
7-47	7 M1	1.812	0.9	.1532		2.663			22 - 6

TABLE C-3a

DATA FOR SEVEN-CALIBER MODELS (CONTD)

Model No.	Type	M	$\overline{\delta^2}$	K_D	K_A	K_M	K_N	$(R_2)_L$ (inches)	$N - N_T$
7-48	7 M1	1.841	0.9	.1497					- 6
7-49	7 M2	2.509	4.7			2.615	1.22	.12	22 - 5
7-50	7 M2	2.514	4.8	.1277	.0056	2.595	1.26	.12	25 - 7
7-51	7 M2	2.566	5.7	.1232	.0048	2.592	1.22	.13	22 - 12
7-61	7 R2	1.268	15.0	.1933	.0086	3.206	1.02	.10	23 - 8
7-62	7 R1	1.308	9.7			3.302	1.04	.23	23 - 5
7-63	7 R1	1.425	5.2			3.365	1.08	.19	23 - 5
7-64	7 R2	1.809	28.1	.1711	.0061	3.635	1.29	.14	23 - 9
7-65	7 R2	1.816	21.9	.1683	.0069	3.586	1.22	.12	22 - 8
7-66	7 R2	1.823	14.4	.1586	.0063	3.617	1.19	.08	22 - 9
7-67	7 R2	1.846	16.0	.1576	.0062	3.601	1.17	.10	23 - 9
7-68	7 R2	2.477	20.0	.1396	.0053	3.589	1.48	.13	22 - 9
7-69	7 R2	2.514	12.2	.1370	.0057	3.572	1.36	.10	22 - 9
7-70	7 R2	2.524	6.0	.1295	.0057	3.574			23 - 9
7-71	7 R2	2.526	25.7	.1452	.0057	3.571	1.55	.15	20 - 7
7-72	7 R2	2.537	20.2			3.612			20 - 5

TABLE C-3b

DATA FOR SEVEN-CALIBER MODELS

Model No.	$\|K_1\|$	$\|K_2\|$	K_H	K_T	$a_1 \times 10^3$	$a_2 \times 10^3$	ν	s	$\bar{s}$
7-01	.0342	.0302	14.3	-.288	.123	.189	.622	5.16	1.19
7-02	.0107	.0107					.627	4.73	
7-03	.0163	.0309	13.1	-.278	.106	.191	.627	4.82	1.25
7-04	.0604	.0399	14.1	-.413	.052	.259	.623	5.32	1.60
7-05	.0514	.0357	15.5	-.419	.078	.262	.624	5.23	1.49
7-06	.0188	.0323	13.0	-.267	.107	.186	.625	4.58	1.22
7-07	.0226	.0151	15.1	-.355	.106	.225	.627	4.97	1.33
7-08	.0758	.0281	18.1	-.606	-.002	.404	.445	2.33	1.78
7-09	.0345	.0138	14.5	-.344	.086	.239	.446	2.18	1.36
7-10	.0498	.0164	17.8	-.557	.016	.386	.446	2.18	1.69
7-11	.0637	.0274	18.3	-.597	.001	.407	.444	2.20	1.73
7-12	.0299	.0232	14.5	-.401	.053	.282	.446	2.43	1.54
7-13	.0185	.0103					.445	2.36	
7-14	.0697	.0290	17.2	-.737	-.096	.475	.443	2.79	2.20
7-15	.0421	.0200	14.9	-.516	-.016	.368	.446	2.49	1.85
7-31	.0236	.0235	8.3	-.018	.263	.065	.630	2.23	0.35
7-32	.0254	.0270	8.9	-.042	.256	.088	.633	2.16	0.63
7-33									
7-34	.0386	.0316	10.1	-.124	.222	.175	.638	2.10	0.91
7-35	.0376	.0215	10.5	-.190	.221	.183	.630	2.06	1.14
7-36							.63		
7-37							.63		
7-38							.63		
7-39	.0178	.0145	12.0	-.149	.257	.207	.629	1.90	0.92
7-40							.63		
7-41							.63		
7-42							.63		
7-43	.0198	.0166	12.3	-.164	.259	.226	.649	1.50	0.96
7-44	.0293	.0189	11.9	-.147	.251	.208	.632	1.88	0.93
7-45	.0175	.0215	12.7	-.235	.273	.164	.419	2.01	0.82
7-46	.0302	.0222	12.7	-.210	.219	.274	.632	1.89	1.08
7-47	.0109	.0111					.633	1.89	

TABLE C-3b

DATA FOR SEVEN-CALIBER MODELS (CONTD)

Model No.	$\lvert K_1 \rvert$	$\lvert K_2 \rvert$	K_H	K_T	$\alpha_1 \times 10^3$	$\alpha_2 \times 10^3$	ν	s	$\bar{s}$
7-48							.63		
7-49	.0215	.0270	12.8	-.287	.238	.207	.422	2.13	0.94
7-50	.0239	.0252	12.8	-.281	.243	.207	.422	2.13	0.94
7-51	.0325	.0236	13.2	-.231	.283	.168	.449	2.47	0.80
7-61	.0400	.0537	7.5	.046	.236	.026	.454	1.42	0.26
7-62	.0381	.0390	7.9	.007	.166	.031	.625	3.22	0.42
7-63	.0232	.0325	8.7	.038	.200	.014	.628	3.18	0.28
7-64	.0575	.0718	10.8	-.055	.248	.044	.449	1.29	0.64
7-65	.0524	.0633	10.2	-.060	.223	.050	.448	1.30	0.67
7-66	.0445	.0489	11.0	-.055	.255	.032	.446	1.28	0.61
7-67	.0395	.0573	10.2	-.054	.233	.039	.447	1.29	0.64
7-68	.0511	.0593	12.3	-.104	.241	.092	.447	1.27	0.78
7-69	.0357	.0494	11.6	-.059	.263	.046	.448	1.29	0.65
7-70	.0179	.0382	11.0	-.087	.226	.059	.447	1.28	0.75
7-71	.0612	.0614	12.3	-.135	.207	.130	.448	1.28	0.70
7-72	.0460	.0580	12.8	-.072	.315	.026	.423	1.17	0.64

TABLE C-4a

DATA FOR NINE-CALIBER MODELS

Model No.	Type	M	$\overline{\delta^2}$	K_D	K_A	K_M	K_N	$(R_2)_L$ (inches)	N - N_T
9-01	9 F2	1.286	1.6	.1884	.0110	2.135	1.06	.06	22 - 11
9-02	9 F1	1.305	0.9	.1883		2.247	1.10	.15	23 - 6
9-03	9 F2	1.310	11.4	.1948	.0097	1.919	1.14	.17	23 - 8
9-04	9 F2	1.311	7.0	.1882	.0098	2.039	1.17	.09	21 - 9
9-05	9 F1	1.319	7.1	.1934		2.084	1.17	.39	23 - 6
9-06	9 F1	1.367	0.7	.1820					- 6
9-07	9 F3	1.377	6.7	.1935	.0092	2.068	1.16	.36	27 - 7
9-08	9 F2	1.390	2.2	.1809	.0100	2.211			22 - 8
9-09	9 F3	1.769	3.3	.1586	.0079	2.493[2]	1.21	.14	29 - 9
9-10	9 F2	1.808	28.1	.1721	.0078	2.355[2]	1.40	.06	22 - 9
9-11	9 F2	1.815	4.9	.1583	.0086	2.460[2]			23 - 9
9-12	9 F3	1.874	17.4	.1626	.0079	2.415[2]			17 - 7
9-13	9 F3	2.488	1.0	.1322	.0070				- 8
9-14	9 F2	2.489	4.6	.1362	.0079	2.475[2]			22 - 7
9-15	9 F3	2.498	1.7	.1357	.0074				- 8
9-16	9 F3	2.508	2.7	.1348	.0070	2.475			25 - 7
9-17	9 F3	2.519	5.7	.1329	.0067	2.482	1.31	.14	20 - 6
9-18	9 F3	2.532	2.5	.1317	.0069	2.498	1.25	.06	28 - 7
9-31	9 M2	1.217	11.8			3.063	1.11	.33	17 - 5
9-32	9 M1	1.295	10.6	.1912		3.107			21 - 6
9-33	9 M1	1.311	4.2	.1852		3.252			24 - 6
9-34	9 M1	1.315	12.0			3.151	1.18	.08	15 - 3
9-35	9 M1	1.703	3.8	.1635					- 7
9-36	9 M1	1.794	3.4	.1654		3.633			22 - 6
9-37	9 M3	1.794	2.2	.1570	.0087	3.658			17 - 7
9-38	9 M1	1.801	16.6	.1734		3.402			21 - 6
9-39	9 M3	1.805	0.8	.1571	.0088				24 - 10

2 K_M determined from one arm and spin

TABLE C-4a

DATA FOR NINE-CALIBER MODELS (CONTD)

Model No.	Type	M	$\overline{\delta^2}$	K_D	K_A	K_M	K_N	$(R_2)_L$ (inches)	N - N_T
9-40	9 M4	2.435	1.1	.1396	.0077	3.825			25 - 7
9-41	9 M4	2.467	9.7	.1438	.0071	3.703	1.32	.06	30 - 9
9-42	9 M4	2.470	1.4	.1364	.0086	3.868			29 - 9
9-61	9 R1	1.323	28.2	.2126		4.416[1]	1.25	.35	22 - 6
9-62	9 R1	1.323	2.1	.1845		4.416[1]	1.08	.08	25 - 7
9-63	9 R1	1.328	13.6			4.429[1]	1.18	.23	23 - 5
9-64	9 R2	1.733	2.1	.1581	.0080	4.686			- 9
9-65	9 R2	1.756	1.5	.1607	.0093	4.661			- 10
9-66	9 R2	1.763	19.5	.1745	.0085	4.655	1.38	.11	21 - 10
9-67	9 R2	1.784	10.8	.1656	.0086	4.668	1.25	.07	19 - 9
9-68	9 R2	1.849	20.3	.1724	.0088	4.708	1.36	.12	19 - 10
9-69	9 R3	2.405	1.0	.1334	.0066	4.944			29 - 9
9-70	9 R3	2.457	0.6	.1337	.0073				- 9
9-71	9 R3	2.488	2.2	.1320	.0064	5.003	1.23	.07	27 - 9

1. Note position of c.m. for this model type

TABLE C-4b

DATA FOR NINE-CALIBER MODELS

Model No.	$\|K_1\|$	$\|K_2\|$	K_H	K_T	$\alpha_1 x10^3$	$\alpha_2 x10^3$	ν	s	$\bar{s}$
9-01	.0194	.0098					.445	1.50	
9-02	.0123	.0111	25.3	-.637	-.045	.279	.635	3.06	2.20
9-03	.0512	.0214					.443	1.64	
9-04	.0420	.0140					.444	1.57	
9-05	.0412	.0204	22.5	-.554	-.033	.248	.632	3.36	2.11
9-06							.630		
9-07	.0495	.0195	21.8	-.463	-.009	.222	.631	3.14	1.90
9-08	.0247	.0062	25.4	-.584	-.095	.348	.444	1.46	2.03
9-09	.0280	.0145	27.9	-.709	-.084	.353	.557	2.06	2.20
9-10	.0762	.0115	32.5	-1.102	-.381	.704	.444	1.38	2.83
9-11	.0338	.0079	30.0	-.863	-.276	.574	.444	1.30	2.46
9-12	.0778	.0080					.444	1.39	
9-13							.555	1.98	
9-14	.0324	.0058					.446	1.29	
9-15							.548	1.98	
9-16	.0285	.0070	29.0	-.669	-.057	.340	.554	2.03	2.02
9-17	.0365	.0133	29.4	-.779	-.110	.400	.550	1.99	2.27
9-18	.0265	.0070					.552	2.02	
9-31	.0425	.0350	15.8	-.173	.135	.103	.631	3.19	0.89
9-32	.0526	.0184	20.8	-.350	-.046	.419	.625	1.24	1.61
9-33	.0328	.0137	18.4	-.279	-.014	.356	.627	1.18	1.50
9-34	.0536	.0257	19.9	-.245	.066	.302	.625	1.21	1.29
9-35							.639	1.12	
9-36	.0267	.0104					.637	1.09	
9-37	.0236	.0117	26.8	-.426	.161	.246	.442	1.29	1.06
9-38	.0697	.0112	30.0	-.504	-.149	.710	.603	1.16	1.57
9-39	.0141	.0074					.443	1.29	

TABLE C-4b

DATA FOR NINE-CALIBER MODELS (CONTD)

Model No.	$\lvert K_1 \rvert$	$\lvert K_2 \rvert$	K_H	K_T	$\alpha_1 \times 10^3$	$\alpha_2 \times 10^3$	ν	s	$\bar{s}$
9-40	.0155	.0084	24.1	-.314	.042	.213	.553	1.26	1.33
9-41	.0492	.0169	31.8	-.605	-.075	.389	.546	1.30	1.74
9-42	.0180	.0094	30.0[1]	-.734[1]	.002	.299	.539	1.25	2.14
9-61	.0341	.0550	11.3[1]	.142[1]	.173	-.036	.631	1.85	0.08
9-62	.0140	.0206	10.0[1]	.146[1]	.160	-.042	.630	1.86	0.21
9-63	.0341	.0550	13.8[1]	.078[1]	.170	-.014	.633	1.84	0.18
9-64	.0240	.0074					.443	1.23	
9-65	.0072	.0192					.443	1.23	
9-66	.0576	.0513	17.3	-.116	.130	.053	.445	1.24	0.80
9-67	.0400	.0395	17.8	-.097	.151	.031	.443	1.22	0.70
9-68	.0538	.0593	16.5	-.088	.139	.038	.443	1.21	0.74
9-69	.0100	.0133	22.5	-.180	.138	.069	.553	1.78	0.79
9-70							.554	1.78	
9-71	.0150	.0207	22.4	-.163	.146	.065	.553	1.74	0.74

1. Note position of c.m. for this model type.

RESTRICTED---Security Information

TABLE C-5

DATA FOR MODELS WITH LARGE YAW[1]

Model No.	Type	M	$\overline{\delta^2}$	K_D	K_A	K_M	K_N	$(R_2)_L$ (inches)	N - N_T
5-91	5 M4	1.305	32.0	.1930	.0053	1.518	1.04	.26	18 - 7
7-91	7 F2	1.569	41.5	.1902	.0062	1.586	1.24	.56	22 - 10
7-92	7 M1	1.263	30.6	.2067		2.349	1.11	.30	19 - 6
9-91	9 F1	1.297	60.1			1.187	1.62	1.28	17 - 4
9-92	9 F1	1.306	49.5	.2219		1.469	1.39	.94	22 - 6
9-93	9 F2	1.881	45.9	.1965	.0078	2.196	1.64	.13	18 - 7
9-94	9 M2	1.731	61.3	.2064	.0084	3.166	1.45	.07	20 - 8
9-95	9 M4	2.436	38.1	.1640	.0067	3.273	1.62	.31	18 - 9
9-96	9 R2	1.757	30.9	.1856	.0086	4.650	1.49	.15	20 - 9
9-97	9 R2	2.472	37.5	.1622	.0062	4.879	1.25	.06	18 - 9

Model No.	$\lvert K_1 \rvert$	$\lvert K_2 \rvert$	K_H	K_T	$\alpha_1 \times 10^3$	$\alpha_2 \times 10^3$	ν	s	$\bar{s}$
5-91	.0744	.0616	4.9	-.107	.381	.242	.449	2.27	0.82
7-91	.1062	.0296	20.7	-.762	-.046	.505	.443	2.41	1.93
7-92	.0789	.0521	10.1	-.186	.154	.250	.641	2.18	1.18
9-91	.1280	.0266	47.8	-1.722	-.241	.680	.633	5.23	2.95
9-92	.1120	.0267	43.5	-1.414	-.180	.575	.631	4.65	2.70
9-93	.1002	.0157	38.1	-1.419	-.482	.863	.442	1.44	3.07
9-94	.1281	.0208	39.3	-1.344	-.178	.746	.443	1.50	1.98
9-95	.0641	.0568	46.6	-1.152	-.204	.653	.545	1.46	2.15
9-96	.0720	.0648	18.1	- .147	.122	.073	.445	1.24	0.88
9-97[2]	.0980	.0352					.445	1.17	

1. $\overline{\delta^2} > 30$

2. Damping rates and hence K_H and K_T for 9-97 could not be determined because of an unfavorable station distribution.

RESTRICTED---Security Information

TABLE C-6

MAGNUS DATA

Model No.	Type	M	$\overline{\delta^2}$	K_F	CP_F	$(R_2)_F$ (inches)
5-09	5 F3	1.805	4.4	.11	4.46	.02
5-12	5 F3	2.480	4.2	.18	3.04	.06
5-13	5 F3	2.498	1.5	.21	2.89	.05
5-68	5 R3	1.306	26.7	.16	3.63	.02
5-70	5 R3	1.722	21.6	.14	3.85	.03
5-91	5 M4	1.305	32.0	.18	3.61	.03
7-01	7 F1	1.208	6.9	.19	4.76	.06
7-03	7 F1	1.275	4.2	.12	5.57	.06
7-04	7 F1	1.283	17.4	.27	4.78	.19
7-05	7 F1	1.289	13.2	.23	5.07	.14
7-06	7 F1	1.297	4.9	.23	4.41	.08
7-07	7 F1	1.310	2.4	.20	5.02	.04
7-08	7 F2	1.741	22.4	.44	4.63	.04
7-11	7 F2	1.798	16.1	.31	5.18	.03
7-12	7 F2	2.357	5.1	.19	5.36	.02
7-14	7 F2	2.454	19.5	.35	5.36	.06
7-15	7 F2	2.487	7.3	.33	4.82	.03
7-62	7 R1	1.308	9.7	.17	4.76	.03
7-63	7 R1	1.425	5.2	.22	4.63	.03
7-91	7 F2	1.569	41.5	.35	5.43	.08
7-92	7 M1	1.263	30.6	.38	4.52	.08
9-03	9 F2	1.310	11.4	.36		.03
9-05	9 F1	1.319	7.1	.37	5.50	.09
9-07	9 F3	1.377	6.7	.36	5.29	.09
9-09	9 F3	1.769	3.3	.34	6.09	.03
9-17	9 F3	2.519	5.7	.32	6.43	.02
9-31	9 M2	1.217	11.8	.20	5.92	.04
9-61	9 R1	1.323	28.2	.43	5.74	.09
9-63	9 R1	1.328	13.6	.37	5.86	.05
9-91	9 F1	1.297	60.1	.62	7.78	.36
9-92	9 F1	1.306	49.5	.42	7.36	.22

TABLE C-7

AVERAGE STATISTICAL ERRORS[1]

Type	ν	K_D	K_A	K_M	K_N	K_F	K_H	K_T
5F	.25	.0002	.0002	.006	.02		.37	.019
5F	.45	.0002	.0002	.006	.02	.04	.37	.019
5M	.20	.0002	.0002	.004	.02		.25	.015
5M	.45	.0002	.0002	.004	.02	.04	.25	.015
5M	.64	.0002	.0002	.004	.02		.25	.015
5R	.45	.0002	.0002	.004	.02	.04	.25	.012
5R	.64	.0002	.0002	.004	.02		.25	.012
7F	.45	.0004	.0002	.013	.03	.06	1.04	.022
7F	.63	.0004	.0002	.013	.03	.05	1.04	.022
7M	.45	.0003	.0001	.007	.03		.44	.015
7M	.63	.0003	.0001	.007	.03	.05	.44	.015
7R	.45	.0007	.0002	.004	.04		.44	.012
7R	.63	.0007	.0002	.004	.04	.05	.44	.012
9F	.45	.0004	.0003	.025	.04	.09	4.00	.060
9F	.55	.0004	.0003	.019	.04	.07	2.30	.030
9F	.63	.0004	.0003	.017	.04	.06	1.50	.037
9M	.45	.0002	.0002	.015	.06		2.22	.060
9M	.55	.0002	.0002	.010	.05		2.00	.050
9M	.63	.0002	.0002	.015	.06	.10	2.22	.044
9R	.45	.0004	.0003	.007	.06		1.18	.012
9R	.55	.0004	.0003	.007	.06		1.04	.017
9R	.63	.0004	.0003	.007	.06	.10	1.04	.017

Accuracy of Physical Measurements

A ~ .1%, B ~.1% m ~.03%, c.m.~ ± .0006 cal., d~ ± .0002 cal, L ~ ± .0006 cal.
Error in swerve fit ~.012 in., error in yaw fit ~.001 rad., error in time fit ~ .5 microsec.

1. Standard errors.

TABLE C-8

TURNING RATES[1]

Type	v rad/cal	ϕ_1' rad/cal	ϕ_2' rad/cal	Type	v rad/cal	ϕ_1' rad/cal	ϕ_2' rad/cal
5 F1	.25	.0205	.0033	9 F1	.63	.0136	.0013
5 F2	.25	.0181	.0033	9 F2	.45	.0080	.0022
5 F3	.45	.0323	.0015	9 F3	.45	.0077	.0024
5 M1	.20	.0106	.0046	9 F3	.55	.0111	.0018
5 M1	.27	.0192	.0026	9 F3	.63	.0131	.0013
5 M1	.30	.0225	.0023	9 M1	.63	.0097	.0045
5 M3	.64	.0498	.0030	9 M2	.45	.0117	.0034
5 M4	.40	.0279	.0054	9 M2	.63	.0201	.0019
5 M4	.45	.0331	.0041	9 M3	.45	.0114	.0040
5 M5	.42	.0335	.0013	9 M4	.54	.0089	.0034
5 R2	.64	.0608	.0022	9 R1	.63	.0137	.0026
5 R3	.42	.0346	.0037	9 R2	.45	.0095	.0038
5 R3	.45	.0363	.0037	9 R3	.55	.0137	.0027
7 F1	.63	.0230	.0013				
7 F2	.45	.0152	.0021				
7 M1	.63	.0206	.0037				
7 M2	.42	.0217	.0035				
7 R1	.63	.0263	.0025				
7 R2	.42	.0125	.0056				
7 R2	.45	.0141	.0050				

1. Turning rates at the middle of the range can be converted to degrees per foot by the factor 874.89 $\frac{\text{o/ft.}}{\text{rad/cal}}$

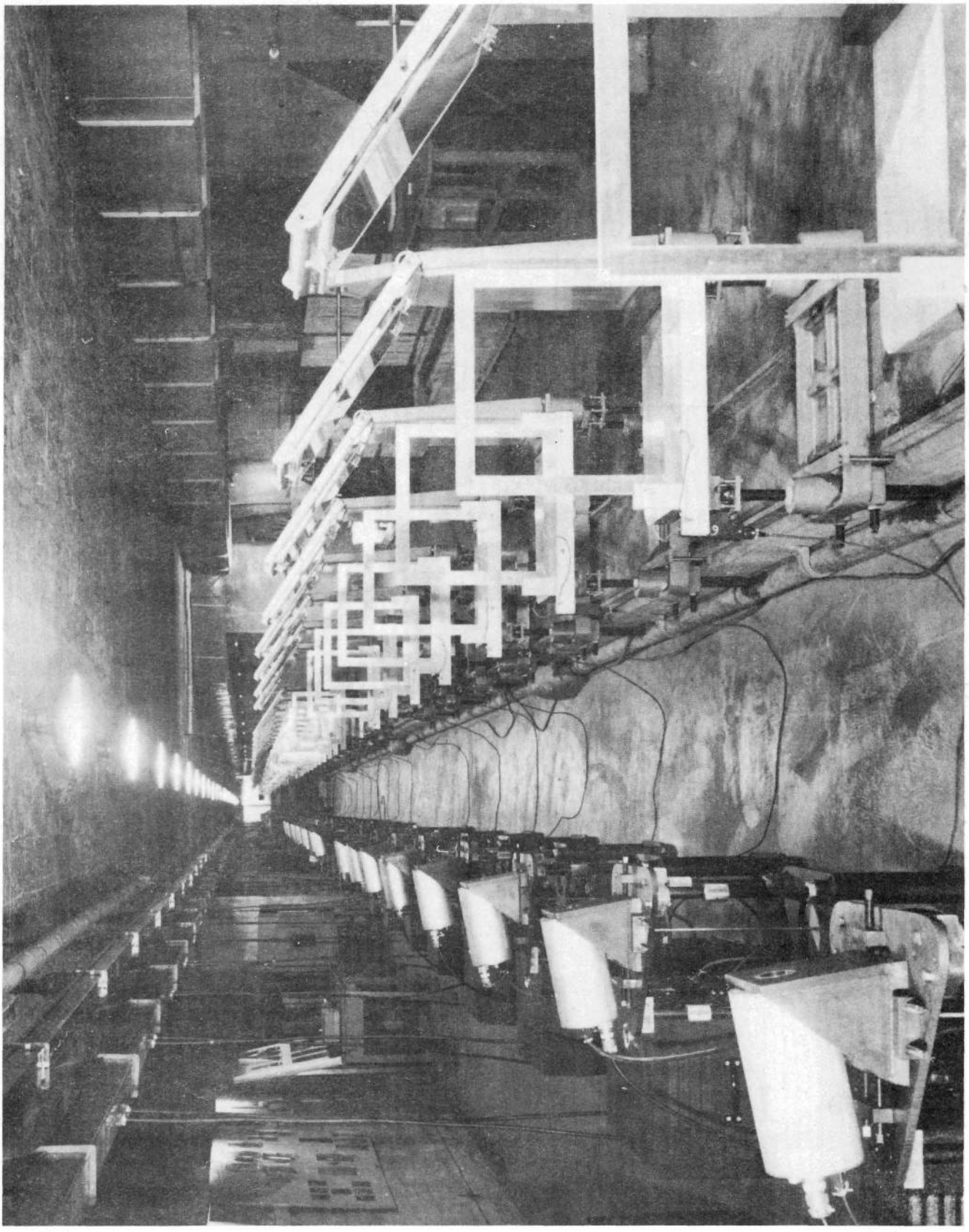

FIG. 1

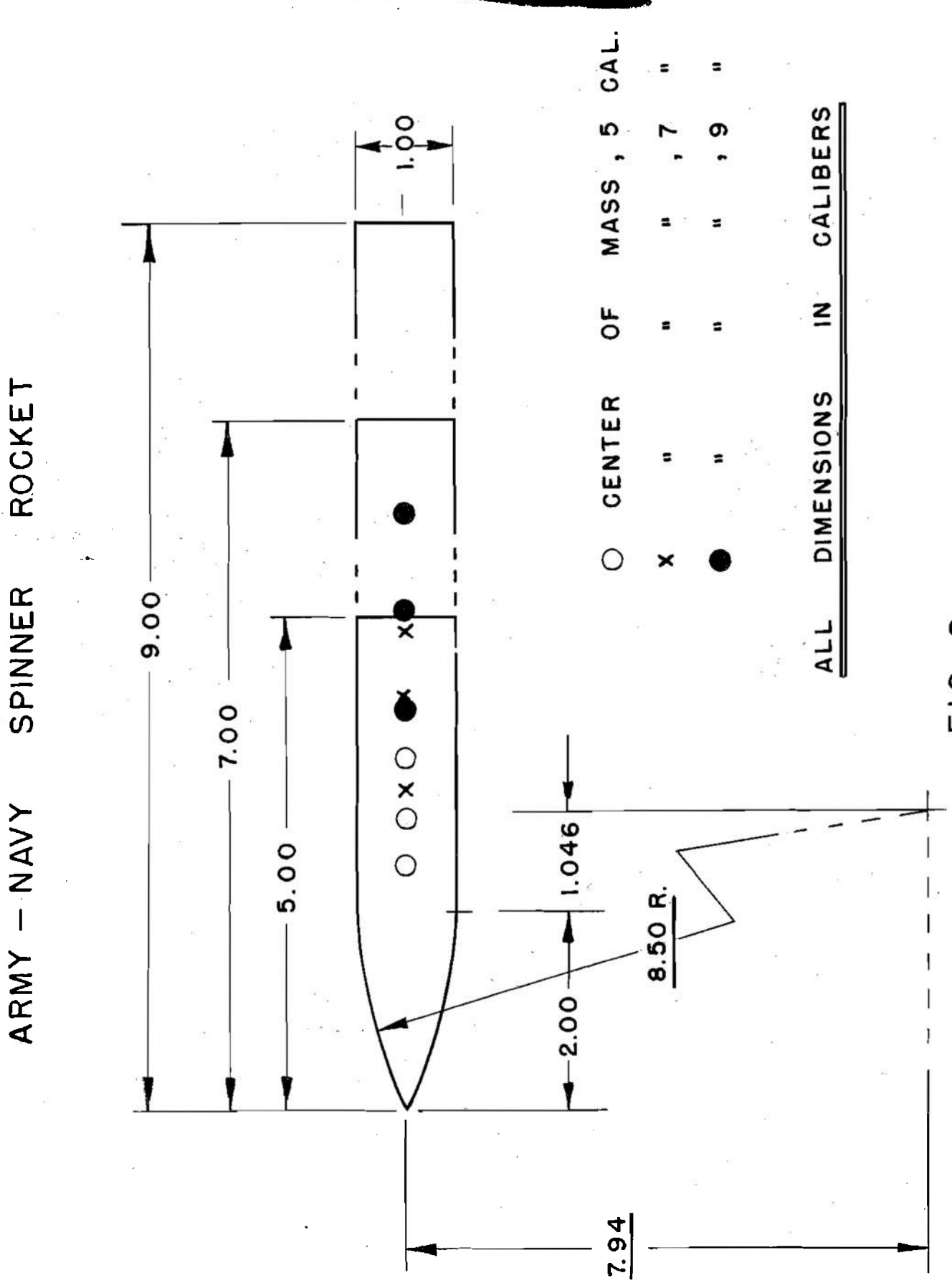
ARMY — NAVY SPINNER ROCKET
1.00
9.00
7.00
5.00
1.046
8.50 R.
2.00
7.94
○ CENTER OF MASS, 5 CAL.
× " " , 7 "
● " " , 9 "
ALL DIMENSIONS IN CALIBERS

FIG. 2

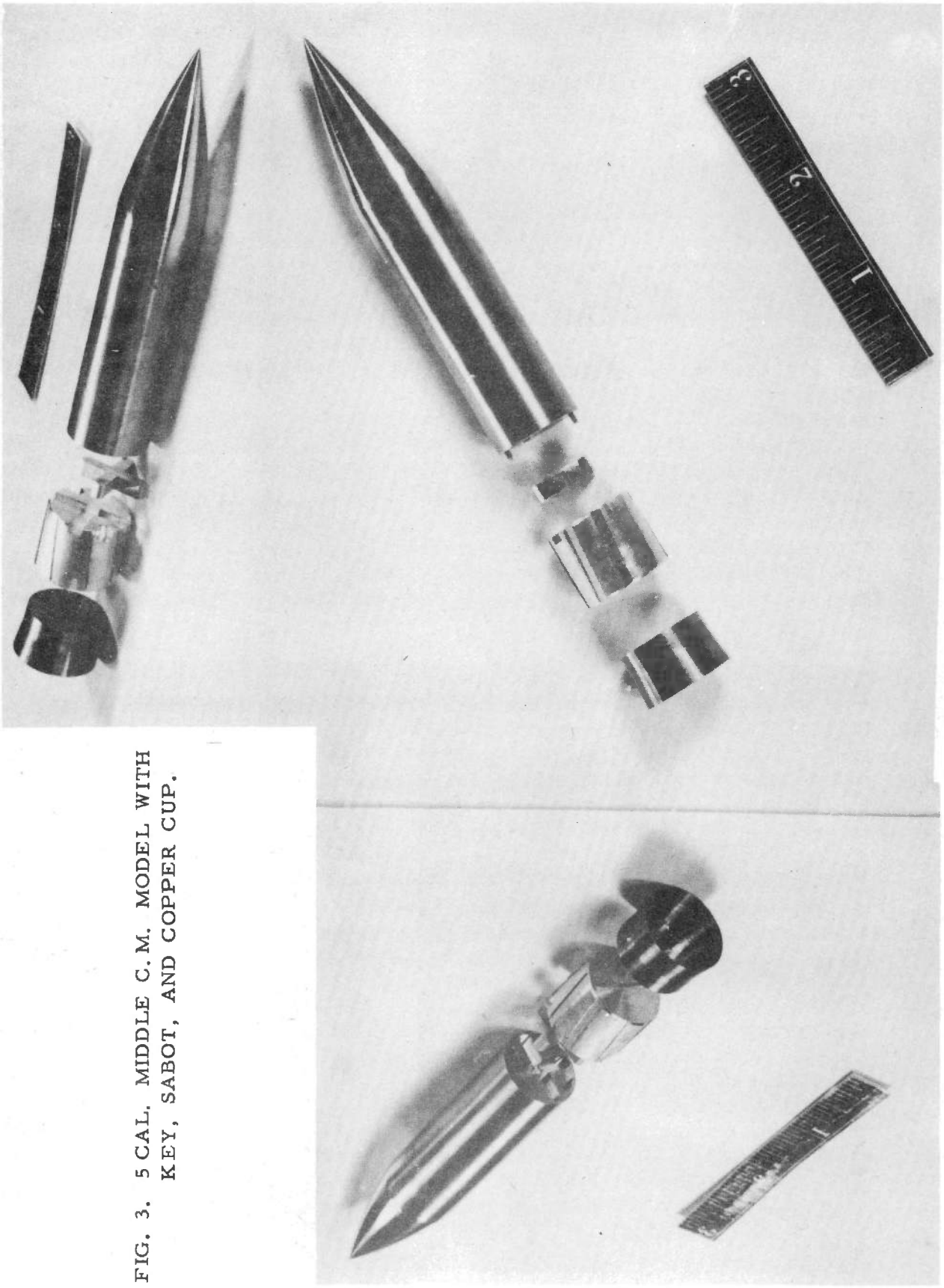

FIG. 3. 5 CAL. MIDDLE C.M. MODEL WITH KEY, SABOT, AND COPPER CUP.

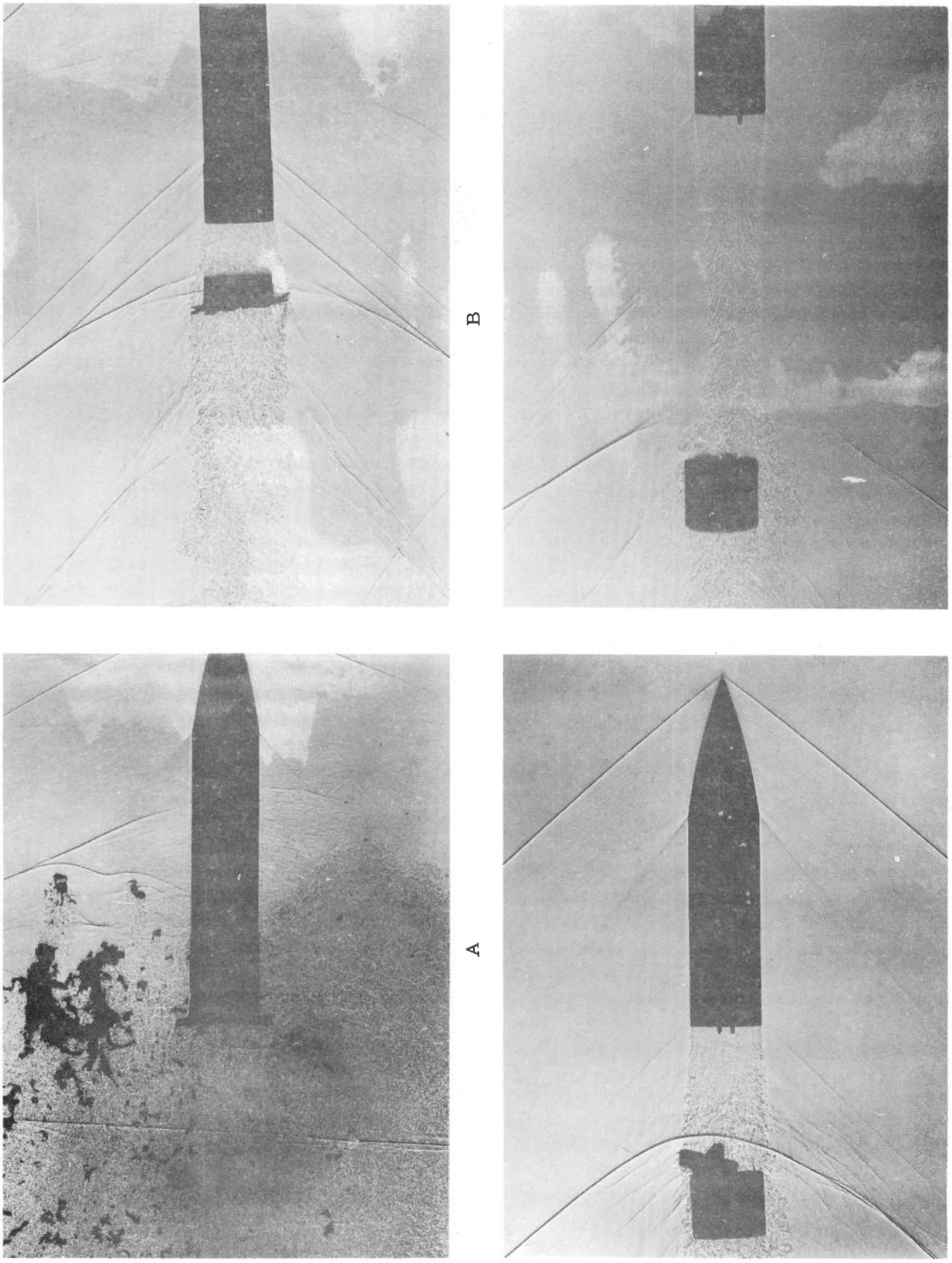

B D A C

FIG. 4

LAUNCHING EFFICIENCY RATIO

NO. OF ROUNDS WITH YAW REDUCTIONS

TO

NO. OF ROUNDS FIRED

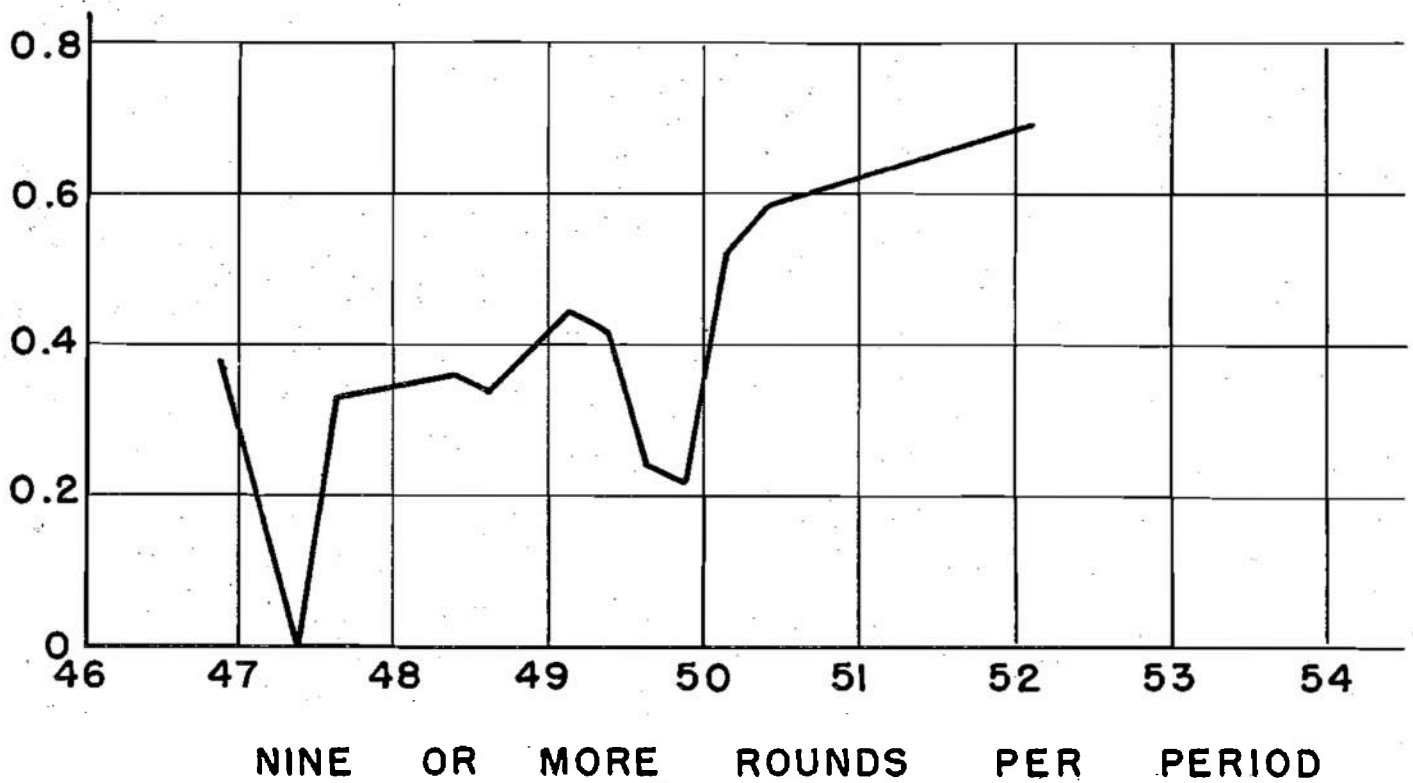

FIG. 5

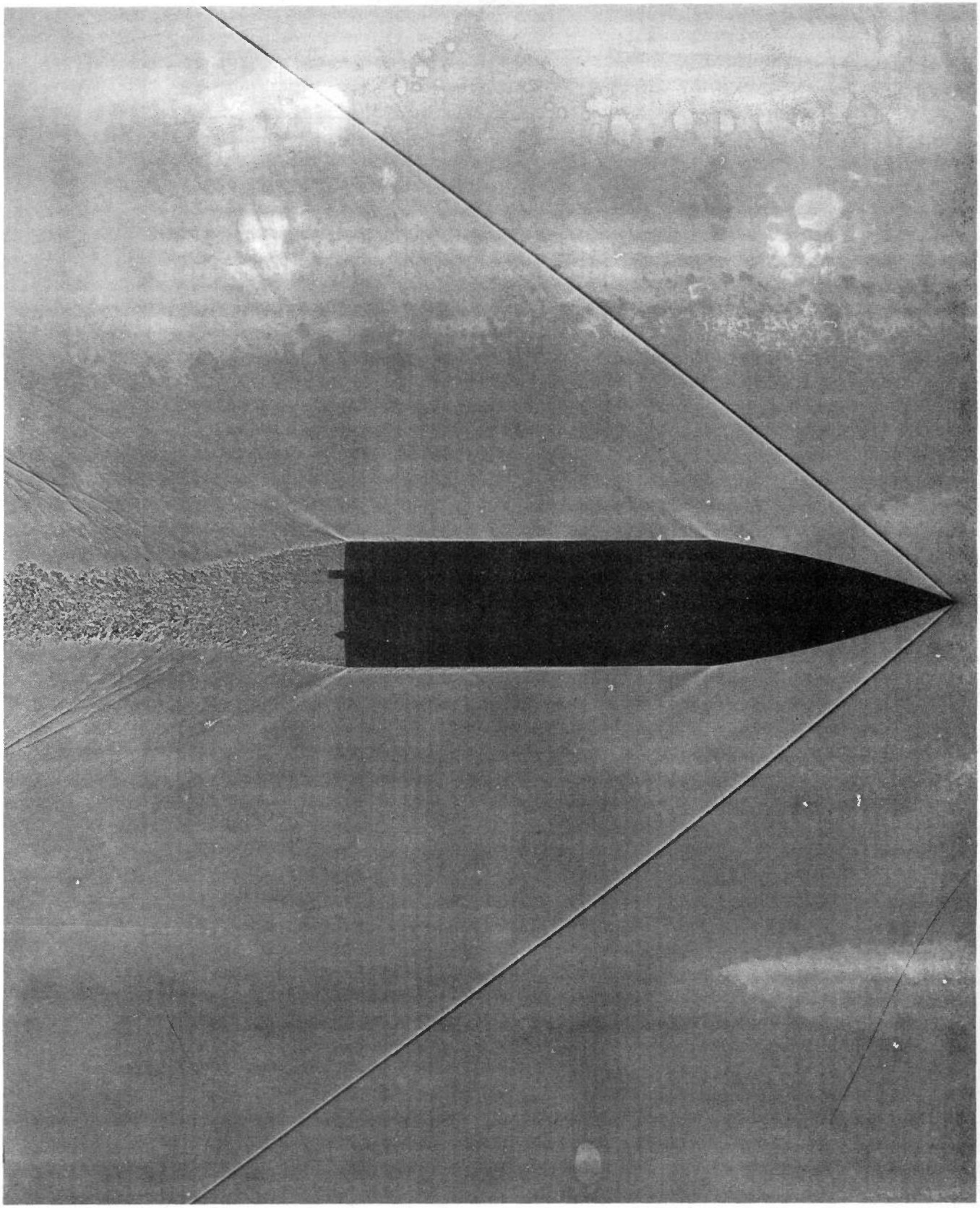

FIG. 6

PRESSURE DISTRIBUTION

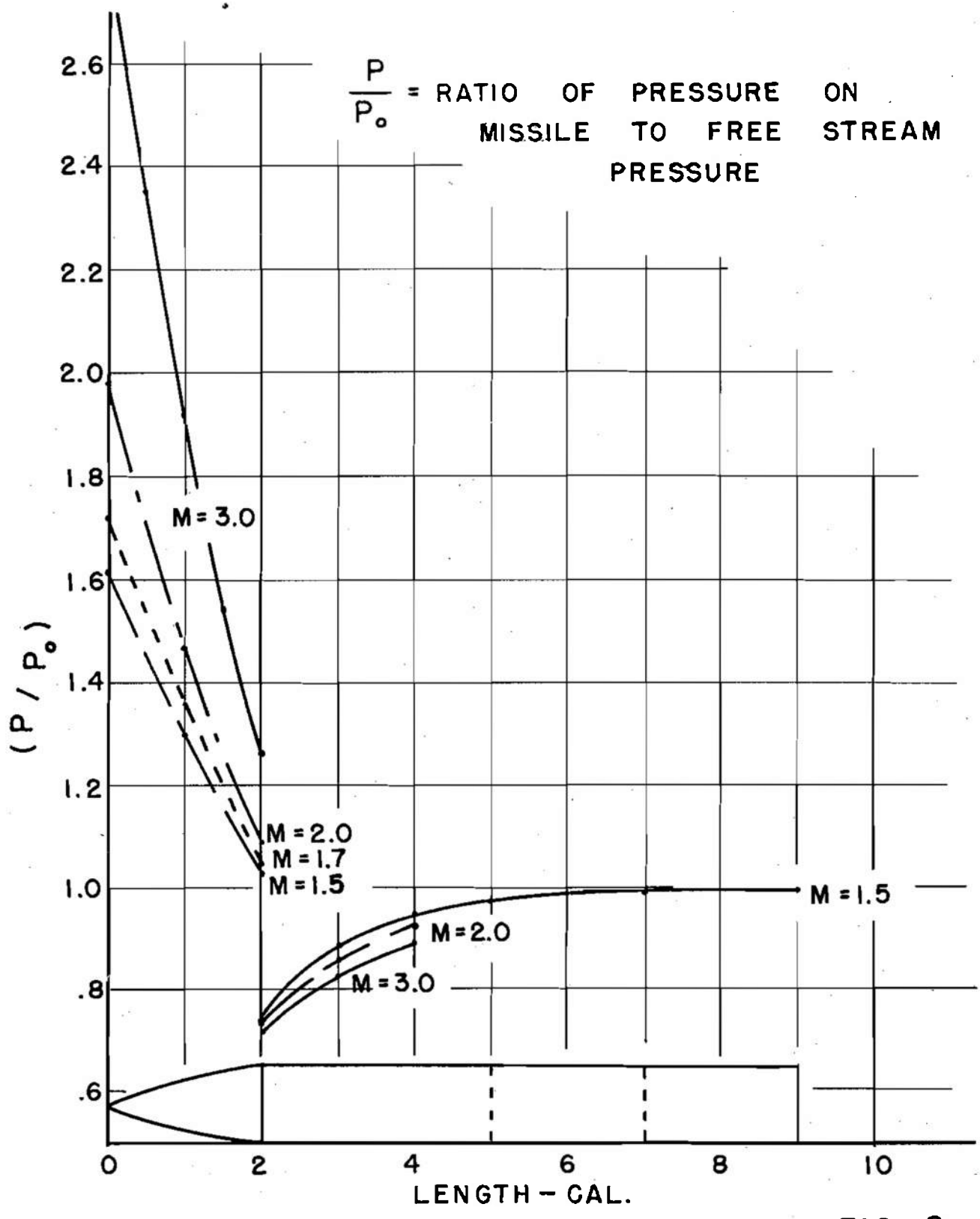

FIG. 8

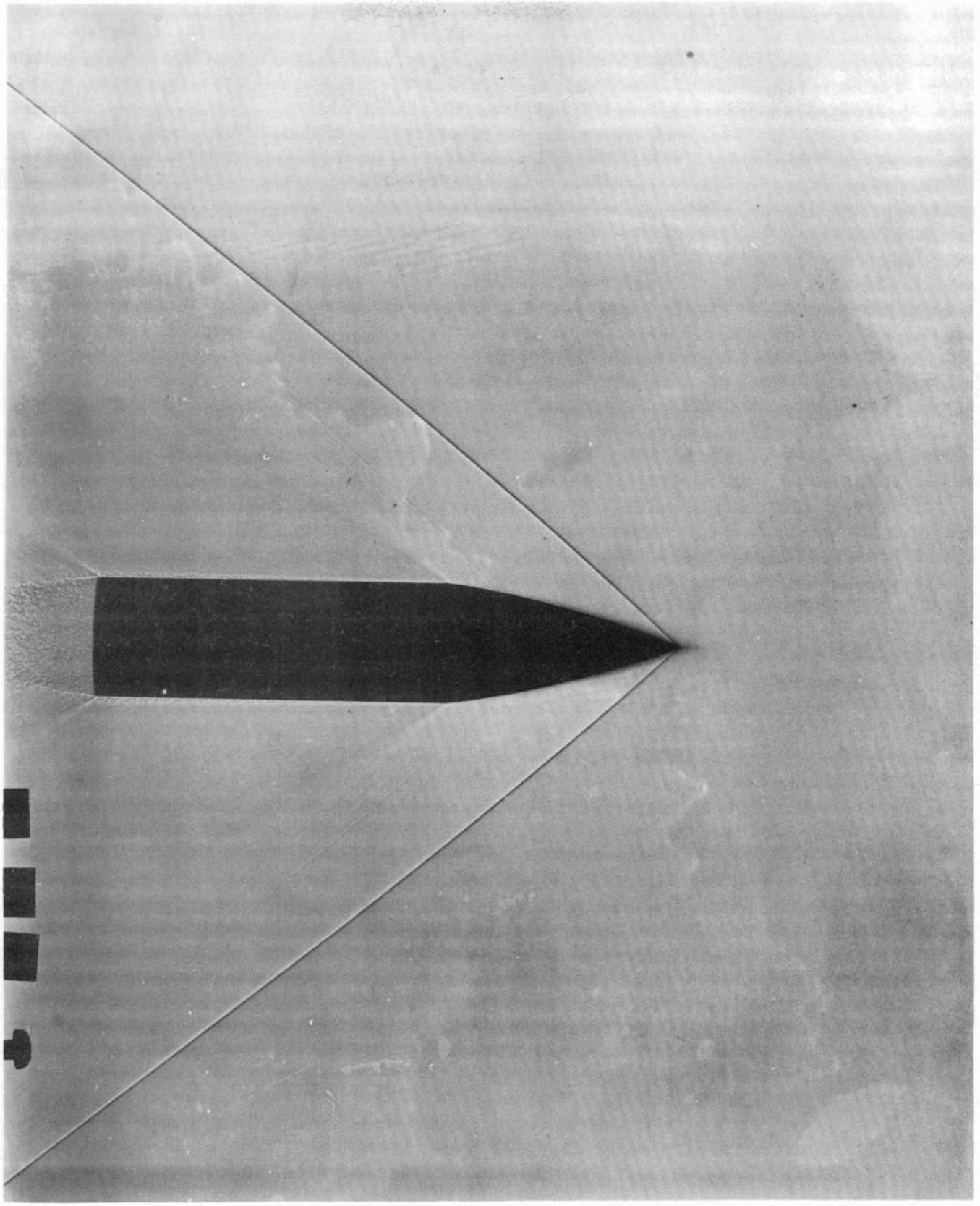

FIG. 7

ZERO – YAW DRAG COEFFICIENT VS MACH NO.

5 CALIBER

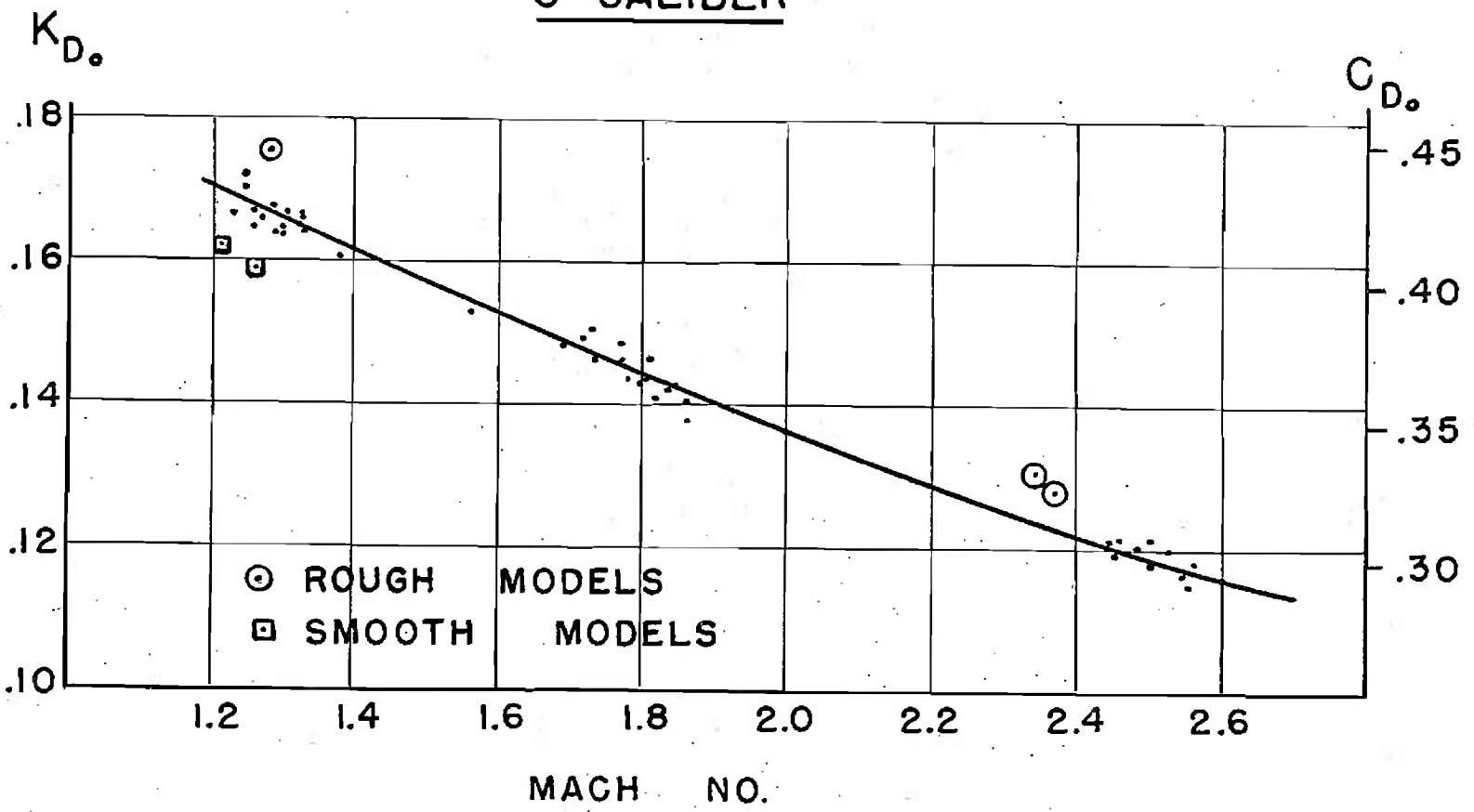

FIG. 9

ZERO – YAW DRAG COEFFICIENT

VS

MACH NO.

7 CALIBER

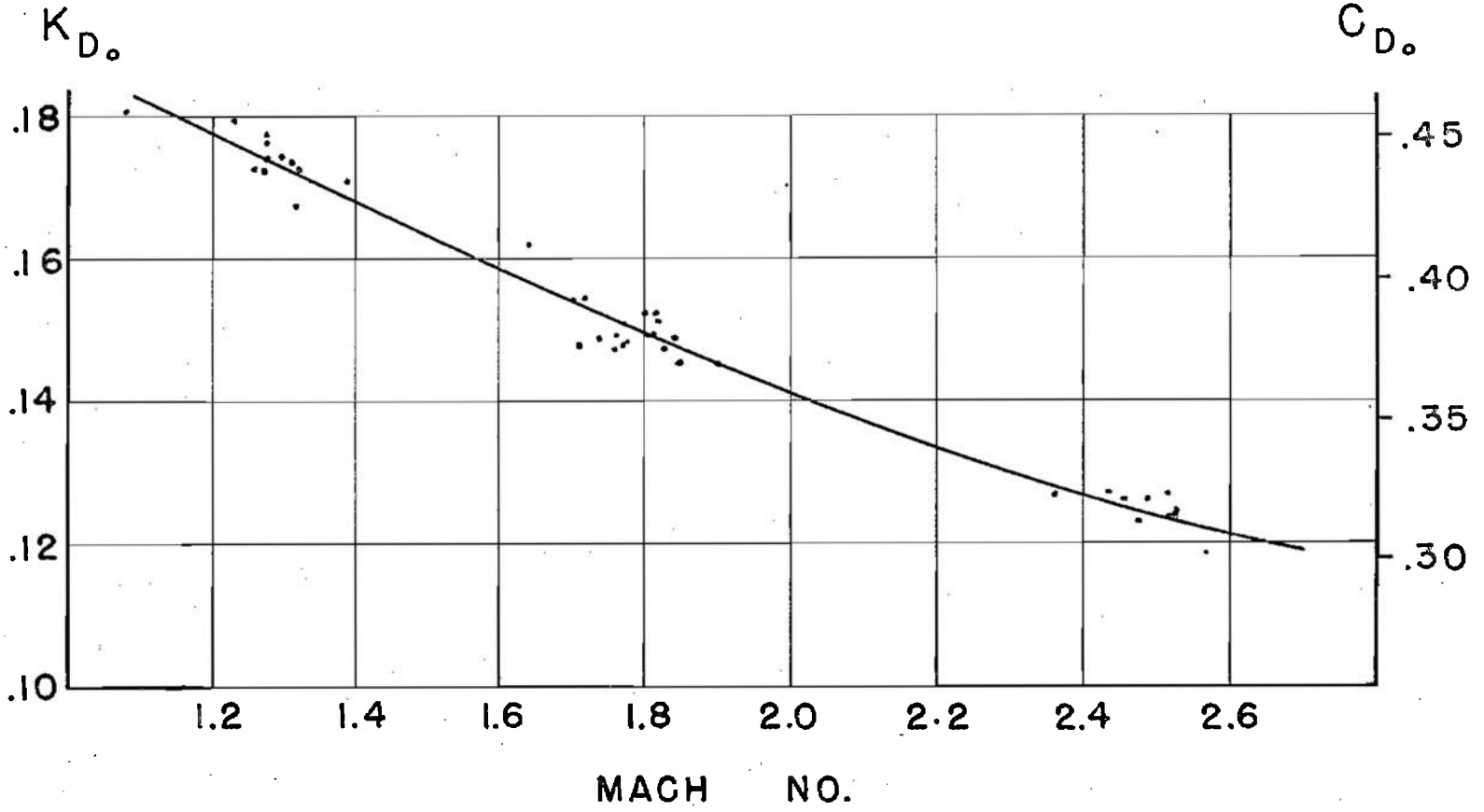

FIG. 10

ZERO – YAW DRAG COEFFICIENT VS MACH NO.

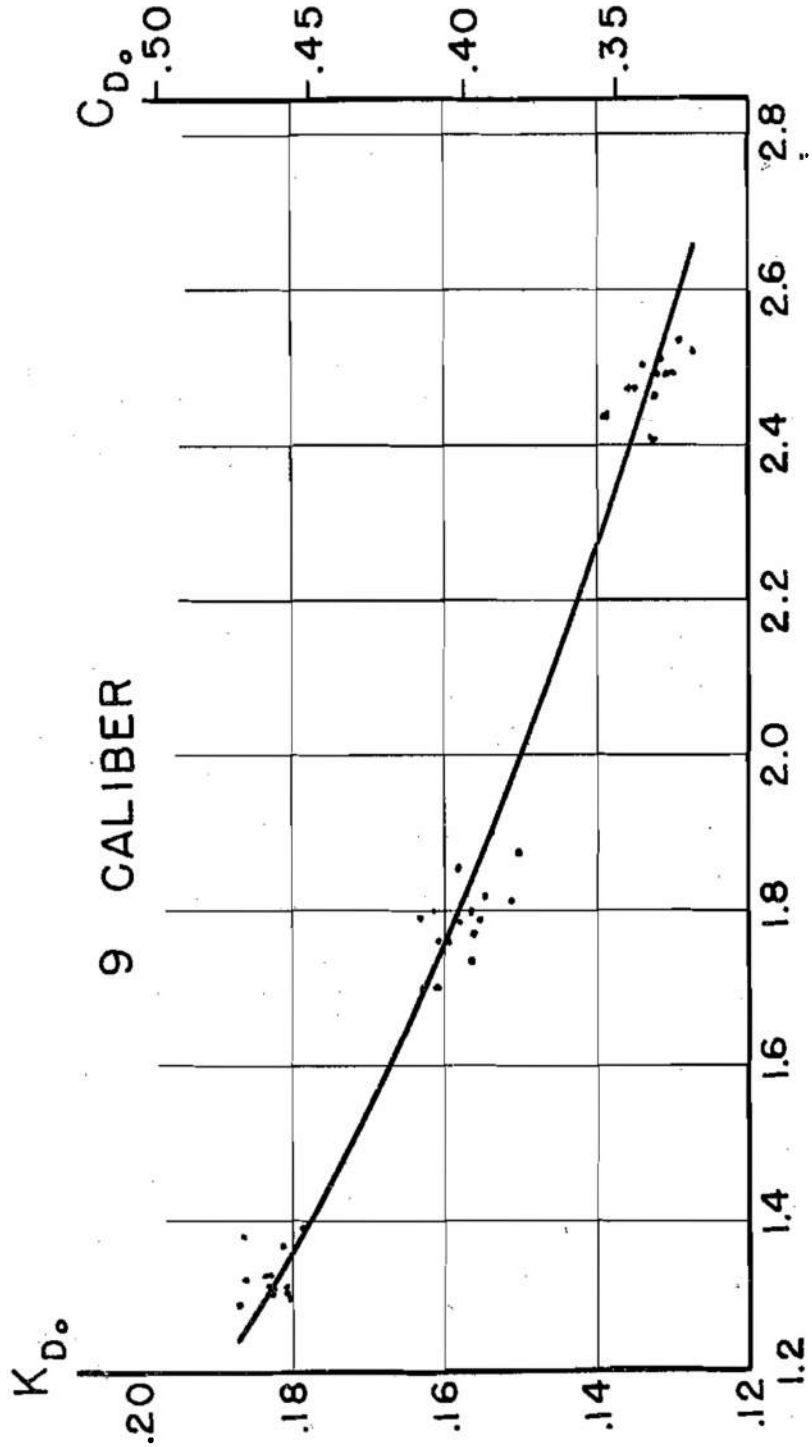

FIG. 11

SPIN DECELERATION MOMENT COEFFICIENT

VS

MACH NO.

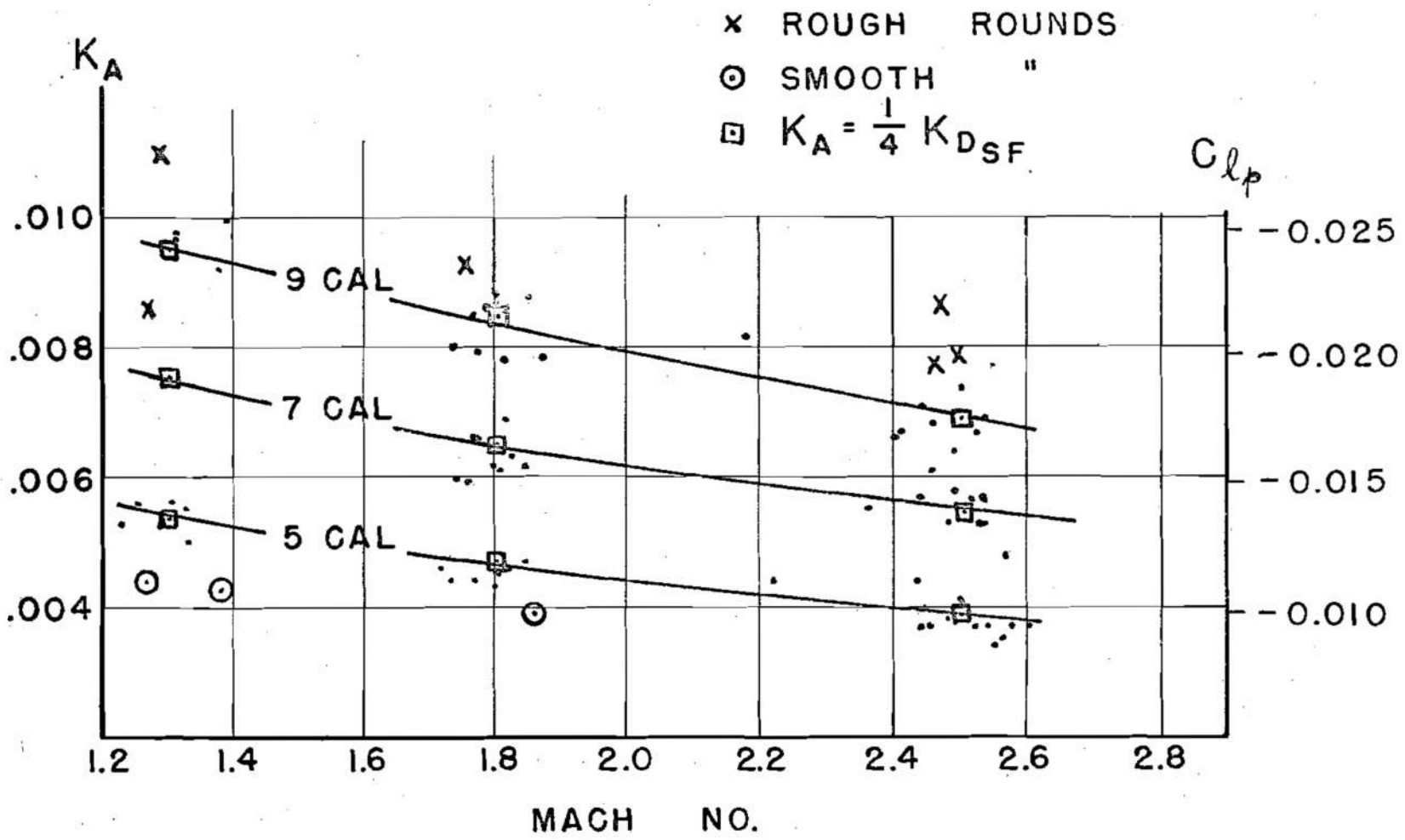

FIG. 12

SPIN DECELERATION MOMENT COEFFICIENT

VS

LENGTH

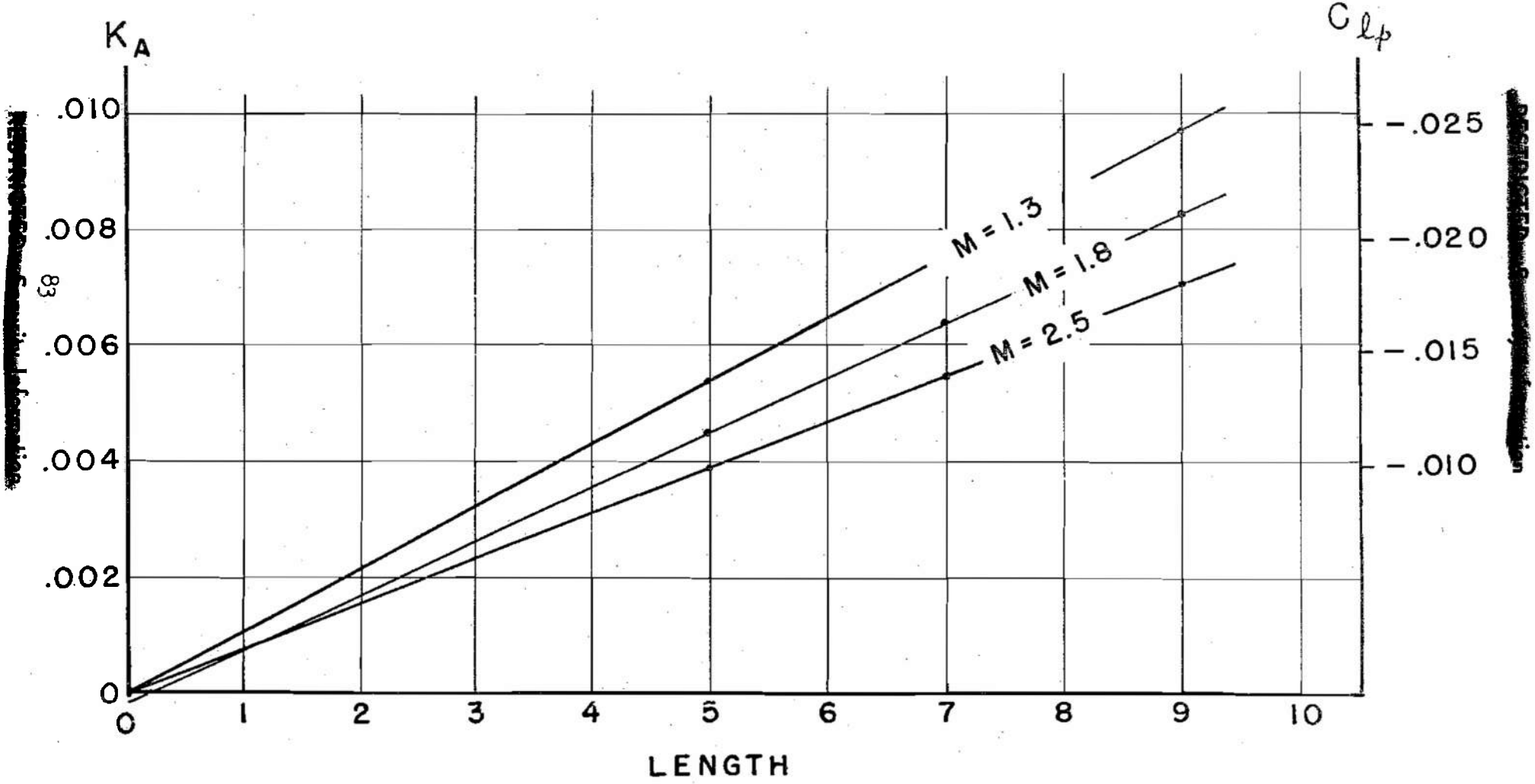

FIG. 13

ZERO – YAW OVERTURNING MOMENT COEFFICIENT VS MACH NO.

5 CALIBER

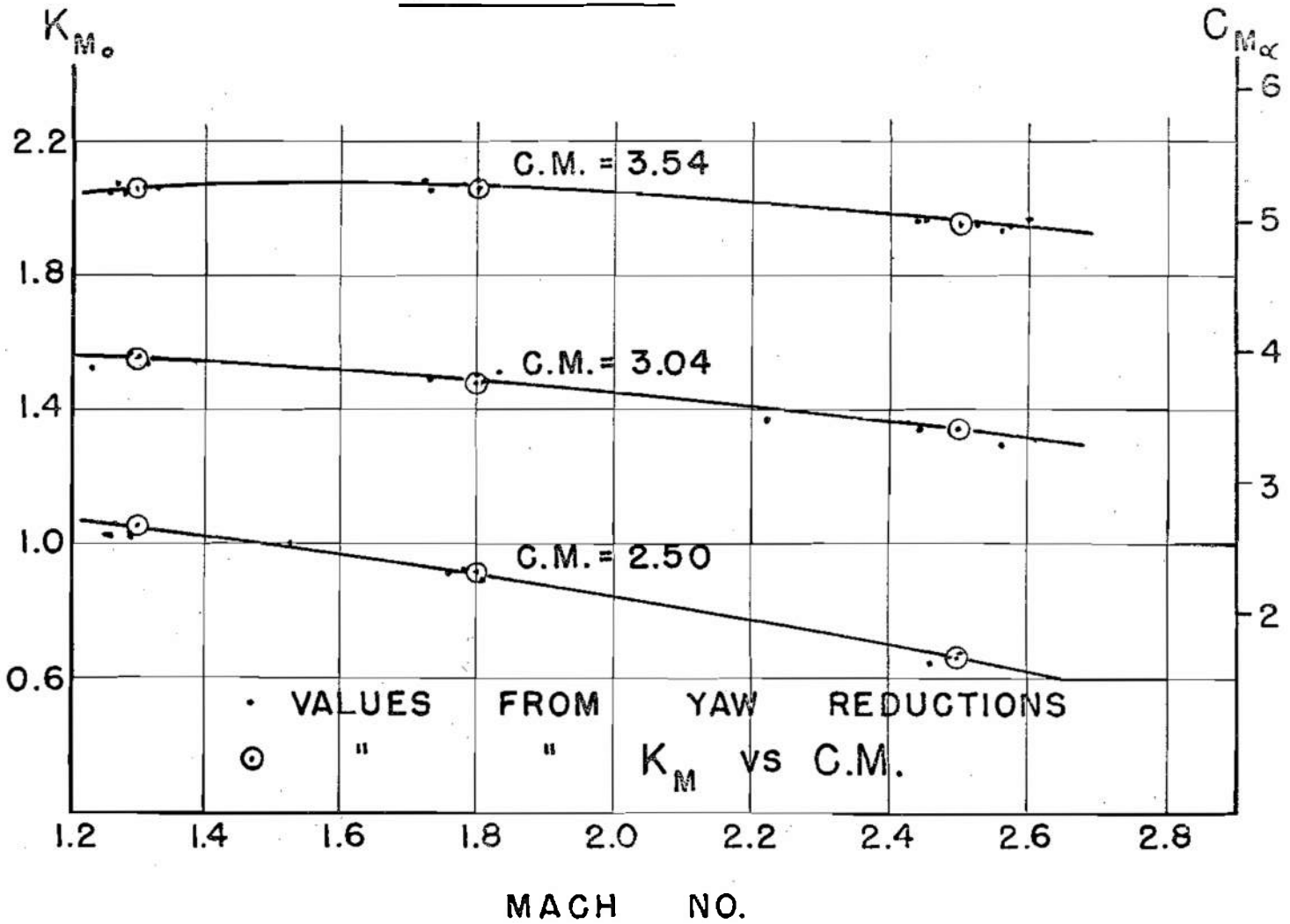

FIG. 14

ZERO - YAW OVERTURNING MOMENT COEFFICIENT VS MACH NO.

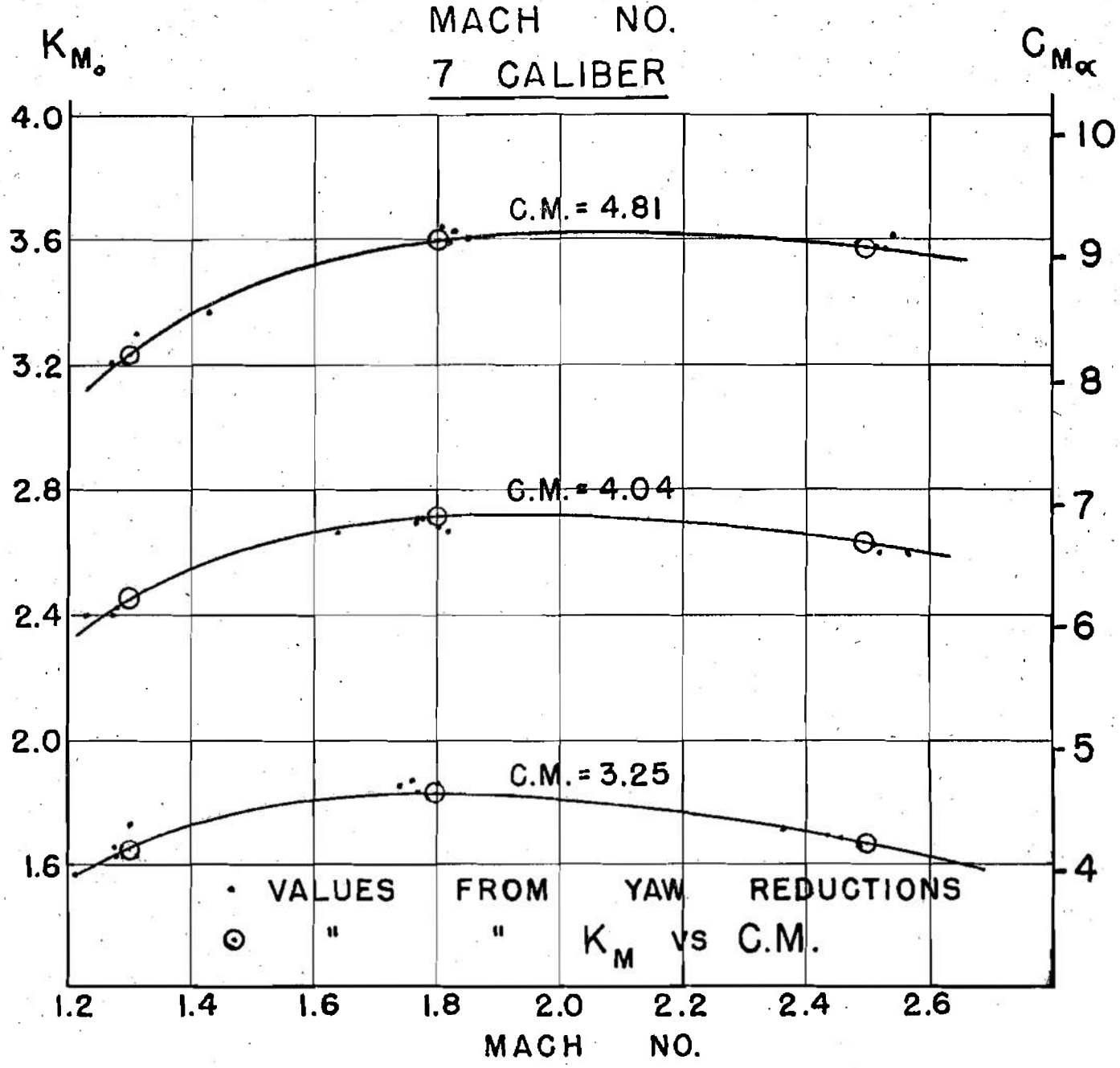

FIG. 15

ZERO – YAW OVERTURNING MOMENT COEFFICIENT
VS
MACH NO.

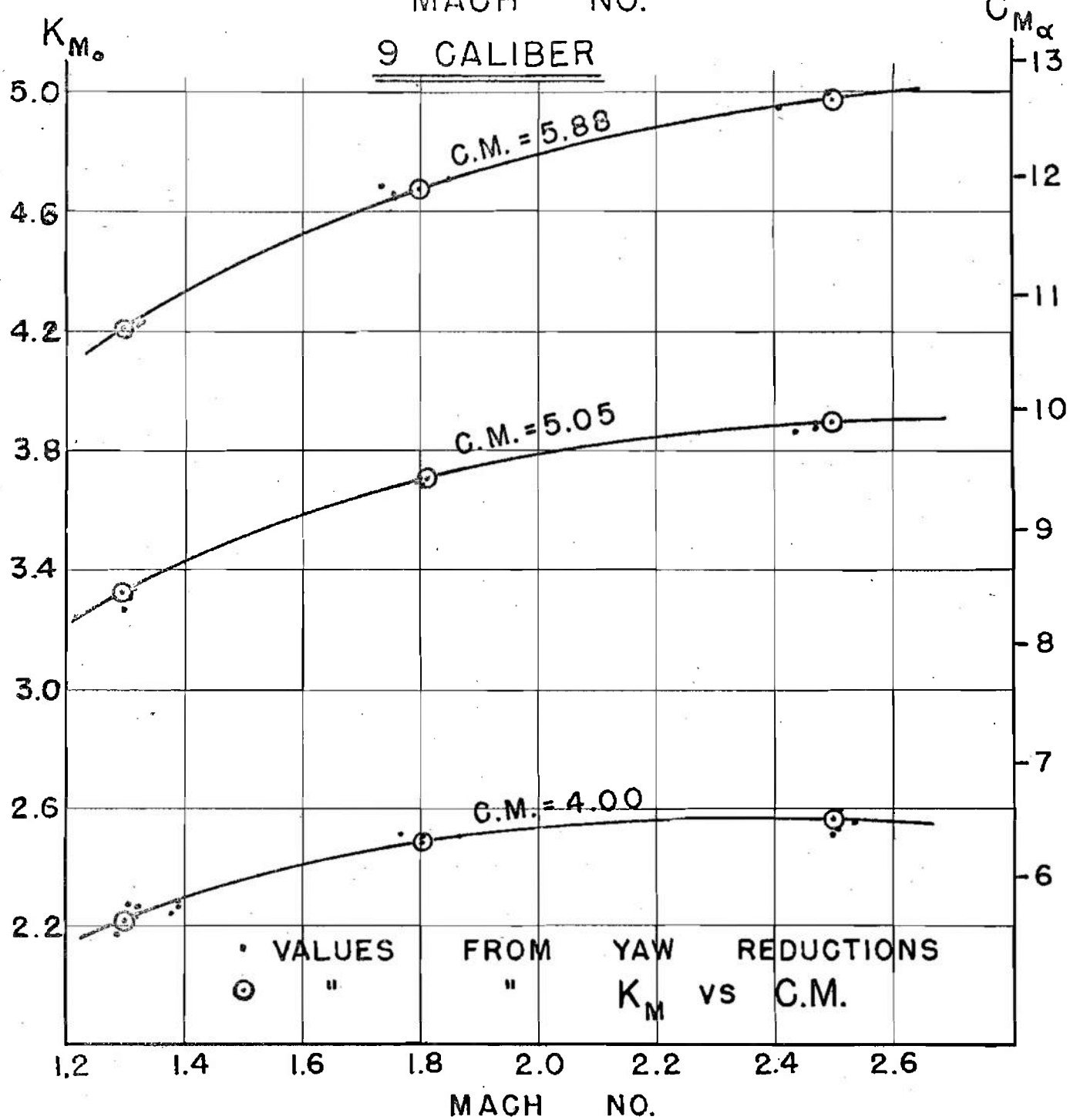

FIG. 16

ZERO – YAW NORMAL FORCE COEFFICIENT VS MACH NO.

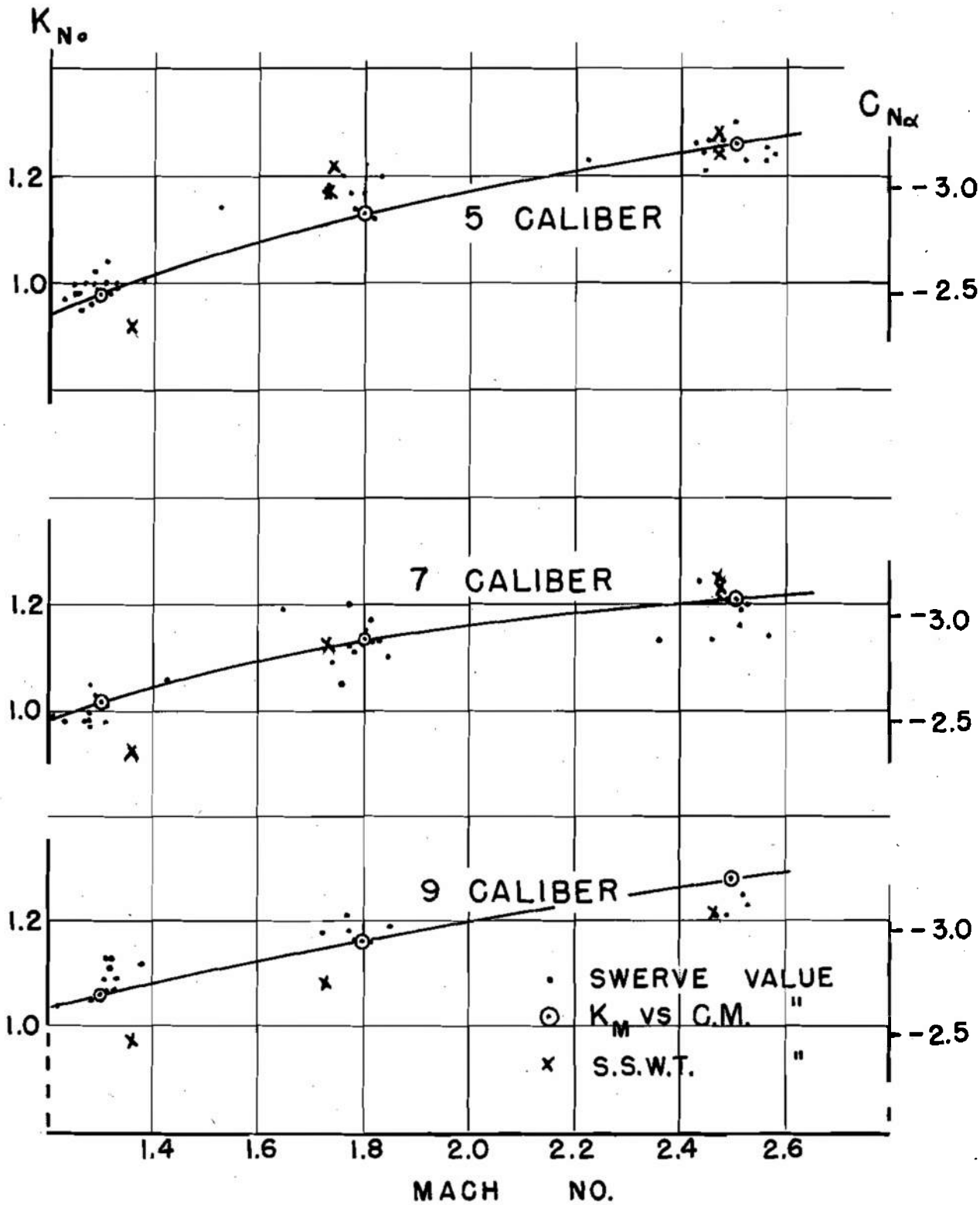

FIG. 17

ZERO - YAW NORMAL FORCE CENTER OF PRESSURE VS MACH NO.

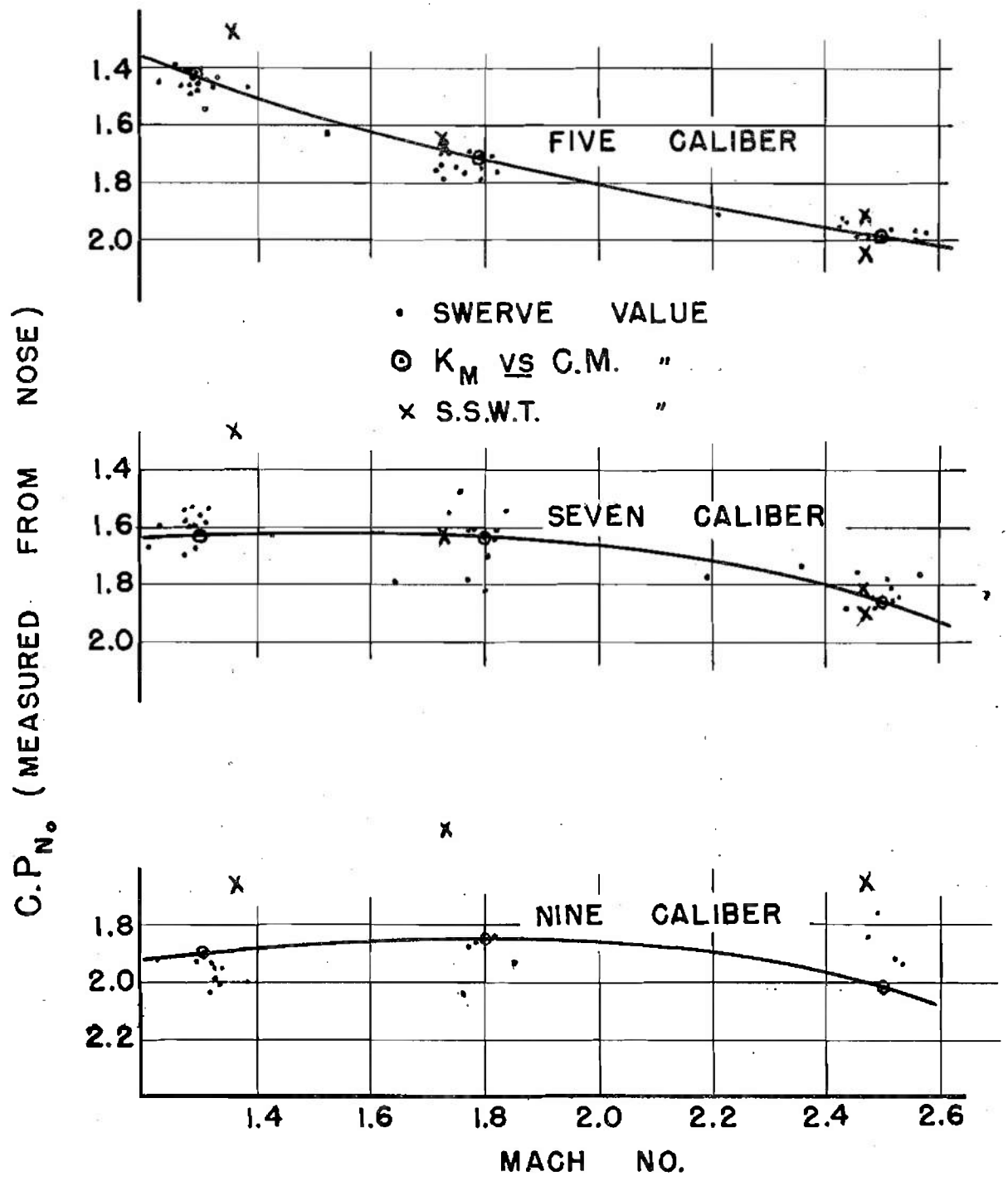

FIG. 18

THE CENTERS OF PRESSURE OF THE NORMAL AND MAGNUS FORCES VS LENGTH

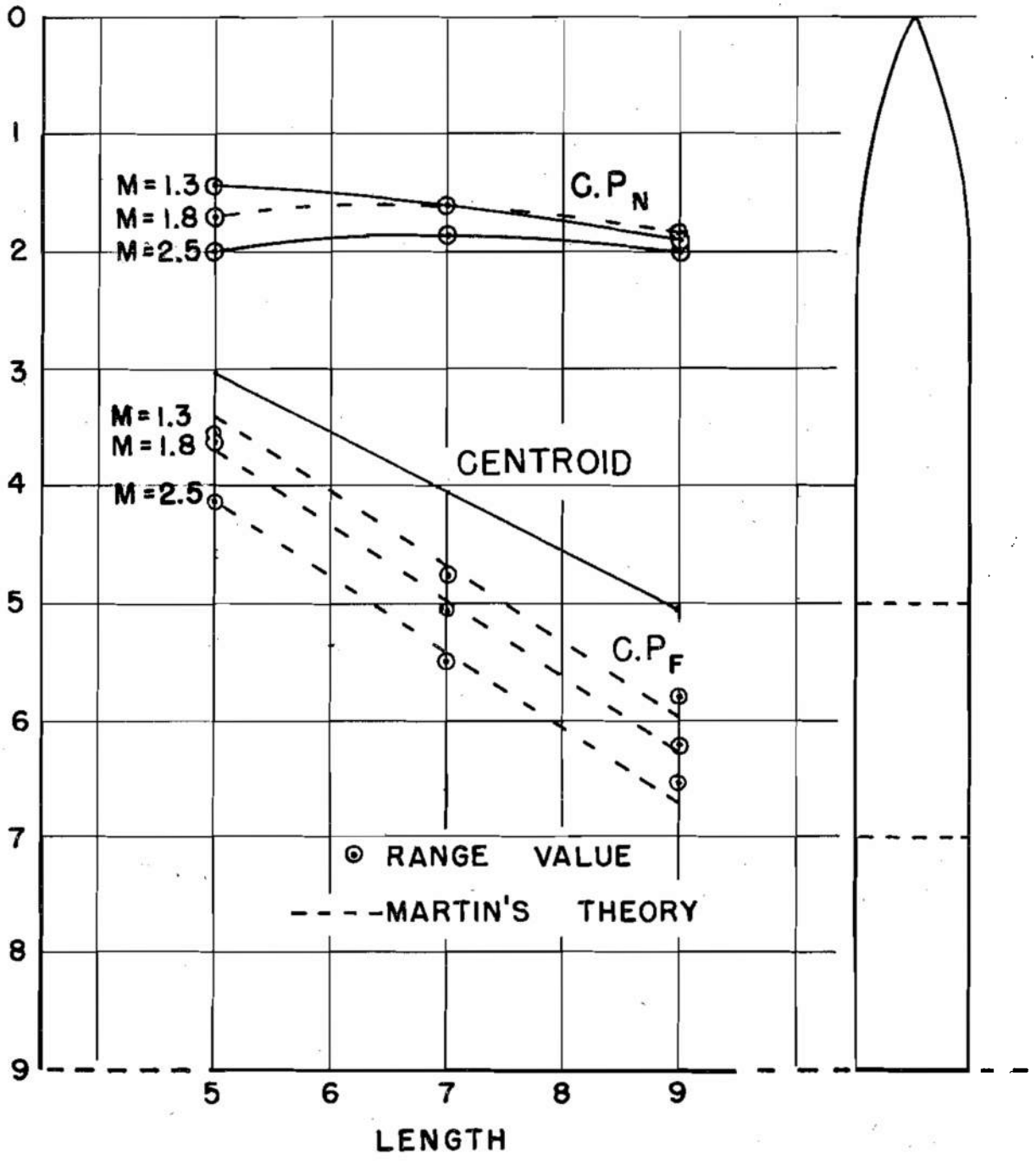

FIG. 19

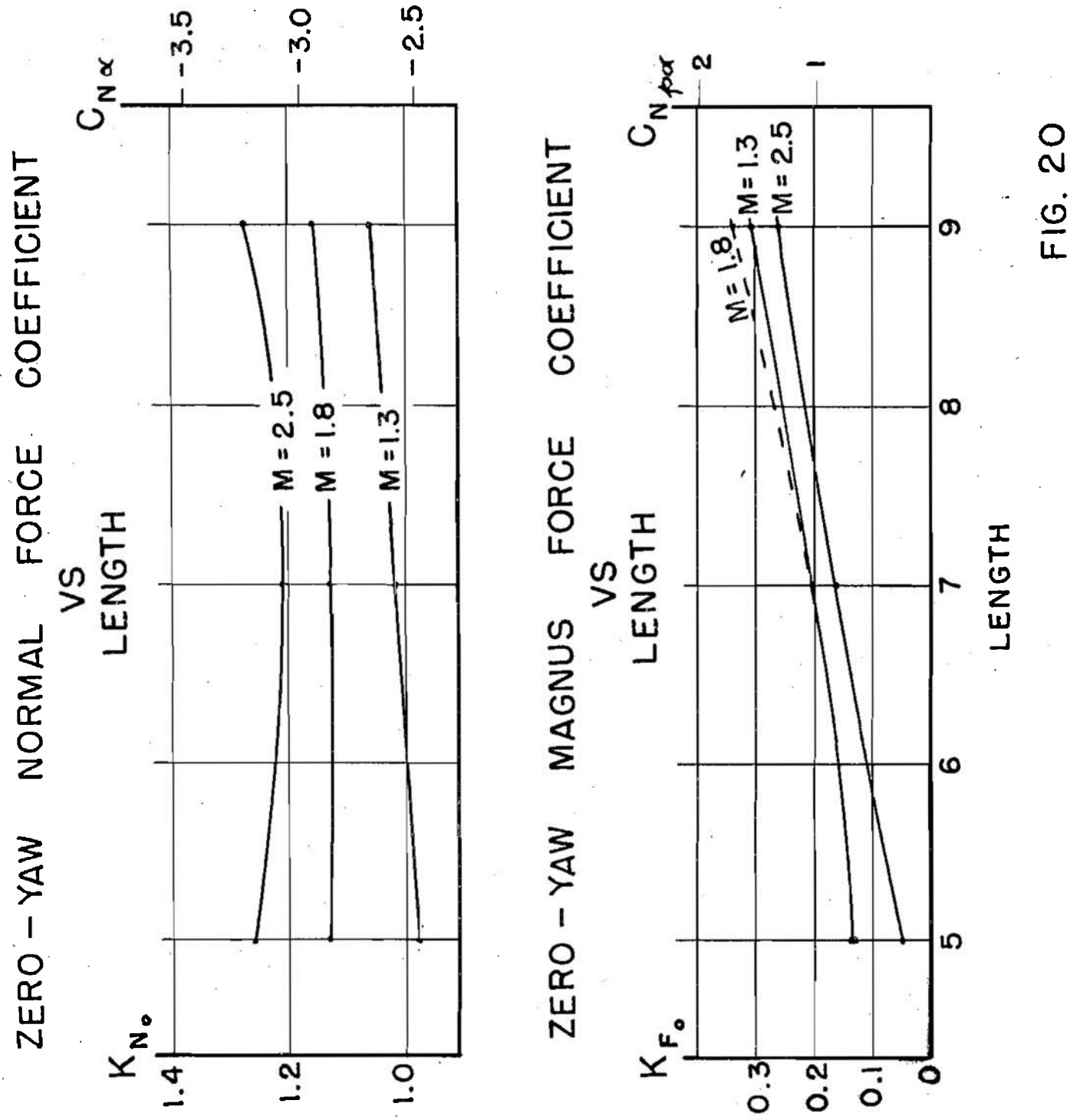
ZERO – YAW NORMAL FORCE COEFFICIENT
VS
LENGTH
$C_{N\alpha}$
-3.5
-3.0
-2.5
K_{N_o}
1.4
1.2
1.0
M = 2.5
M = 1.8
M = 1.3
ZERO – YAW MAGNUS FORCE COEFFICIENT
VS
LENGTH
$C_{N_{pqr}}$
2
1
K_{F_o}
0.3
0.2
0.1
0
5
6
7
8
9
LENGTH
M = 1.3
M = 2.5
M = 1.8

FIG. 20

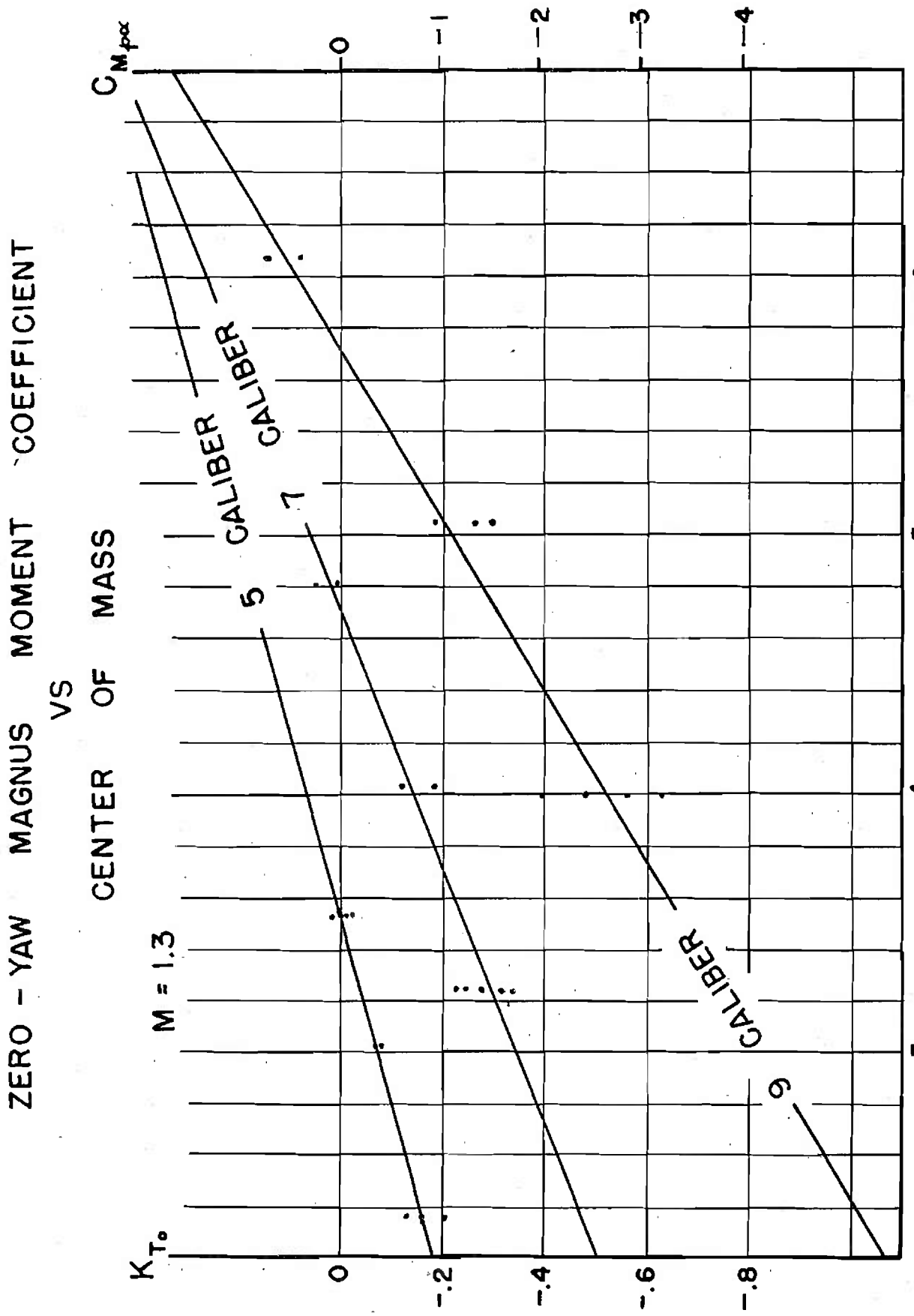
ZERO - YAW MAGNUS MOMENT COEFFICIENT
VS
CENTER OF MASS
M = 1.3
$C_{M_{p\alpha}}$
K_{T_o}
0
-1
-2
-3
-4
-.2
-.4
-.6
-.8
3
4
5
6
C.M. FROM NOSE
5 CALIBER
7 CALIBER
9 CALIBER

FIG. 21

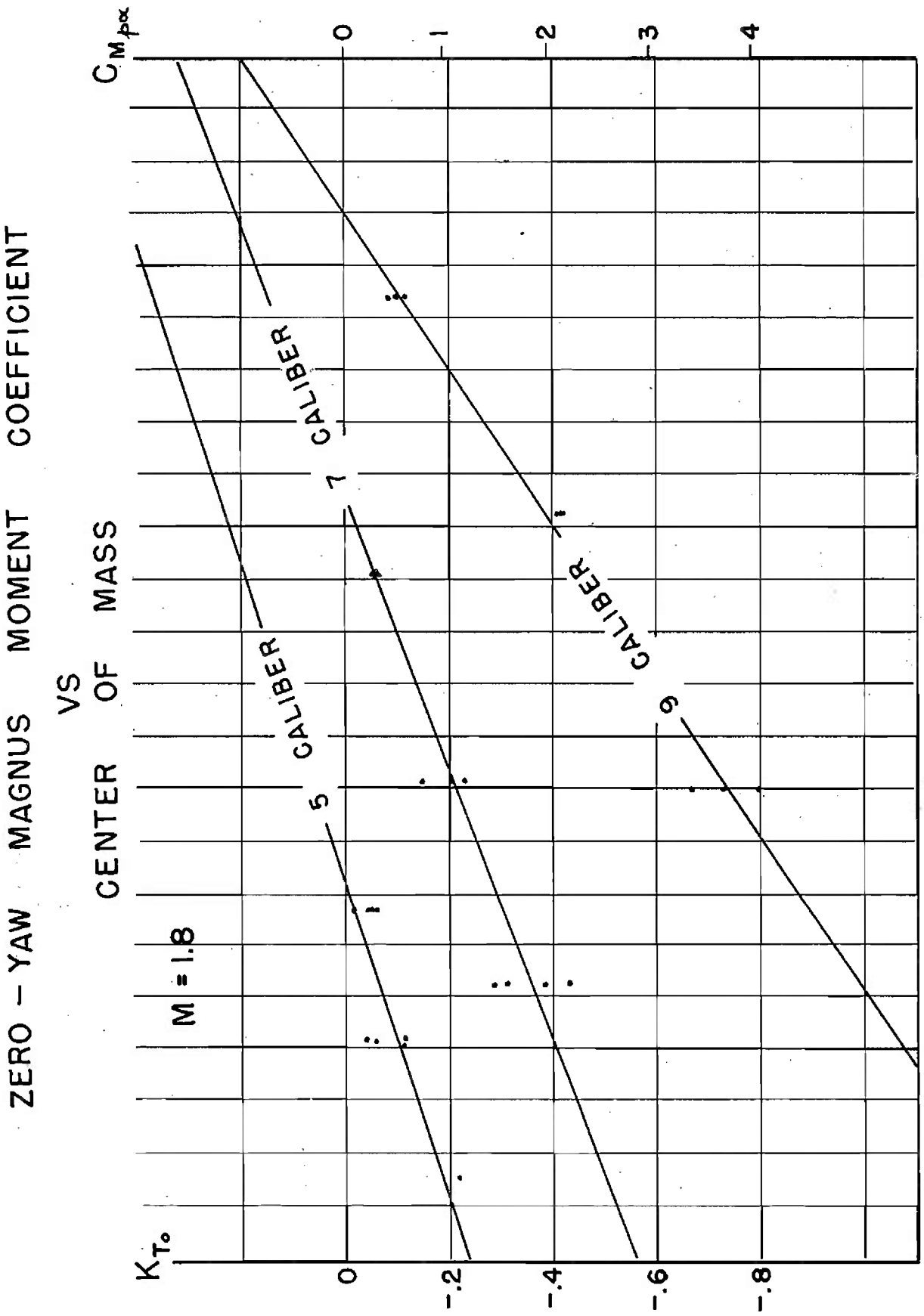

FIG. 22

ZERO – YAW MAGNUS MOMENT COEFFICIENT VS CENTER OF MASS

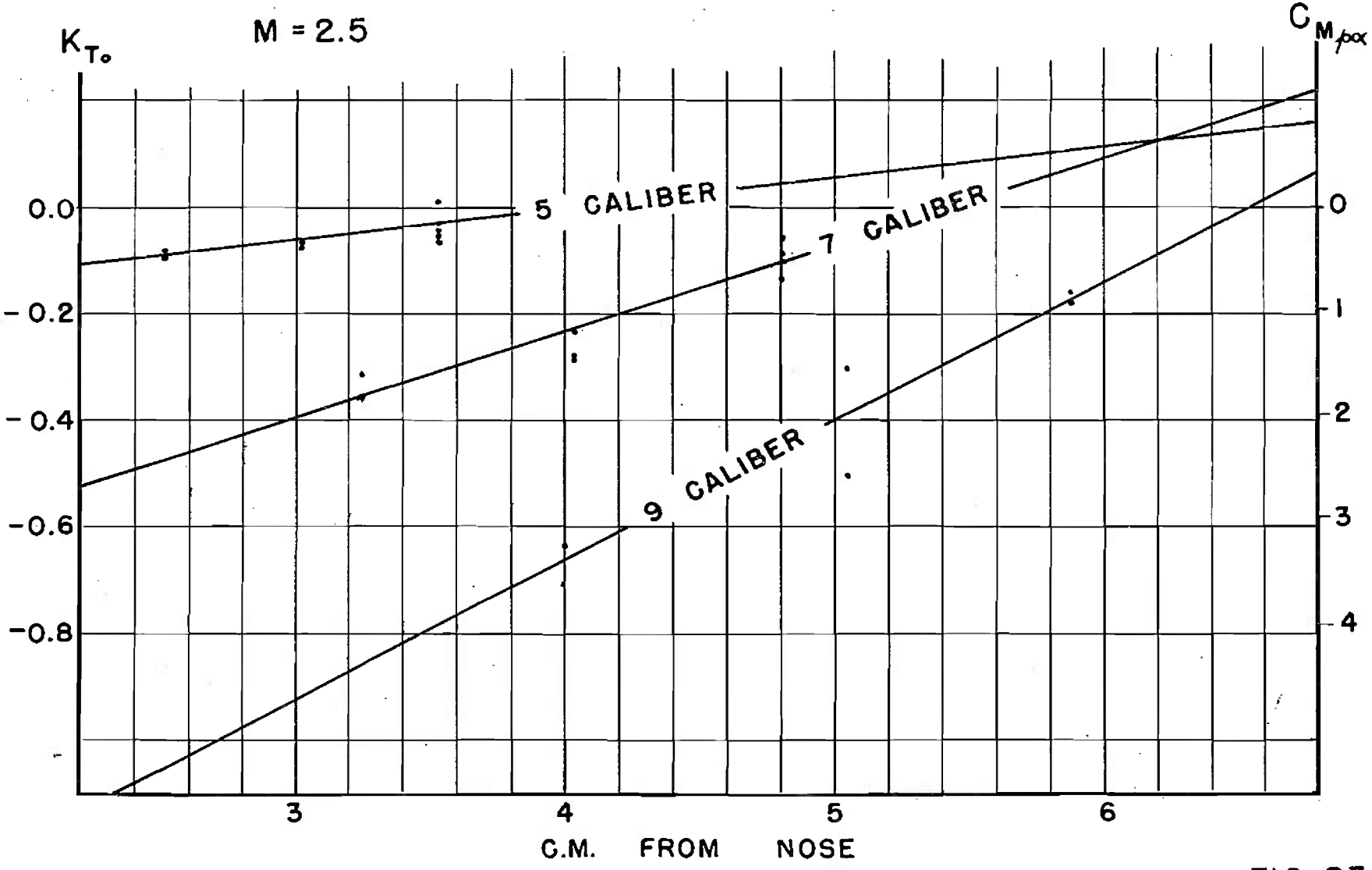

FIG. 23

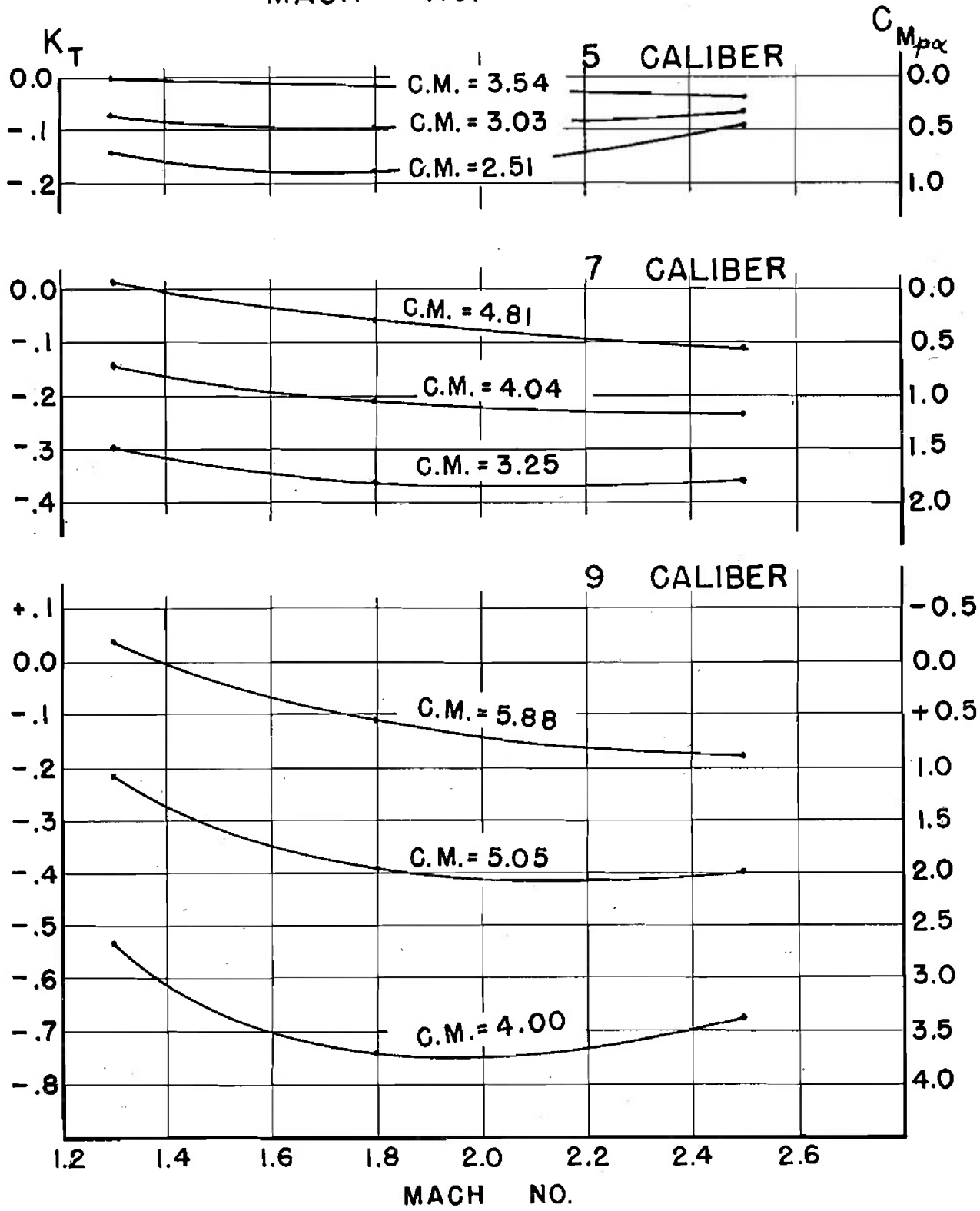
MAGNUS MOMENT COEFFICIENT
VS
MACH NO.
K_T
$C_{M_{p\alpha}}$
5 CALIBER
C.M. = 3.54
C.M. = 3.03
C.M. = 2.51
0.0
-.1
-.2
0.0
0.5
1.0
7 CALIBER
C.M. = 4.81
C.M. = 4.04
C.M. = 3.25
0.0
-.1
-.2
-.3
-.4
0.0
0.5
1.0
1.5
2.0
9 CALIBER
C.M. = 5.88
C.M. = 5.05
C.M. = 4.00
+.1
0.0
-.1
-.2
-.3
-.4
-.5
-.6
-.7
-.8
-0.5
0.0
+0.5
1.0
1.5
2.0
2.5
3.0
3.5
4.0
1.2
1.4
1.6
1.8
2.0
2.2
2.4
2.6
MACH NO.

FIG. 24

MAGNUS FORCE COEFFICIENT VS MACH . NO.

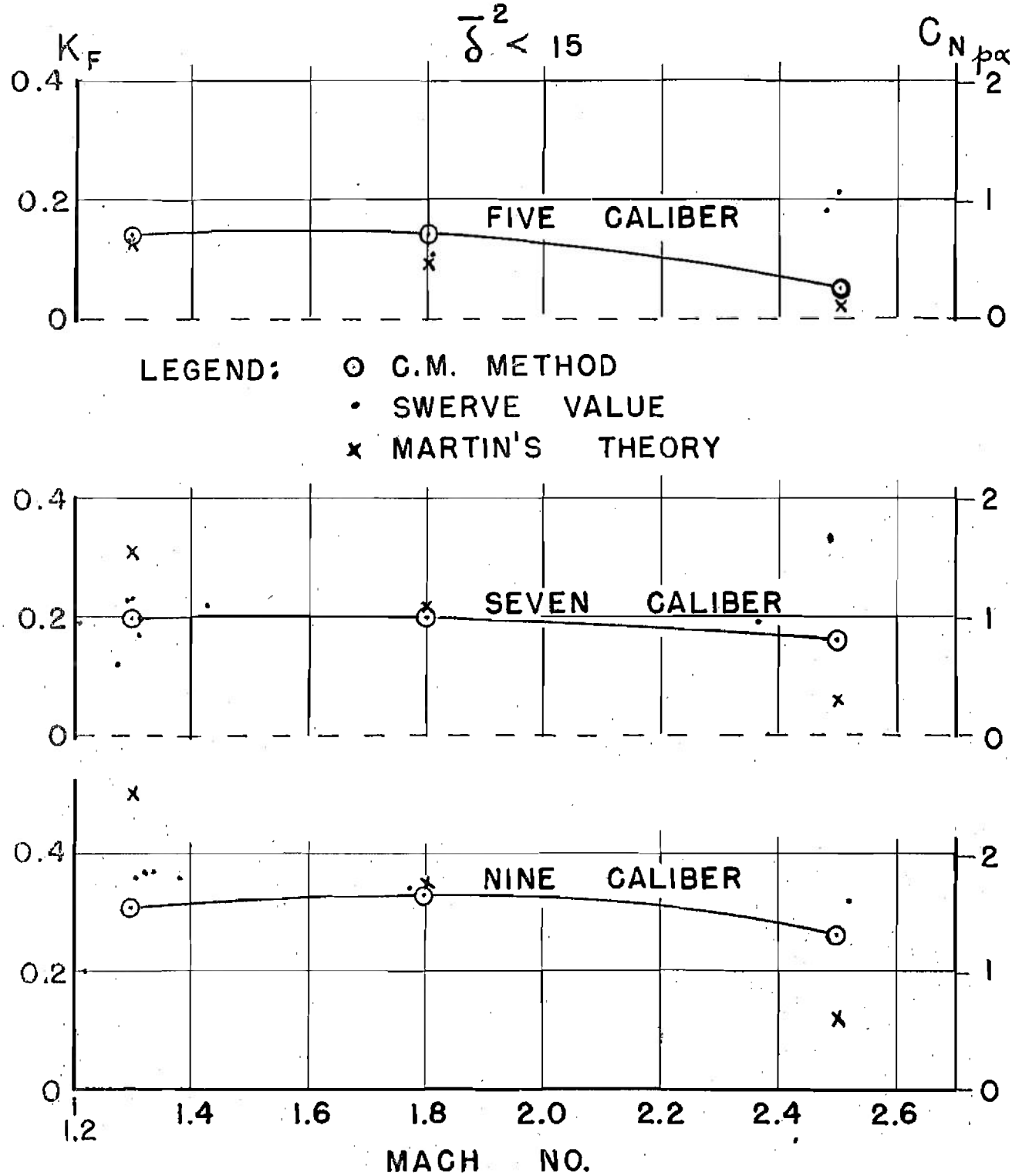

FIG. 25

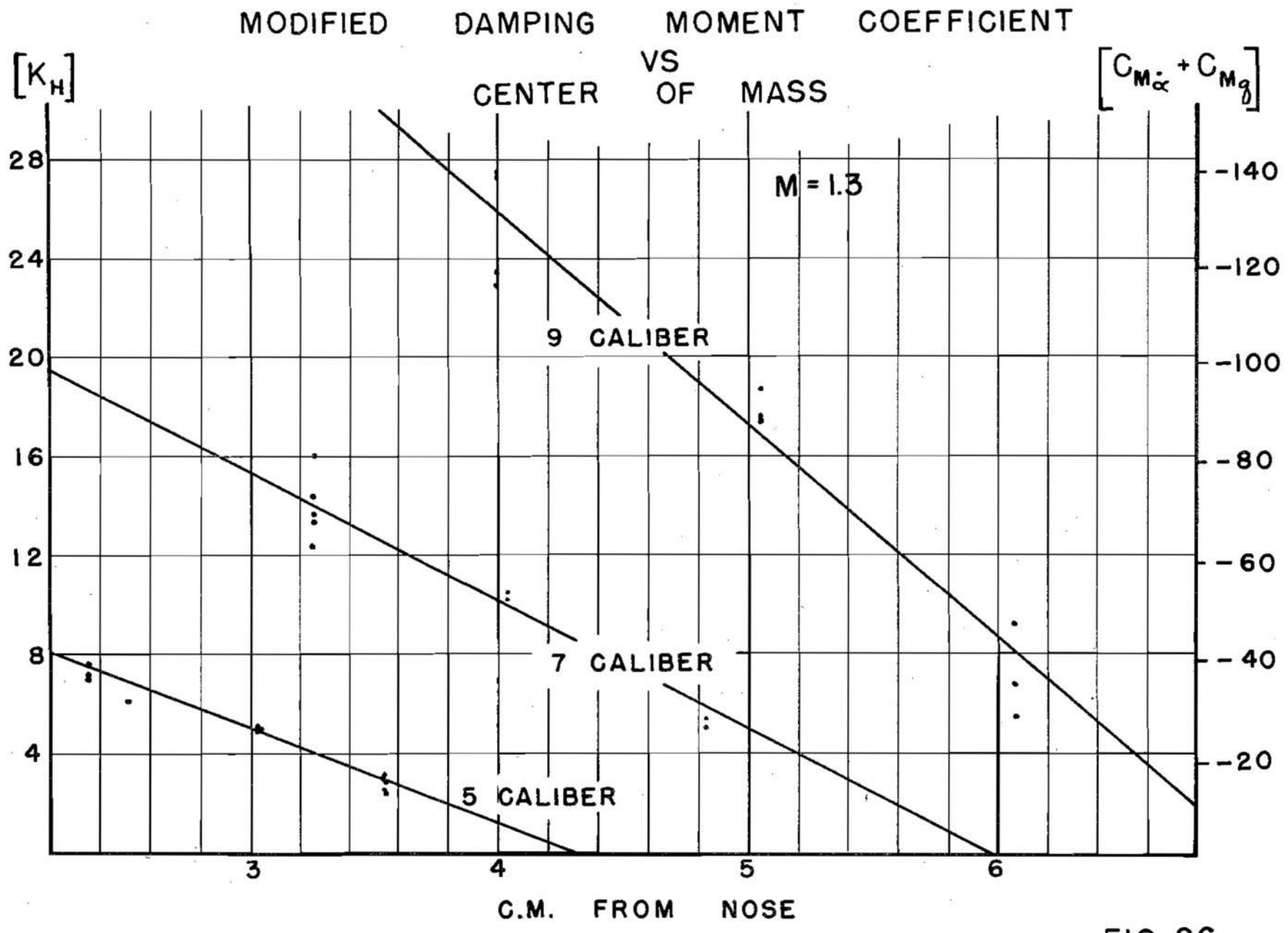
MODIFIED DAMPING MOMENT COEFFICIENT
VS
CENTER OF MASS
$[K_H]$
$[C_{M\dot{\alpha}} + C_{M_q}]$
M = 1.3
9 CALIBER
7 CALIBER
5 CALIBER
28
24
20
16
12
8
4
-140
-120
-100
-80
-60
-40
-20
3
4
5
6
C.M. FROM NOSE

FIG. 26

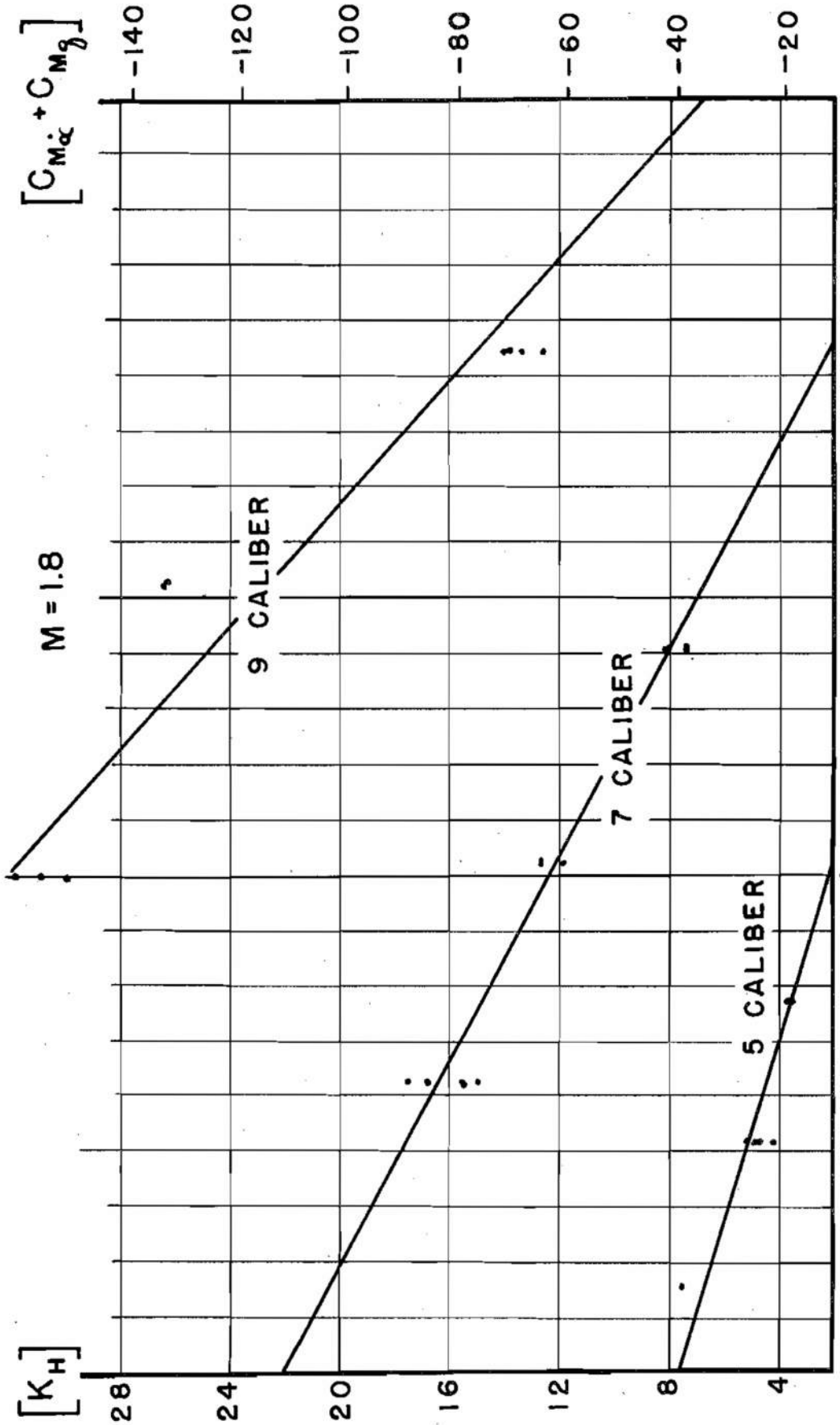
MODIFIED DAMPING MOMENT COEFFICIENT
VS
CENTER OF MASS
M = 1.8
9 CALIBER
7 CALIBER
5 CALIBER
$[K_H]$
$[C_{M\dot{\alpha}} + C_{M_q}]$
C.M. FROM NOSE
28
24
20
16
12
8
4
-140
-120
-100
-80
-60
-40
-20
3
4
5
6

FIG. 27

ZERO – YAW MODIFIED DAMPING MOMENT COEFFICIENT
VS
CENTER OF MASS

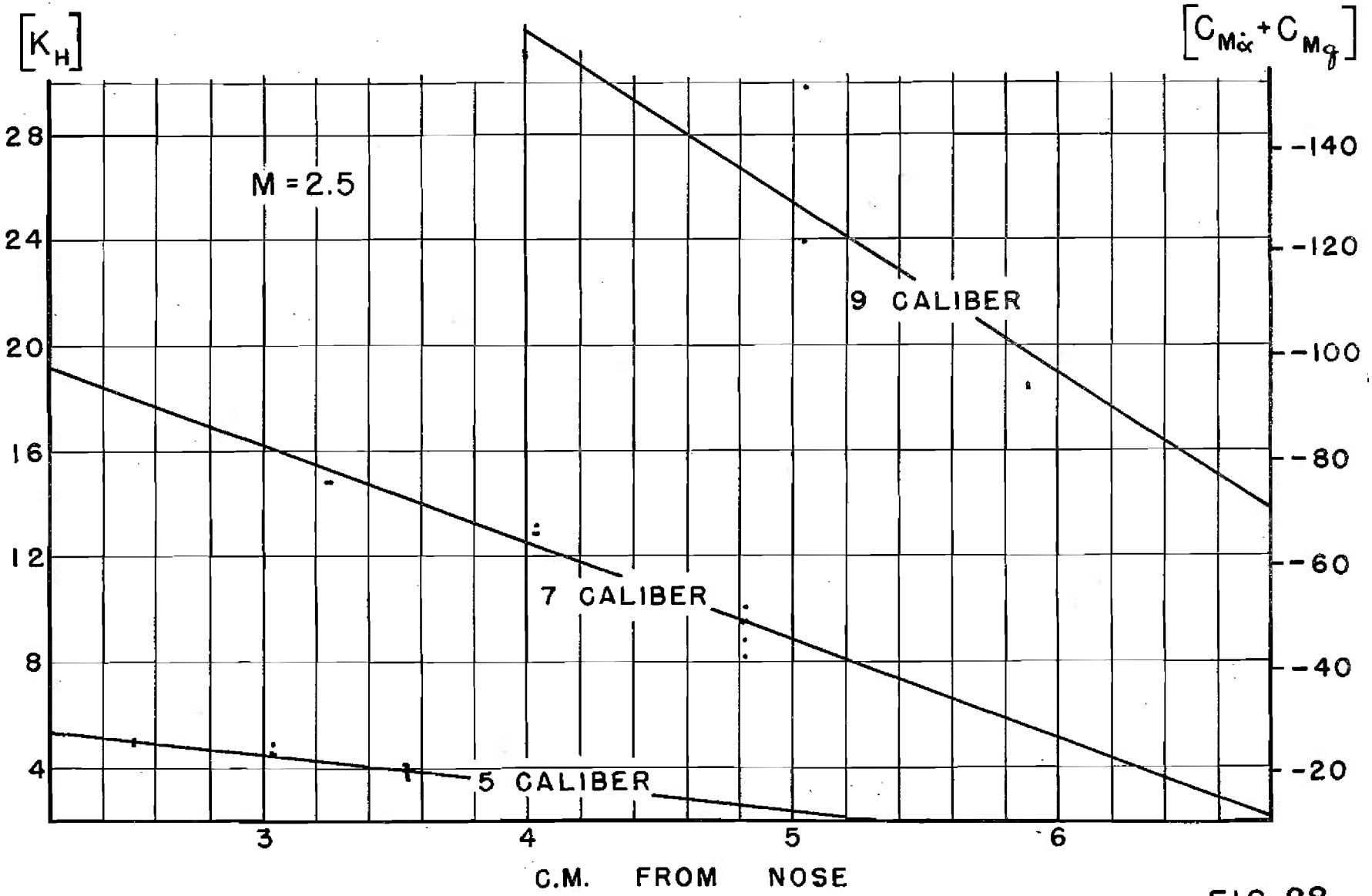

FIG. 28

DAMPING FORCE COEFFICIENT AT CENTROID
VS
MACH NO.

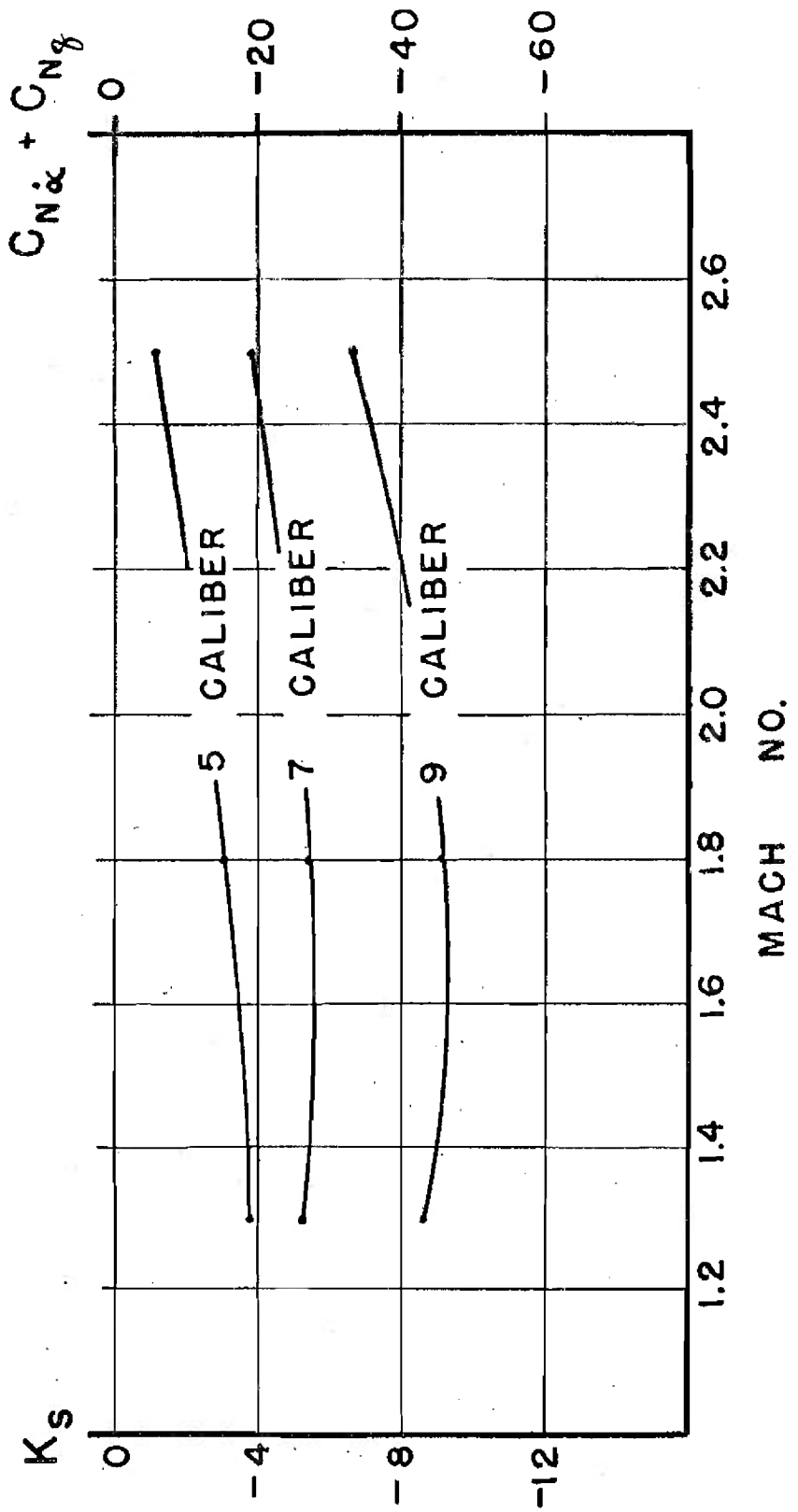

FIG. 29

DAMPING MOMENT COEFFICIENT AT CENTROID VS MACH NO.

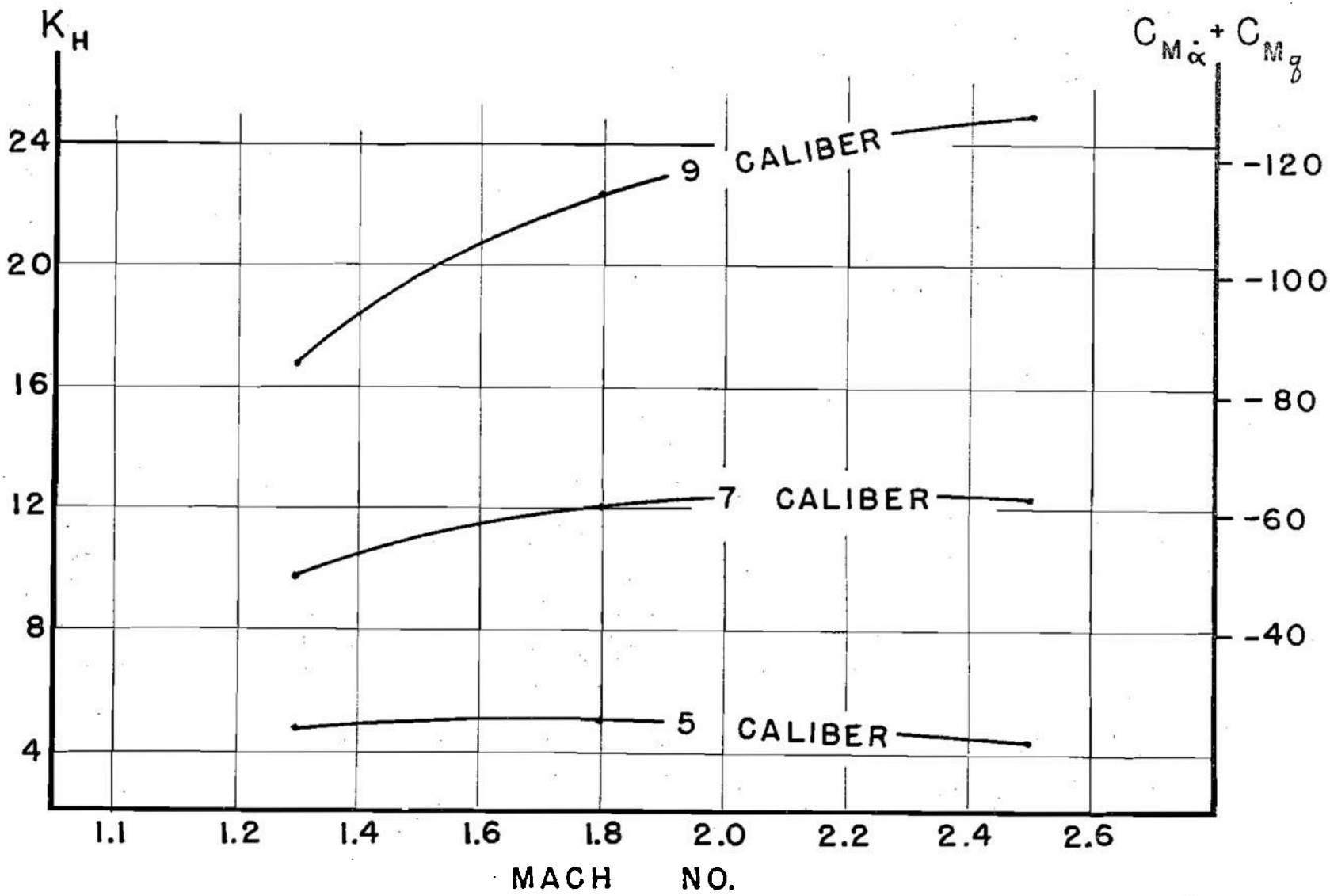

FIG. 30

DAMPING FORCE COEFFICIENT AT CENTROID VS LENGTH

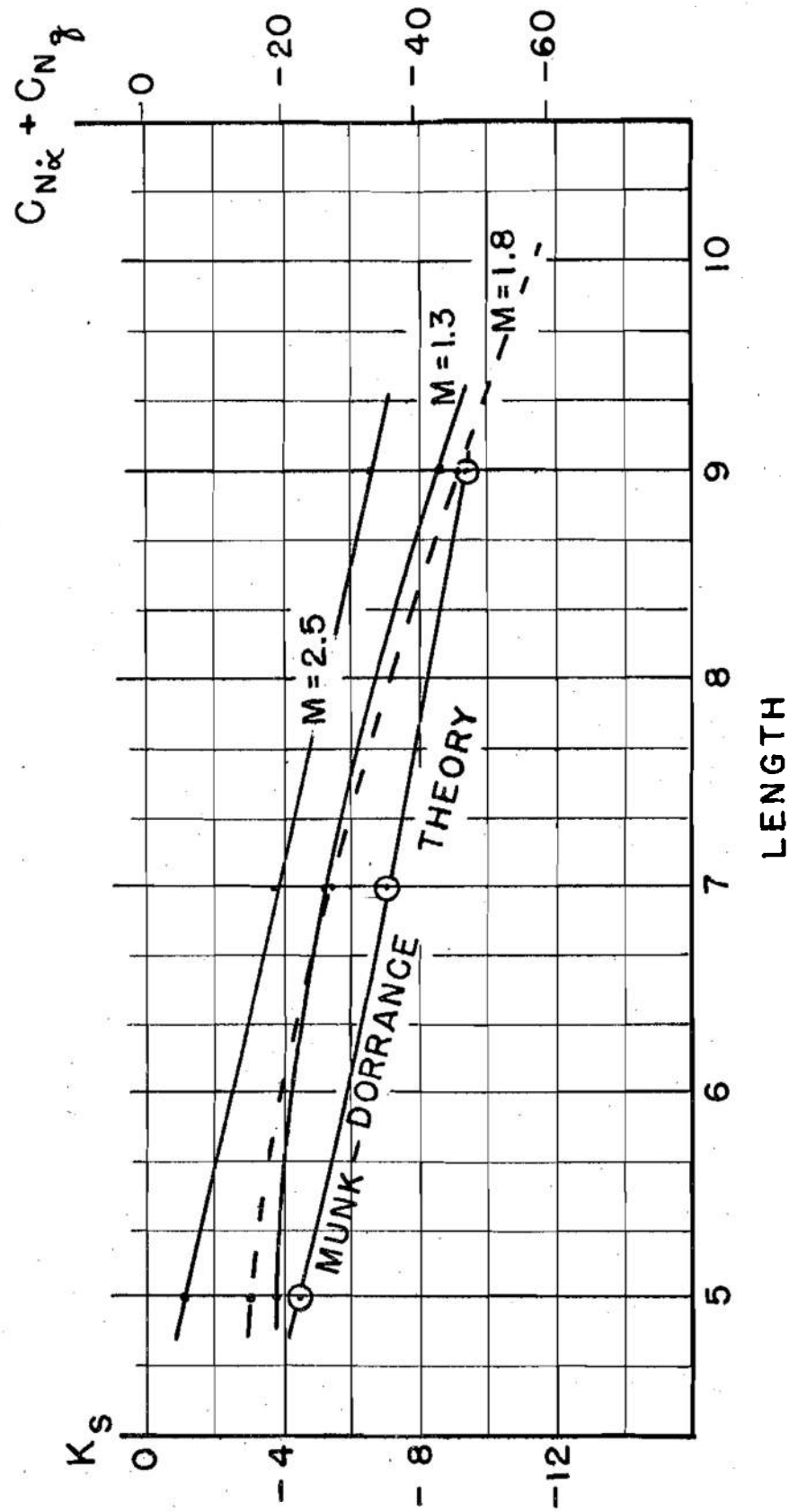

FIG. 31

DAMPING MOMENT COEFFICIENT AT CENTROID VS LENGTH

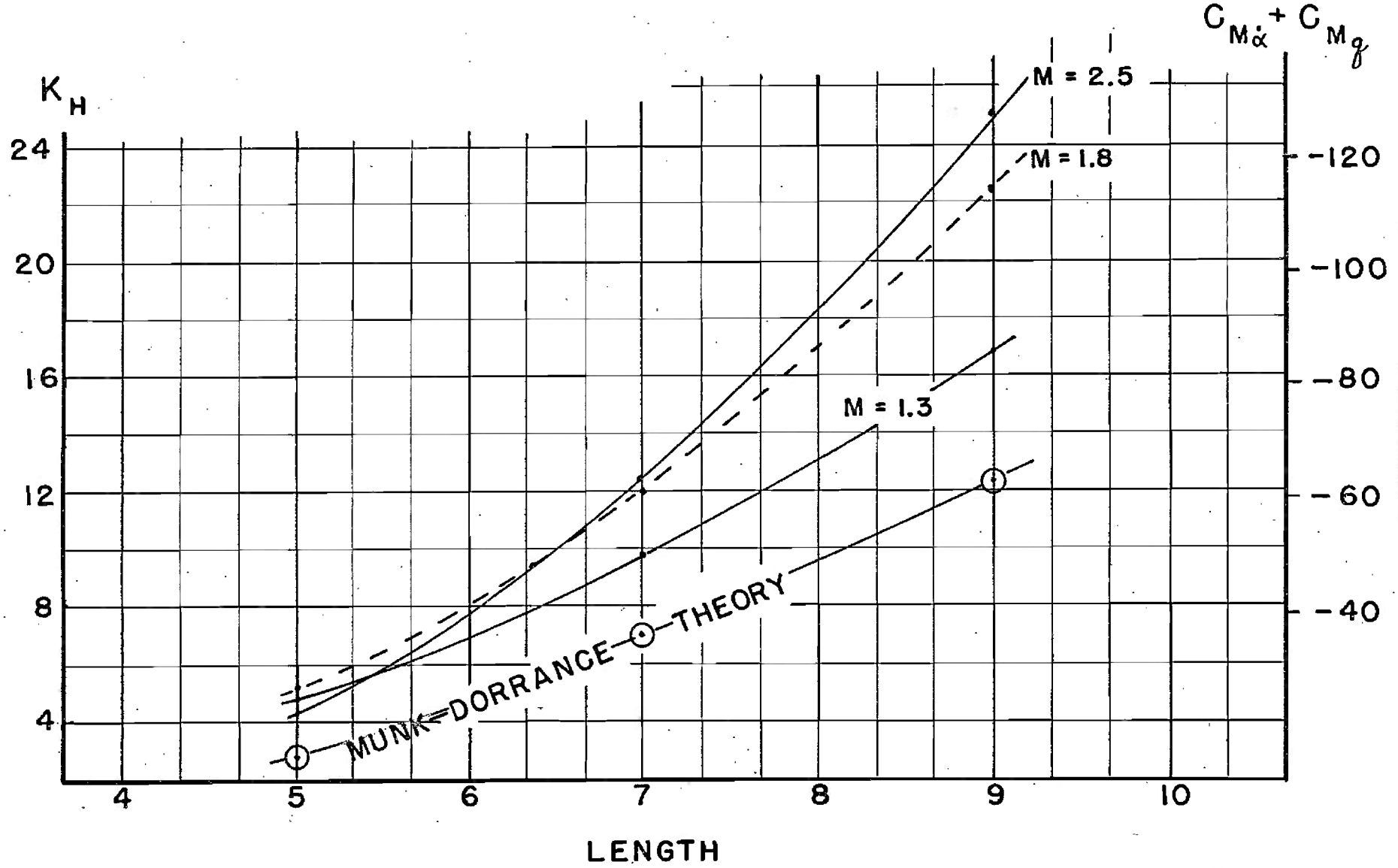

FIG. 32

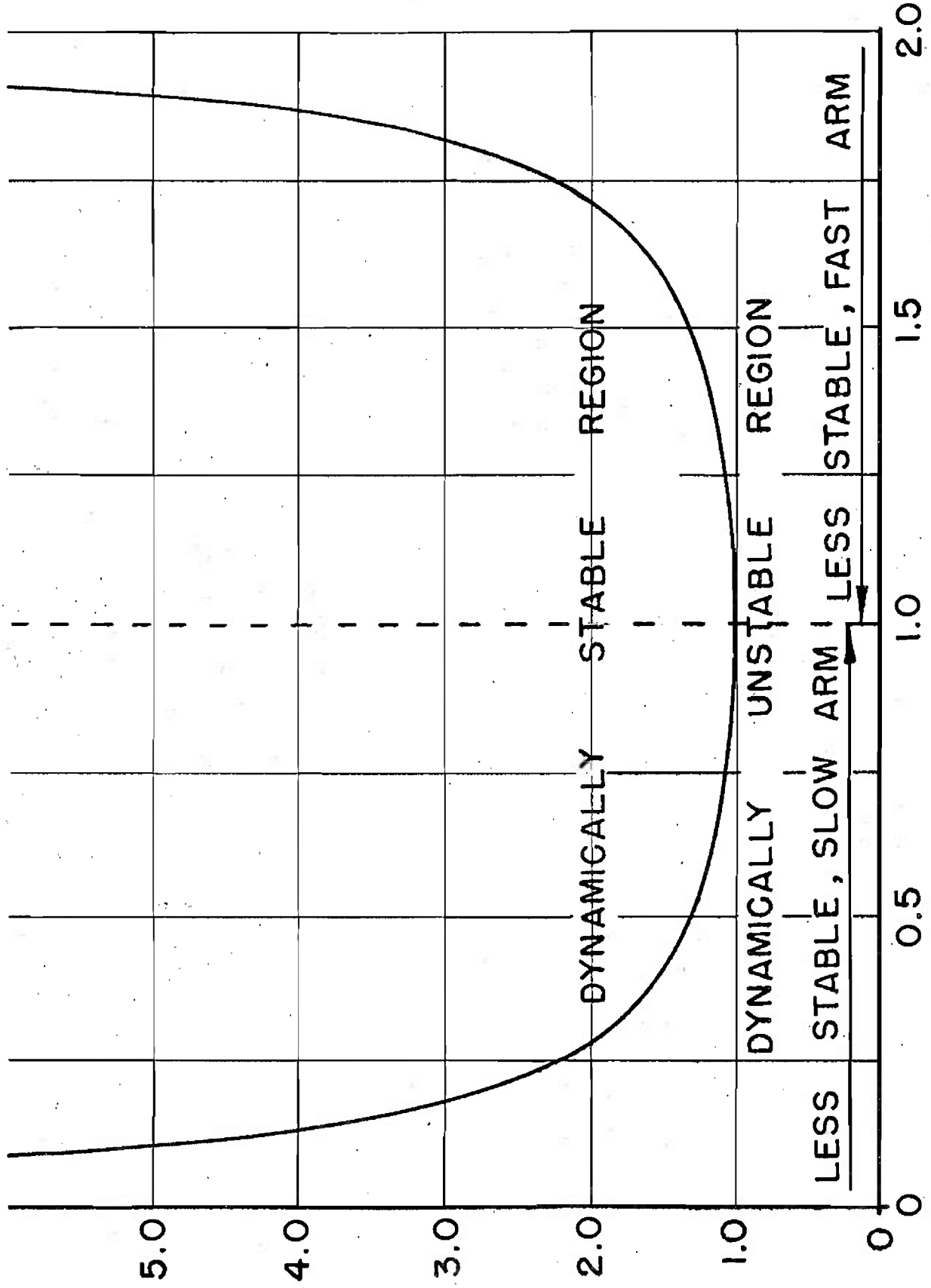
GYRO. STAB. FACTOR (S)
5.0
4.0
3.0
2.0
1.0
0
0
0.5
1.0
1.5
2.0
DYNAMIC STABILITY FACTOR ($\bar{S}$)
LESS STABLE, SLOW ARM
DYNAMICALLY UNSTABLE REGION
LESS STABLE, FAST ARM
DYNAMICALLY STABLE REGION

FIG. 33

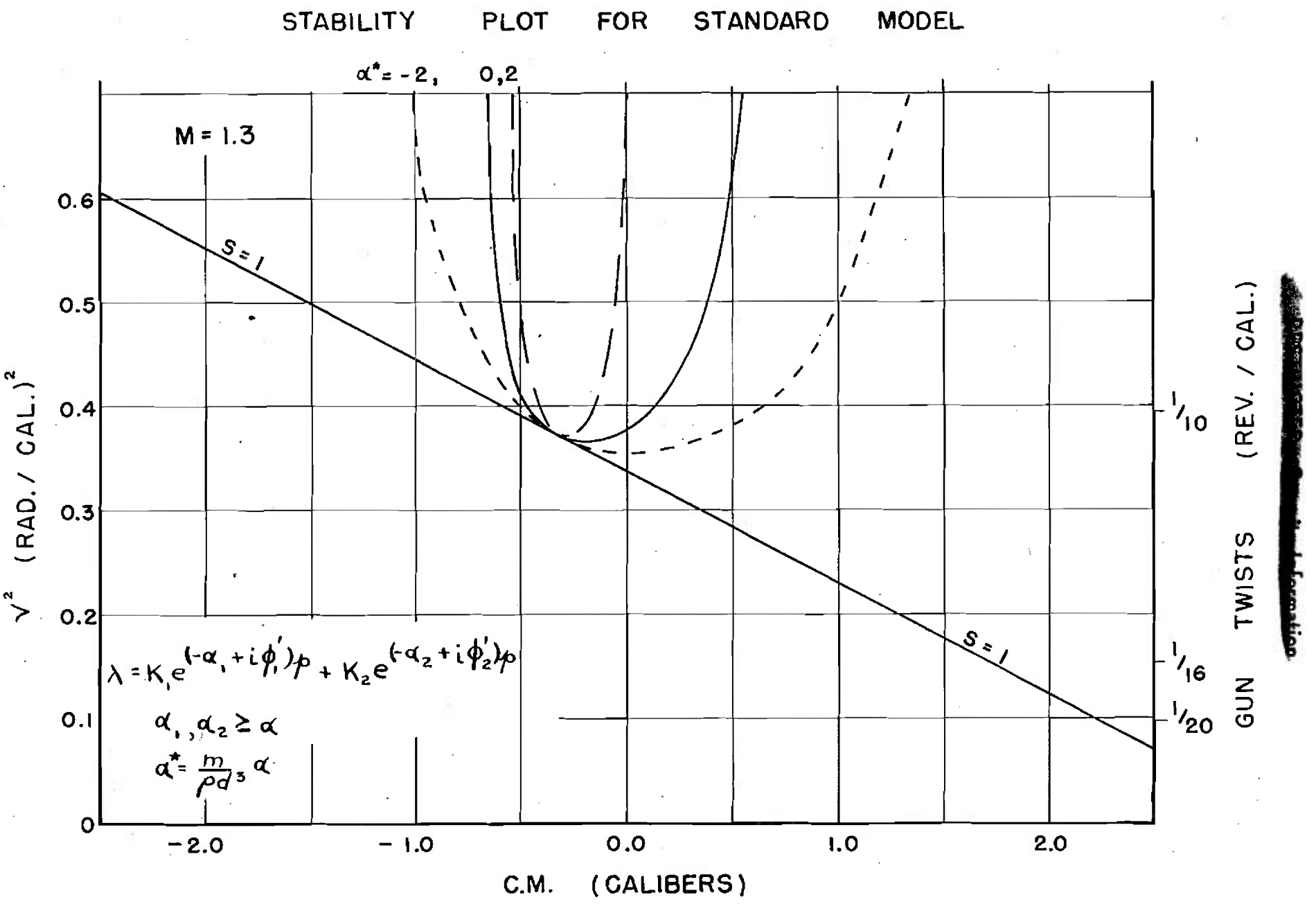
STABILITY PLOT FOR STANDARD MODEL
α* = -2, 0,2
M = 1.3
S = 1
S = 1
0.6
0.5
0.4
0.3
0.2
0.1
0
V² (RAD. / CAL.)²
λ = K₁e^((-α₁ + iφ₁')/p) + K₂e^((-α₂ + iφ₂')/p)
α₁, α₂ ≥ α
α* = m/ρd³ α
-2.0
-1.0
0.0
1.0
2.0
C.M. (CALIBERS)
1/10
1/16
1/20
GUN TWISTS (REV. / CAL.)

FIG.34

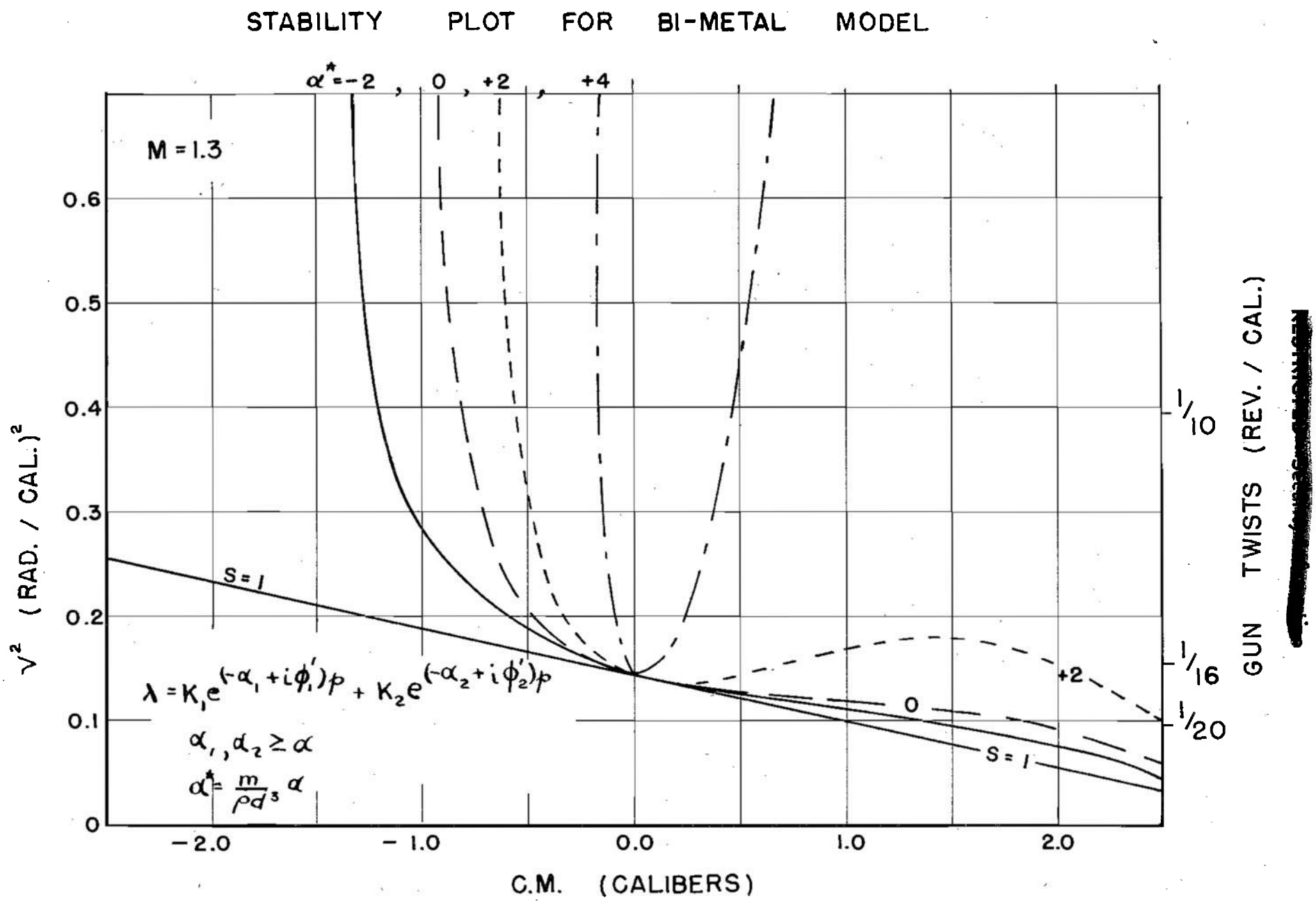

DISTRIBUTION LIST

No. of Copies	Organization
6	Chief of Ordnance Department of the Army Washington 25, D. C. Attn: ORDTB - Bal Sec
10	British - ORDTB for distribution
4	Canadian Joint Staff - ORDTB for distribution
3	Chief, Bureau of Ordnance Department of the Navy Washington 25, D. C. Attn: Re3
2	ASTIA Reference Center Library of Congress Washington 25, D. C.
2	Commander Naval Proving Ground Dahlgren, Virginia
3	Commander Naval Ordnance Laboratory White Oak Silver Spring 19, Maryland Attn: Mr. Nestingen Dr. May
3	Commander Naval Ordnance Test Station Inyokern P. O. China Lake, California Attn: Technical Library W. R. Haseltine
35	Superintendent Naval Postgraduate School Monterey, California
2	Commander Naval Air Missile Test Center Point Mugu, California
1	Commander Naval Air Development Center Johnsville, Pennsylvania
4	Commander Air Research and Development Command P. O. Box 1395 Baltimore 3, Maryland Attn: Deputy for Development
5	Director National Advisory Committee for Aeronautics 1724 F Street, N. W. Washington 25, D. C. Attn: Division Research Information
1	Commanding Officer and Director David W. Taylor Model Basin Washington 7, D. C. Attn: Aerodynamics Laboratory
1	Director Operations Research Office 6410 Connecticut Avenue Chevy Chase, Maryland
1	Chief, Armed Forces Special Weapons Project P. O. Box 2610 Washington 25, D. C. Attn: Capt. Bert F. Brown, USN
5	Director Armed Services Technical Information Agency Documents Service Center Knott Building Dayton 2, Ohio Attn: DSC - SA
2	Director National Advisory Committee for Aeronautics Ames Laboratory Moffett Field, California Attn: Dr. A. C. Charters Mr. H. J. Allen

DISTRIBUTION LIST

No. of Copies	Organization
1	Commander Arnold Engineering Development Center Tullahoma, Tennessee Attn: Deputy Chief of Staff, R&D
1	Commanding Officer Chemical Corps Chemical and Radiological Lab. Army Chemical Center, Maryland
3	Commanding General Redstone Arsenal Huntsville, Alabama
3	Commanding Officer Picatinny Arsenal Dover, New Jersey
1	Commanding Officer Frankford Arsenal Philadelphia, Pennsylvania
1	Prof. George F. Carrier Division of Applied Science Harvard University Cambridge 38, Massachusetts
1	Prof. Francis H. Clauser Department of Aeronautics Johns Hopkins University Baltimore 18, Maryland
1	Prof. Clark B. Millikan Guggenheim Aeronautical Laboratory 1500 Normandy Drive California Institute of Technology Pasadena 4, California
1	Dr. A. E. Puckett Hughes Aircraft Co. Florence Avenue at Teal St. Culver City, California
1	Dr. L. H. Thomas Watson Scientific Computing Laboratory 612 West 116th Street New York 27, New York
1	Arthur D. Little, Inc. Cambridge 42, Massachusetts Attn: Dr. C. S. Keevil THRU: District Chief Boston Ordnance District Boston Army Base Boston 10, Massachusetts
1	Professor J. W. Cell North Carolina State College Raleigh, North Carolina THRU: District Chief Philadelphia Ordnance District 1500 Chestnut Street Philadelphia 2, Pennsylvania
2	Armour Research Foundation Illinois Institute of Technology Technology Center Chicago 16, Illinois Attn: Mr. W. Casler Dr. A. Wundheiler THRU: District Chief Chicago Ordnance District 209 W. Jackson Boulevard Chicago 6, Illinois
1	Wright Aeronautical Corp. Wood-Ridge, New Jersey Attn: Sales Dept. (Government) THRU: AFPR, Wright Aeronautical Corp. Wood-Ridge, New Jersey

DISTRIBUTION LIST

No. of Copies	Organization
2	Applied Physics Laboratory 8621 Georgia Avenue Silver Spring, Maryland Attn: Mr. George L. Seielstad THRU: Naval Inspector of Ordnance Applied Physics Laboratory 8621 Georgia Avenue Silver Spring, Maryland
1	Cornell Aeronautical Laboratory, Inc. Buffalo, New York Attn: Miss Elma T. Evans Librarian THRU: Bureau of Aeronautics Representative Cornell Aeronautical Laboratory, Inc. P. O. Box 235 Buffalo 21, New York
1	M. W. Kellogg Co. Foot of Danforth Avenue Jersey City 3, New Jersey Attn: Mr. Robert A. Miller THRU: Inspector of Naval Material Naval Industrial Reserve Shipyard Building 13, Port Newark Neward 5, New Jersey
1	General Electric Co. Project HERMES Schenectady, New York Attn: Mr. J. C. Hoffman THRU: Project HERMES Resident Ord Officer Campbell Ave. Plant, General Elec. Co. Schenectady 5, New York
2	California Institute of Technology Jet Propulsion Laboratory Pasadena, California Attn: Mr. Irl E. Newlan Reports Group THRU: District Chief Los Angeles Ordnance District 35 N. Raymond Avenue Pasadena 1, California
1	University of Michigan Willow Run Research Center Willow Run Airport Ypsilanti, Michigan Attn: Mr. J. E. Corey THRU: Commanding Officer Central Air Procurement District West Warren and Lonyo Ave. Detroit 32, Michigan
1	Massachusetts Institute of Technology Instrumentation Laboratory 155 Massachusetts Avenue Cambridge 39, Massachusetts Attn: Dr. C. S. Draper THRU: Inspector of Naval Material Massachusetts Institute of Technology Cambridge 39, Massachusetts Attn: Development Contract Dept.
1	The Firestone Tire and Rubber Co. Defense Research Division Akron 17, Ohio Attn: Peter J. Ginge THRU: District Chief Cleveland Ordnance District Auditorium Building 1367 East Sixth Street Cleveland 14, Ohio

DISTRIBUTION LIST

No. of Copies	Organization
2	Sandia Corp. Sandia Base P. O. Box 5800 Albuquerque, New Mexico Attn: Mrs. Wynne K. Cox THRU: Field Manager U. S. Atomic Energy Commission P. O. Box 5900 Albuquerque, New Mexico
1	United Aircraft Corp. Research Department East Hartford 8, Connecticut Attn: Mr. Robert C. Sale THRU: Bureau of Aeronautics Representative Pratt and Whitney Aircraft Division United Aircraft Corp. East Hartford 8, Connecticut
1	Aerophysics Development Corp. P. O. Box 657 Pacific Palisades, California Attn: Dr. William Bollay THRU: District Chief Los Angeles Ordnance District Pasadena 1, California
1	University of Southern California Engineering Center Los Angeles 7, California Attn: Mr. H. R. Saffell Director THRU: BuAer Representative c/o Aerojet Engineering Corp. 6352 North Irvindale Avenue Azusa, California
1	Consolidated Vultee Aircraft Corp. Ordnance Aerophysics Laboratory Daingerfield, Texas Attn: Mr. J. E. Arnold THRU: Assistant Inspector of Naval Material Ordnance Aerophysics Lab. Daingerfield, Texas
1	Dr. Z. Kopal Department of Electrical Engineering Massachusetts Institute of Technology Cambridge 39, Massachusetts THRU: Inspector of Naval Material Boston District (Development Contract Officer) Massachusetts Inst. of Technology Cambridge 39, Massachusetts
1	Northrop Aircraft, Inc. Hawthorne, California Attn: Mr. Selna THRU: District Chief L. A. Ordnance District Pasadena 1, California